Source apportionment of highly time resolved trace elements during a firework episode from a rural freeway site in Switzerland

Pragati Rai[1], Markus Furger[1], Jay Slowik[1], Francesco Canonaco[1], Roman Fröhlich[1], Christoph Hüglin[2], María Cruz Minguillón[3], Krag Petterson[4], Urs Baltensperger[1] and André S.H. Prévôt[1]

[1] Laboratory of Atmospheric Chemistry, Paul Scherrer Institute, Villigen PSI, 5232, Switzerland
[2]Laboratory for Air Pollution / Environmental Technology, Empa, 8600 Dübendorf, Switzerland
[3]Institute of Environmental Assessment and Water Research (IDAEA), CSIC, 08034 Barcelona, Spain
[4]Cooper Environmental Services (CES), 9403 SW Nimbus Avenue, Beaverton, OR 97008, USA

Correspondence to: André S. H. Prévôt (andre.prevot@psi.ch) and Markus Furger (markus.furger@psi.ch)

Response to Reviewer #1

We thank Reviewer#1 for the careful revision and comments which helped improving the overall quality of the manuscript. A point-by-point answer (in regular typeset) to the reviewers' remarks (in italic typeset) follows. Changes to the manuscript are indicated in blue font.

In the following page and lines references refer to the manuscript version reviewed by anonymous Reviewer#1.

GENERAL COMMENTS

The manuscript describes a study to determine the sources impacting on PM10 in a traffic oriented site using a high resolution elemental dataset and processing data with the SoFi tool based on ME-2 receptor model algorithm. The manuscript is well organized, the language is clear and the English style is appropriate.

According to the authors, the SA study was conducted to characterize the source emissions at a traffic-influenced site. This is confusing because receptor models are normally carried out at the receptor site to characterize the source contributions rather than the source emissions. The authors claim the novelty of the work is due to the limited number of studies for trace element emission sources with high time resolution. However, as the same authors state, many studies were carried out using rotating drum and streakers that, despite being off-line, provide comparable information that can be processed in the same manner as this study.

We agree with reviewer#1 that receptor models characterize the source contributions. Therefore we have replaced "emissions" by "contributions" to make it clear.

The novelty of this work mainly highlights the inclusion of a strong fireworks event in the PMF input data set. Typically such strong, isolated events are excluded from PMF analysis to avoid distortion of the solution. However, here we established that unmixed fireworks can be apportioned by ME-2, without disturbing the model solutions, in contrast to conventional/unconstrained PMF.

We agree with the reviewer that highly time-resolved trace element measurements can be obtained by rotating drum and streaker techniques, and in principle provide similar information as the Xact. However, these samplers require offline analysis, including accessibility and significant beam time availability at accelerator facilities. In practice, this leads to undesirable trade-offs between time resolution and data coverage even for short duration field campaigns, whereas highly time-resolved long-term measurements are impractical. In contrast, the Xact 625 is an online system which has been developed and commercialized for rapid, long-term and semi-continuous detection of the ambient aerosol particle's elemental composition. This is a novel and highly useful analytical capability, and characterization of the instrument's measurement and source apportionment capabilities is therefore of significant interest.

We have rewritten page 3 line 1 as follows:

In practice, the offline samplers lead to undesirable trade-offs between time resolution and data coverage even for short duration field campaigns, whereas highly time-resolved long-term measurements are impractical. A recently introduced online high time resolution instrument can collect samples and perform analysis for elements simultaneously in a near real time scenario for long-term measurements without waiting for laboratory analysis.

SA of the entire PM based only on trace elements representing only a limited fraction of the PM mass (in this case 20%) is very uncertain because a considerable amount of information is missing about the main components of PM: elemental carbon, ions and the organic fraction. The risk is to overestimate the contribution of sources for which the elements are markers and neglect sources where elements are less relevant in particular the secondary organic fraction. In addition, the identification of factors into sources is hindered because the chemical profiles contain few diagnostic species or combination of species.

It is important to know where the inorganic elements / metals come from. Every source apportionment typically focuses on the components that are measured. For example, all the PMF of organic aerosol just does a source apportionment of the organic aerosol. We do not attempt to provide a full source apportionment of the atmospheric aerosol, but rather focus on the inorganic elements / metals. This has been done to a much lesser extent than for the organic aerosol, but it is actually important, and may become more important in the next years, due to the discussion of the possible health effects of metals.

In addition, we have used BC, NO_x and Q-ACSM data to compare the SA results with the time trends of those components. We did not claim to do a SA of PM_{10} just with the elements measured by the Xact. We fully agree with reviewer#1 that it would introduce a lot of uncertainties if we attempted to scale our element SA to the full PM_{10}, however, as mentioned, this is not the case here. We believe that SA of trace elements alone is already interesting. Some elements are directly health-relevant and many are closely related to specific sources. The total SA including elemental carbon, ions, organic fraction and trace elements is quite complicated, requiring blending of data from several instruments. It is also suboptimal for identifying sources of trace elements because it can reduce them to minor factors (in comparison to organics or non-refractory inorganics). In addition, the combined SA would require combining measurements with different size cuts, e.g. Xact with $PM_{10,}$ ACSM with PM_1 and BC with $PM_{2.5}$.

The authors claim MAAP and Q-ACSM were collected in parallel so it is not clear why they didn't use this information to obtain more robust SA results. The impression is that the authors are splitting the study in pieces to make more publications.

As already mentioned above combining different data sets from different instruments into one ME-2 model is challenging due to differences in error propagation. In our opinion, the combination of PM_1 data for Q-ACSM, $PM_{2.5}$ for MAAP and PM_{10} data for Xact may introduce artefacts in the ME-2 analysis. We have used MAAP and Q-ACSM data sets in the manuscript to compare some of the ME-2 factor time series and diurnal patterns. We are not planning to publish any other paper on the additional data. A major focus was the exploration of the use of the Xact for source apportionment in Europe where the concentrations are considerably lower than in polluted areas in Asia.

We have added in the manuscript as follows on page 3 line 7:

The main focus of this work is the exploration of the use of the Xact for source apportionment in Europe where the concentrations are considerably lower than in polluted areas in Asia.

The study location is not well described. A map is needed to help the reader understanding the characteristics of the site.

We have added a map in the manuscript on page 22.

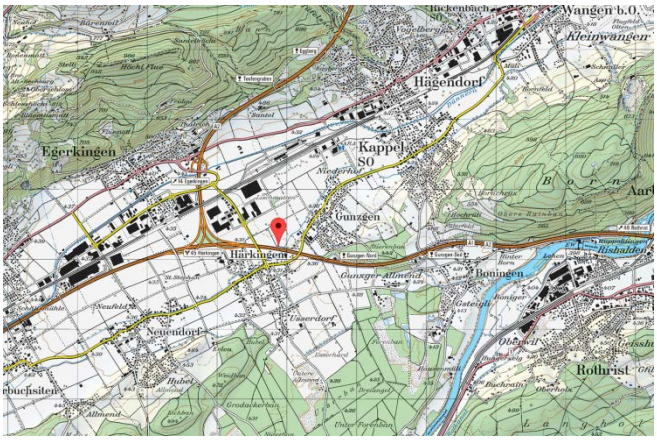

Figure 1: Map of the sampling location (NABEL site in Haerkingen), The site is marked with red google pin. Map reproduced by permission of swisstopo (JA100119).

The Conditional Bivariate Polar Function (CBPF) analysis is an important part of this work, there is a dedicated sub-chapter in the methodology section. However, there are no graphs about the results of this technique in the paper. The supplementary material is supposed to be used to provide information that supports the main findings of the work not to place essential results of the work.

This issue was also raised by reviewer #2. We have modified the graph and moved it into the main text of the revised manuscript.

The conclusion that the study result emphasizes the large influence of highway traffic on the composition of PM10 is trivial considering the study was conducted at a traffic site. In addition, this is not in line with the declared objective of characterizing the emissions.

We have mentioned in the objective that we conducted SA using PMF to characterize the source contributions of highly time-resolved metals during a three-week campaign at a traffic-influenced and otherwise rural site in Härkingen, Switzerland. Therefore, we decided to mention a brief overview of results in the conclusions including the smallest and largest contributions of sources, which is in line with the objective. In fact, the high contribution of traffic is not trivial and not easily accessible with 24-hours sampling. In addition, it is important in the light of the role elements may have concerning health effects. In contrast, the contribution of traffic is minor for organics, also at such a site and also for other components it is not clear how much the rather local source would contribute in comparison to other more regionally influenced components.

In this manuscript there is a contrast between the highly sophisticated data treatment and the limited data input. The model allocates all the PM10 mass on the basis on the predictive capabilities of only 14 elements which do not provide enough information to properly identify all the factors and to allocate the PM10 mass to each of them reliably. This is due to lack of markers to allocate the carbonaceous fraction and part of the secondary inorganic (nitrate). As a consequence there are not well resolved factors (e.g. the two fireworks and the two dust factors and the road dust with the traffic-related factor).

Again, we are not attempting a source apportionment of the full PM_{10}, but rather of the inorganic elements / metals concentrations. For these components, we have been able to retrieve quite well resolved factors, in contrast to the reviewer's opinion. Examples are the strong influence of the fireworks episode and the wind direction dependency. In addition, the high time resolution of the Ca and Si data set make the separation of two dust factors with distinct factor time series possible, while the traffic-related factor shows much stronger diurnal patterns, similar to BC and NO_x as compared to the road dust factor. The BC time series yields a strong correlation with the traffic-related factor (Pearson's $r = 0.86$) while it shows a weak correlation with the road dust factor ($r = 0.34$). The two fireworks factors are resolved due to difference in elemental ratios in the factors as well as based on the residual structure during fireworks days. Fig. 4 in the manuscript shows that we indeed need two fireworks factors to explain the time series of elements related to fireworks.

Source apportionment with receptor models is a routine technique and alone does not represent a scientific novelty. In addition, the application of these models with only trace elements does not fulfill the minimum requirements to obtain robust PM source apportionment because of the absence of important information to allocate the entire PM10 mass.

Some source apportionment applications may be regarded as a routine technique. This is mostly the case for standardized chemical mass balance (CMB) or positive matrix factorization (PMF). The use of partial constraints in ME-2, hybrids of CMB and PMF, is not routine. In addition, it has so far mostly been applied to the organic aerosol,

and much less to inorganic elements / metals. And, to reiterate, we did not attempt to allocate the entire mass to sources but rather a sub-fraction like it has been done frequently for the organic aerosol, but in this case mostly for trace elements which are partially specifically toxic.

SPECIFIC COMMENTS

Page 1 line 29: the literature about the health impacts of PM need to be improved.

We have already added several references for health impacts before line 29. We added a line in the manuscript on page 1 line 30 related to health impact of coarse fraction of PM as follows:

In Stockholm, Meister et al. (2012) estimated a 1.7% increase in daily mortality per 10 µg m^{-3} increase in coarse fraction of PM.

Meister, K., Johansson, C., and Forsberg, B.: Estimated short-term effects of coarse particles on daily mortality in Stockholm, Sweden, Environ. Health Perspect., 120, 431–436, https://doi.org/10.1289/ehp.1103995, 2012.

Page 3 line 6: the study by Park et al was carried out with XACT 620.

We have added in the text some more references in this paragraph as follows: "The Xact 620, 625 and the newer 625i ambient metals monitors (Cooper Environmental Services, Beaverton, Oregon, USA) based on XRF have been developed in recent years and have been used in several field studies (Fang et al., 2015; Cooper et al., 2010; Furger et al., 2017; Park et al., 2014; Phillips-Smith et al., 2017; Tremper et al., 2018; Chang et al., 2018; Liu et al., 2019; Ji et al., 2018). However, only six studies included SA on Xact data (Park et al., 2014; Fang et al., 2015; Phillips-Smith et al., 2017; Chang et al., 2018; Liu et al., 2019; Ji et al., 2018)."

Cooper, J. A., Petterson, K., Geiger, A., Siemers, A., and Rupprecht, B.: Guide for developing a multi-metals, fenceline monitoring plan for fugitive emissions using X-ray based monitors, Cooper Environmental Services, Portland, Oregon, 1–42, 2010.

Fang, T., Guo, H., Verma, V., Peltier, R. E., and Weber, R. J.: $PM_{2.5}$ water-soluble elements in the southeastern United States: automated analytical method development, spatiotemporal distributions, source apportionment, and implications for health studies, Atmos. Chem. Phys., 15, 11667–11682, https://doi.org/10.5194/acp-15-11667-2015, 2015.

Phillips-Smith, C., Jeong, C.-H., Healy, R. M., Dabek-Zlotorzynska, E., Celo, V., Brook, J. R., and Evans, G.:
Sources of particulate matter components in the Athabasca oil sands region: investigation through a comparison of trace element measurement methodologies, Atmos. Chem. Phys., 17, 9435–9449, https://doi.org/10.5194/acp-17-9435–2017, 2017.

Liu, Y., Zheng, M., Yu, M., Cai, X., Du, H., Li, J., Zhou, T., Yan, C., Wang, X., Shi, Z., Harrison, R. M., Zhang, Q., and He, K.: High-time-resolution source apportionment of $PM_{2.5}$ in Beijing with multiple models, Atmos. Chem. Phys., 19, 6595–6609, https://doi.org/10.5194/acp-19-6595-2019, 2019.

Ji, D., Cui, Y., Li, L., He, J., Wang, L., Zhang, H., Wang, W., Zhou, L., Maenhaut, W., Wen, T., and Wang, Y.: Characterization and source identification of fine particulate matter in urban Beijing during the 2015 Spring Festival, Sci. Total Environ., 430–440, 628–629, https://doi.org/10.1016/j.scitotenv.2018.01.304, 2018.

Page 6 line 2: is it reasonable to use 10% analytical uncertainty for all the species?

An estimated analytical uncertainty of 10% for all species has been used to derive the uncertainty data set in several previous studies (Kim et al., 2005; Kim and Hopke, 2007; Tian et al., 2016; Ji et al., 2018), which did not impact the interpretability of the PMF results. We also tried metal specific analytical uncertainty from Phillips-Smith et al. (2017) and Jeong et al. (2016) but it did not change the PMF results.

We have modified line 2 on page 6 as follows:

In this study, an estimated analytical uncertainty (p_j) of 10 % was used to derive the error matrix data set (Kim et al., 2005; Kim and Hopke, 2007; Tian et al., 2016; Ji et al., 2018), which did not change the PMF solution. The metal-specific analytical uncertainty was also considered from the previous studies (Jeong et al., 2016; Phillips-Smith et al., 2017), where it was calculated on the basis of high/medium-concentration metal standards laboratory experiments and the additional 5-10% flow rate accuracy, which yielded similar PMF solutions compared to an overall 10 % analytical uncertainty.

Kim, E., Hopke, P. K., and Qin, Y.: Estimation of organic carbon blank values and error structures of the speciation trends network data for source apportionment, J. Air Waste Manage. Assoc., 55, 8, 1190–1199, https://doi.org/10.1080/10473289.2005.10464705, 2005.

Kim, E. and Hopke, P. K.: source identifications of airborne fine particles using positive matrix factorization and U.S. environmental protection agency positive matrix factorization, J. Air Waste Manage. Assoc., 57, 7, 811–819, https://doi.org/10.3155/1047-3289.57.7.811, 2007.

Tian, S. L., Pan, Y. P., and Wang, Y. S.: Size-resolved source apportionment of particulate matter in urban Beijing during haze and non-haze episodes, Atmos. Chem. Phys., 16, 1–19, https://doi.org/10.5194/acp-16-1-2016, 2016.

Jeong, C.-H., Wang, J. M., and Evans, G. J.: Source Apportionment of Urban Particulate Matter using Hourly Resolved Trace Metals, Organics, and Inorganic Aerosol Components, Atmos. Chem. Phys. Discuss., https://doi.org/10.5194/acp-2016-189, 2016.

Ji, D., Cui, Y., Li, L., He, J., Wang, L., Zhang, H., Wang, W., Zhou, L., Maenhaut, W., Wen, T., and Wang, Y.: Characterization and source identification of fine particulate matter in urban Beijing during the 2015 Spring Festival, Sci. Total Environ., 430–440, 628–629, https://doi.org/10.1016/j.scitotenv.2018.01.304, 2018.

Phillips-Smith, C., Jeong, C.-H., Healy, R. M., Dabek-Zlotorzynska, E., Celo, V., Brook, J. R., and Evans, G.: Sources of particulate matter components in the Athabasca oil sands region: investigation through a comparison of trace element measurement methodologies, Atmos. Chem. Phys., 17, 9435–9449, https://doi.org/10.5194/acp-17-9435–2017, 2017.

Page 7 line 18: how do you know salt is from sea and not road salt?

This point is discussed later in the detailed presentation of the sea salt factor (section 4.2, "sea salt"). As mentioned in the manuscript the observed Mg / Na ratios for sea salt events (0.13 and 0.16) are in line with the expected ratio for marine aerosol (0.135 to 0.185). The measured Cl / K and Cl / Ca ratios (0.27 and 0.33 respectively) from Xact do not lie in the range of road salt snow samples (150±39 and 103±22, respectively) collected near the roadside (≤50 m) in the USA (Williams et al., 2000). The CBPF plot (Fig. 5) and backward trajectories (Fig. S11) also validate the occurrence of the sea salt event. Moreover, during summer (mean temperature 21 ^{0}C), we do not expect de-icing salt on the road.

We have added a line on Page 9 line 17 as follows:

The measured Cl / K and Cl / Ca ratios (0.27 and 0.33 respectively) from Xact do not lie in the range of road salt snow samples (150±39 and 103±22, respectively) collected near the roadside (≤50 m) in USA (Williams et al., 2000), which validates our interpretation as a sea salt factor.

Williams, A. L., Stensland, G. J., Peters, C. R., and Osborne, J.: Atmospheric dispersion study of deicing salt applied to roads: first progress report, Illinois State Water Surv. Contract Report, 2000-05, Champaign, IL, 2000.

Page 7 line 25: the expression factor composition is not clear. Do you mean factor profile?

Yes, the factor composition expression represents the factor profile. The mathematical expression for factor composition is mentioned in line 26 of that page. We replaced "factor composition" with "factor profile" to avoid confusion for readers.

Page 9 line 14: the comparison between the on-line and off-line data is not clear. In the text are mentioned 28th and 30th July but the Mg/Na ratio is similar to marine aerosol also on 31st July.

We apologize for the misunderstanding. Here we discuss the offline measurements of Na and Mg, which were not measured by the Xact, and their ratio in sea salt aerosols. The Mg / Na ratio on 31st July (0.28) does not lie in the range for marine aerosol but it is close to literature values (0.132 – 0.185). The sea salt factor time series as well as the time series of Cl from the Xact have a quite flat pattern on 31st July except for the fireworks peak at 23:00 LT with mostly south-east-north wind directions at low wind speeds (1–4 m s^{-1}) (Fig. S10) which may indicates the background concentration. In contrast, during the sea salt event, wind was mostly dominating from west directions at higher wind speeds (5–8 m s^{-1}).

We modified the text on Page 9 line 11 as follows:

Sea salt also includes Na and Mg, which were not measured by the Xact but analysed by ICP-OES for 24-h offline filters.

Page 9 line 21 and foll.: There is not clear evidence to prove there are two different dust factors. The diurnal profiles are almost overlapping (Figure 3) and in the scatter plot of fig S13 there is only one cloud of points. Also the CBPF plots in figure S8 show overlapping wind speed and directions. Soil dust should be farther from the origin than the more local road dust. Split of sources is a typical problem of using only elements in factor analysis source

apportionment. In addition, how do you know that Ca rich is road dust and not other sources? Enriched Ca dust is common in construction works, for instance.

The scatter plot of Si and Ca in Fig. S13 shows quite scattered data points which might be due to influence of more than one source especially during the end of the measurement period. Therefore, there is no strong correlation between Si and Ca elements (Pearson's r^2 0.56). The possible sources for Si and Ca could be the local and regional transport of crustal material partly re-suspended by traffic (south sector) and partly originating from the agricultural area north of the freeway. The factor time series of both factors are not identical except for a few overlapping points. The road dust diurnal pattern shows a maximum traffic rush hour peak similar to NO_x, black carbon (BC), heavy duty vehicle (HDV) count and the traffic-related factor while the background dust factor has no spikes in the diurnals (Fig. 3). Also our interpretation brackets the road dust factor because the road dust resuspension in the road side environment is primarily traffic induced. We have added the modified CBPF plots as well as an explanation about two dust factors in the 2nd referee's general comments section. However we would like to add that the agricultural land immediately to the west and north direction and another freeway (A2) in the northwest direction from the sampling location might be the reason for background dust in the CBPF plot.

We agree that Ca dust is also possible from construction dust. But this hypothesis does not support the Ca rich factor diurnal pattern when we assume that this kind of sources peaked during the day and decreased to almost zero outside of normal working times (08:00 until 17:00 LT). We also found that there is only a weak correlation in the hourly concentrations between Ca and S. If calcium sulfate dihydrate is the main compound in gypsum used for construction work, Ca and S should show a better correlation. The weak correlation could be possible due to the contribution from different sources for Ca (road dust) and S (ammonium sulfate). During the Ca peaks, ACSM PM_1 sulfate and ammonium did not show high peaks. However, comparing the ACSM PM_1 sulfate with PM_{10} S may not be direct because of the existence of coarse sulfate in the form of calcium sulfate. Pure gypsum typically contains 29.4% Ca and 23.5% S, resulting in an elemental ratio of 1.25 which was not found in our measurements except one data point.

We added the text in the manuscript as follows on page 10 line 1:

Ca has been associated with construction activities in previous studies (Bernardoni et al., 2011; Crilley et al, 2016), which have been found to peak during the day and decreased to almost zero outside of normal working times (08:00 until 17:00 LT). This evidence is not supported by the road/background dust factor diurnal pattern in this study. Further evidence of non-construction activity is found in the Xact elemental ratio of Ca / S (0.62) which is not in the agreement with the pure gypsum Ca / S ratio (1.25) used for construction work (Hassan et al., 2014), where they are the main constituents.

Bernardoni, V., Vecchi, R., Valli, G., Piazzalunga, A., Fermo, P.: PM_{10} source apportionment in Milan (Italy) using time-resolved data, Sci. Total Environ., 409, 4788–4795, https://doi.org/10.1016/j.scitotenv.2011.07.048, 2011.

Crilley, L. R., Lucarelli, F., Bloss, W. J., Harrison, R. M., Beddows, D. C., Calzolai, G., Nava, S., Valli, G., Bernardoni, V., and Vecchi, R.: Source apportionment of fine and coarse particles at a roadside and urban background site in London during the 2012 summer ClearfLo campaign, Environ. Pollut., 220, 766–778, https://doi.org/10.1016/j.envpol.2016.06.002, 2016.

Hassan, A. K., Fares, S., and Abd El-Rahma, M.: Natural radioactivity levels and radiation hazards for gypsum materials used in Egypt, J. Environ. Sci. Technol., 7, 56–66, https://doi.org/10.3923/jest.2014.56.66, 2014.

Page 9 line 25: only the Ca scaled residuals improve not those of Si.

The Si scaled residual was also improved a bit (from 6 to 4). Increasing the number of factors further did not improve the Si scaled residual structure.

Page 10 line 17 and foll.: The chemical composition of this factor indicates brake wear mixed to the re-suspended particles as Fe and Si are components of crustal material. Again there is an overlapping in the chemical composition with the so called road dust profile and these two profiles also have very similar diurnal profiles.

Although Fe and Si are components of crustal material, both can be emitted from anthropogenic sources as well. The diurnal pattern of Fe shows traffic rush hour peaks while Si diurnal cycle is not as prominent as Fe. The sources of Fe are already discussed in the manuscript. We added a sentence for Si in the manuscript. If the road dust factor is attributable mainly to abrasion of the road surface and tires, and the resuspension by traffic vortices, a similar diurnal pattern with the traffic-related factor would be expected.
We have added the following text in the manuscript on page 10 line 24:
Si is one of the brake lining components used as abrasive to increase friction, and as fillers to reduce manufacturing costs, respectively (Thorpe and Harrison, 2008; Grigoratos and Martini, 2015).
Thorpe, A. and Harrison, R. M.: Sources and properties of non-exhaust particulate matter from road traffic: A review, Sci. Total Environ., 400, 270–282, https://doi.org/10.1016/j.scitotenv.2008.06.007, 2008.
Grigoratos, T. and Martini, G.: Brake wear particle emissions: a review, Environ. Sci. Pollut. Res., 22, 2491–2504, https://doi.org/10.1007/s11356-014-3696-8, 2015.

Page 10 line 29: the secondary sulfate does not provide any evidence to allocate the ammonium nitrate (another main secondary inorganic component of PM).

Yes, we agree with reviewer#1 that it does not provide evidence to allocate the ammonium nitrate but this is not what we are attempting in this paper. It is outside the scope of this paper to perform an ACSM PMF analysis.

Page 11 line 8: The characterization of the industrial source is weak. There is no connection to any known industrial process. The fact that other studies in completely different areas found the same profile is not proving the industrial origin of this factor. On the contrary, it is unlikely that the same industrial process is present in many different sites.

This factor time series contains a few spikes which correlate with wind direction, indicating a local point source. Based on this hypothesis, we interpreted this factor as industrial source. The other previous studies are mentioned to represent similar factor profiles from local point sources without a specific industrial emission.

We have modified the text in the manuscript on page 11 line 11:

A similar factor profile was observed in previous source apportionment studies (Crilley et al., 2016; Richard et al., 2011) from local point source emissions without any link to specific industrial activities. Amato et al. (2010) and Dall'Osto et al. (2013) also reported a PMF factor with high concentrations of Zn and Pb and attributed it to emissions from smelters in Barcelona, while Vossler et al. (2016) reported a similar factor profile from coal combustion processes in Ostrava.

Crilley, L. R., Lucarelli, F., Bloss, W. J., Harrison, R. M., Beddows, D. C., Calzolai, G., Nava, S., Valli, G., Bernardoni, V., and Vecchi, R.: Source apportionment of fine and coarse particles at a roadside and urban background site in London during the 2012 summer ClearfLo campaign, Environ. Pollut., 220, 766–778, https://doi.org/10.1016/j.envpol.2016.06.002, 2016.

Richard, A., Gianini, M. F. D., Mohr, C., Furger, M., Bukowiecki, N., Minguillón, M. C., Lienemann, P., Flechsig, U., Appel, K., DeCarlo, P. F., Heringa, M. F., Chirico, R., Baltensperger, U., and Prévôt, A. S. H.: Source apportionment of size and time resolved trace elements and organic aerosols from an urban courtyard site in Switzerland, Atmos. Chem. Phys., 11, 8945–8963, https://doi.org/10.5194/acp-11-8945-2011, 2011.

Amato, F., Nava, S., Lucarelli, F., Querol, X., Alastuey, A., Baldasano, J. M., and Pandolfi, M.: A comprehensive assessment of PM emissions from paved roads: Real-world emission factors and intense street cleaning trials, Sci. Total Environ., 408, 4309–4318, https://doi.org/10.1016/j.scitotenv.2010.06.008, 2010.

Dall'Osto, M., Querol, X., Amato, F., Karanasiou, A., Lucarelli, F., Nava, S., Calzolai, G., and Chiari, M.: Hourly elemental concentrations in $PM_{2.5}$ aerosols sampled simultaneously at urban background and road site during SAPUSS – diurnal variations and PMF receptor modelling, Atmos. Chem. Phys., 13, 4375–4392, https://doi.org/10.5194/acp-13-4375-2013, 2013.

Vossler, T., Černikovský, L., Novák, J., and Williams, R.: Source apportionment with uncertainty estimates of fine particulate matter in Ostrava, Czech Republic using positive matrix factorization, Atmos. Pollut. Res., 7, 503–512, https://doi.org/10.1016/j.apr.2015.12.004, 2016.

Figure 4: Not clear what is the added value of this figure with respect to figure 1. Normalized concentration (should be explained in the caption). Why use different units than the other graphs. The percentile box and whisker and the mean -+SD overlaps making the graph difficult to read. Choose one.

PMF results (Fig. 1) describe potentially complex and time-dependent sources as a single factor (or linear combination of factors). This is a fundamental limitation of the model, and may not accurately describe the behaviour or a complex source (e.g., residuals may be significant). In contrast, Fig. 4 provides an estimate of the overall fireworks composition and temporal variability, complementing the PMF results (which are shown for reference). One can then see both the explanatory power and limitations of the SA model for this source.

We moved Fig. 4 to the supplement and removed ± SD from the figure.

We added in the supplement on page 8 line 6:

Fig. S8 provides an estimate of the overall fireworks composition and temporal variability, complementing the PMF results (which are shown for reference). The figure is constructed in two stages. First, the time series of fireworks

contributions to each element is estimated by subtracting the non-fireworks factors (NFF) from the original measurements. Then, the estimated fireworks contribution for each element is normalized by the total fireworks element contribution, and the displayed statistics are calculated. This is represented mathematically below, and the expression has been added to the main text. Note that the variation in fireworks profiles implied by this figure supports the representation of fireworks by 2 fireworks factors.

$$normalized\ concentration_{ij} = \frac{x_{ij} - \left(g_{ik} f_{kj}\right)_{k=NFF}}{\sum_j \left(x_{ij} - \left(g_{ik} f_{kj}\right)_{k=NFF}\right)} \quad \text{(S1)}$$

where X represents the input data matrix for PMF, while G and F represent the factor time series and factor profiles driven by six non-fireworks factors (NFF). Here *i* and *j* denote time series and variables, respectively.

Figure S9: the connection between this data and the days with high "sea salt" is not clear in this figure. It should be better evidenced to allow the reader evaluating if there is a difference between the days with high sea salt and those without it.

We apologise for the misunderstanding. Fig. S9 only shows the Mg / Na ratio for 24-h filter data analysed by ICP-OES along with the literature Mg / Na ratio (0.132 - 0.185) in marine aerosols. In this figure, we presented the existence of sea salt events and non-sea salt events. The sea salt factor time series with high and low concentrations is already shown in Fig.1 and discussed in the manuscript.

We added a line in the caption of Fig. S9 caption on page 9 line 5:

The Mg / Na ratio was 0.13 and 0.16 for 28 July and 30 July, respectively while for the rest of the days it was higher than 0.185.

TECHNICAL CORRECTIONS

Figure S6: not clear why the p25 is a single point while the p75 is a vertical line.

We modified Fig. S6.

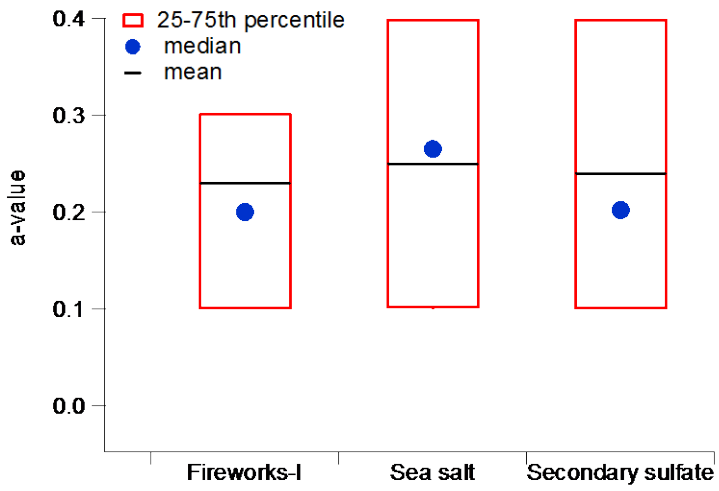

Figure S6: *a*-value statistics of the accepted solutions. *a*-values between 0 to 0.5 were explored during BS analysis. The average *a*-value of the selected solutions was ranging from 0.2 to 0.3 for the constrained factors. The selected *a*-values were homogeneously distributed over that range.

Response to Reviewer #2

We kindly thank the reviewer#2 for taking our manuscript into consideration and we value the comments raised to improve the manuscript. A point-by-point answer (in regular typeset) to the reviewers' remarks (in italic typeset) follows. Changes to the manuscript are indicated in blue font.

In the following page and lines references refer to the manuscript version reviewed by anonymous Reviewer#2.

This paper examines data previously reported by Furger et al (2017) applying PMF source apportionment techniques to a subset of the reported data to provide insight into the chemical composition of different sources. It focuses on firework / burning sources associated with local celebrations (which are a common influence on air quality for short periods in many countries) and to a lesser extent on suspended dust from road and surface sources. The article is generally well written and the approach is methodologically robust. However, the data used is somewhat limited and the authors have not taken advantage of the aerosol mass spectrometer data which was available. I have many suggested edits and some points which require consideration by the authors.

Major Comments –

Pg 5, line 16 – the authors reduce the data set from 24 to 14 based on manufacturer supplied MDLs to produce 'better' source apportionment results. Firstly, even though the measurements are below the detection limit, they could contain 'valuable' information on variability, especially during firework periods as some of the excluded elements are potential firework components (e.g. Cd). They have been excluded based on %below MDL at a rather arbitrary value e.g. Bi at 93% was included while Cd at 87% was not. It would be worth including this data and downweighting rather that excluding it or at least performing sensitivity test. A further 4 elements are excluded based on data quality but no detail on what constitutes data quality is given.

We agree with reviewer#2 and therefore we had included Bi which shows fireworks peaks while for the rest of time it is below MDL. We inspected all the elements before preparing the PMF input data based on MDL. V, Co, As, Se, Cd and Pt were close to or below their Xact MDL. The inter-comparison of Xact vs ICP data for Co, Ni, As, Se, Cd and Hg was not justified based on the weak correlation (r^2). Pt was below MDL (98%), and it was not measured on the filters, therefore no conclusion about the Pt accuracy can be drawn. We did not find any fireworks peaks for any of these elements. The detailed discussion on Xact data quality is described in more detail in the previous study (Furger et al., 2017).

We modified the text on Pg 5 line 20:

Elements (% of data points below MDL, r^2 value) which had more than 50 % of data points below MDL and low r^2 (0.5) between Xact and offline data were not included in the PMF input, such as: V (98 %, 0.57), Co (100 %, 0.05), Ni (32 %, 0.22), As (96 %, 0.5), Se (62 %, 0.3), Cd (87 %, 0.18), Sn (15 %, 0.27), Sb (6%, 0.42), Hg (13 %, 0.12) and Pt (98 %, not measured on the filters). The element Bi (93% data points below MDL) was an exception to include in the PMF input due to an excellent correlation between Xact and offline data (r^2 = 0.98) during fireworks peaks. The detailed description of the Xact data quality is given in the previous study (Furger et al., 2017).

Furger, M., Minguillón, M. C., Yadav, V., Slowik, J. G., Hüglin, C., Fröhlich, R., Petterson, K., Baltensperger, U., and Prévôt, A. S. H.: Elemental composition of ambient aerosols measured with high temporal resolution using an online XRF spectrometer, Atmos. Meas.Tech., 10, 2061–2076, https://doi.org/10.5194/amt-10-2061-2017, 2017.

Pg 8 Line 4 and later – The CBPF is an important analysis which is used to justify the identification of sources and the charts should not be shunted to the appendix. Further, the reliance on 90th percentile to identify the sources is flawed when considered on its own, especially when the distribution of measurements is heavily skewed (as it is with Cl). A range of CBPFs should be presented (at least in the supplementary) to support the interpretation. The authors should also consider the use of the min bin statistic to ensure that individual points are not skewing the interpretation. Finally, the conclusion that the two dust sources are from different sources (based on these plots) when their direction is broadly similar is rather weak.

We agree that it would be helpful moving the CBPF plots from the Supplement to the main manuscript. We presented a range of CBPF plots in the supplementary for these four factors (as shown in the figure below). We partially agree with reviewer#2 for min bin statistics. The min bin parameter provides the minimum number of points required to provide a result in a wind speed/wind direction bin and is 1 in this analysis. If we set it >1, there is the risk of removing real data. Concerning the two dust factors, comparing the two CBPF ranges, there are indeed differences in terms of source directions. The road dust factor is quite consistent with southerly winds except for a few low concentration data points (at the 50th percentile) while the background dust source direction is quite variable for different ranges of data.

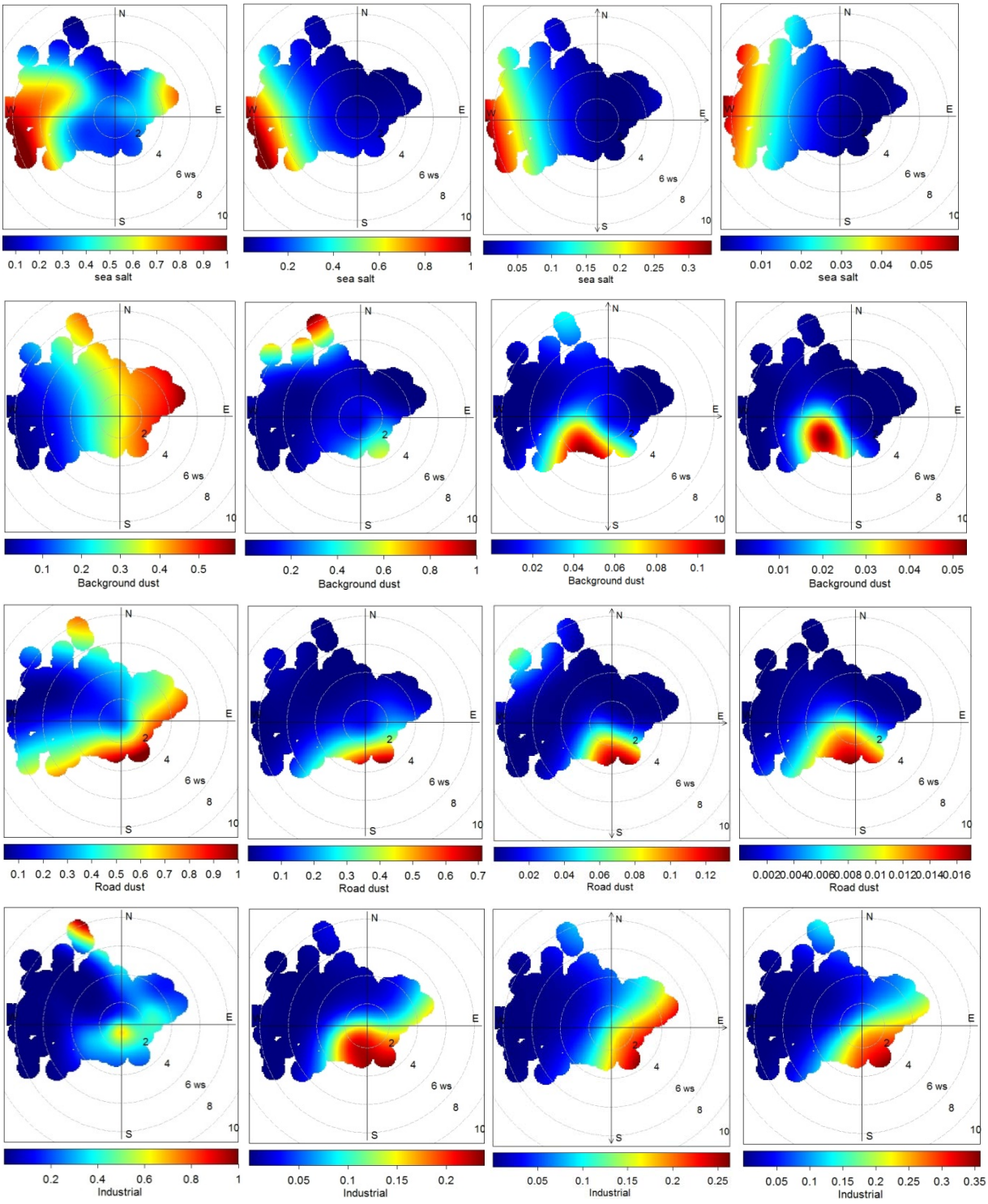

Figure S16: CBPF analysis (from left to right: 50th, 75th, 90th, 95th percentiles) of factors (sea salt, background dust, road dust, industrial) in terms of wind speed (m s^{-1}) and wind direction. The color code represents the probability of the factor contribution.

Pg 8 Line 9 and later – KNO3 is quoted as comprising 74% of fireworks. In which case NO3 could be a useful tracer for unburnt firework material - it was measured but is not reported. A recognition of this point, even to say that there was no correlation would help. The same is true of the other mass concentrations and m/z measured by the ACSM – were these examined or even considered for inclusion in the PMF or data analysis?

We added a figure in the supplement to show the ACSM inorganics concentration along with NO_2 and NO_x during the fireworks episode. From the figure it is very obvious that neither particulate nitrate nor ammonium is generated in the fireworks in significant amounts. The ACSM nitrate showed a quick drop immediately before the main fireworks (1 August 2015 23:00 LT). The sulphate peaks coincide with a strong drop of the nitrate concentration, which indicates that ammonium nitrate may have reacted with sulfuric acid, releasing nitric acid to the gas phase. The absence of fireworks nitrate has been observed previously (Drewnick et al., 2006) and indicates that most of the black powder nitrate is converted to other forms of nitrogen species. We calculated the measured NO_2 / K mass ratio for enhanced NO_2 concentration during the fireworks based on K concentration. The ratio was 1.66 on the main fireworks hour (1 August 23:00 LT) which is close to the atomic ratio of NO_2 / K (1.17). This measured ratio is in-line with the NO_2 / K^+ (2.03) ratio measured during Chinese Spring Festival in Shanghai (Yao et al., 2019).
We have added the following text in the revised manuscript on pg8 line 10:
The ACSM inorganics concentrations during the fireworks episodes indicate that neither particulate nitrate nor ammonium is generated in the fireworks in significant amounts (Fig. S7). Consistent with previous measurements of submicron fireworks aerosol (Drewnick et al., 2006; Vecchi et al., 2008; Jiang et al., 2015), nitrate was not enhanced during the fireworks period, suggesting conversion of KNO_3 to other forms of nitrogen. The NO_2 / K mass ratio (1.66) on the main fireworks hour (1 August 23:00 LT) is close to the atomic ratio of NO_2 / K (1.17). This measured ratio is also in agreement with the NO_2 / K^+ (2.03) ratio observed during Chinese Spring Festival in Shanghai (Yao et al., 2019). However, the NO_2 and/or NO_x variation was not significant during the fireworks peaks in the present study (Fig. S7), which is in agreement with the former studies (Vecchi et al., 2008; Retama et al., 2019; Yao et al., 2019).

Drewnick, F., Hings, S. S., Curtius, J., Eerdekens, G., and Williams, J.: Measurement of fine particulate and gas-phase species during the New Year's fireworks 2005 in Mainz, Germany, Atmos. Environ., 40, 4316–4327, https://doi.org/10.1016/j.atmosenv.2006.03.040, 2006.

Vecchi, R., Bernardoni, V., Cricchio, D., D'Alessandro, A., Fermo, P., Lucarelli, F., Nava, S., Piazzalunga, A., and Valli, G.: The impact of fireworks on airborne particles, Atmos. Environ., 42, 1121–1132, https://doi.org/10.1016/j.atmosenv.2007.10.047, 2008.

Jiang, Q., Sun, Y. L., Wang, Z., and Yin, Y.: Aerosol composition and sources during the Chinese Spring Festival: fireworks, secondary aerosol, and holiday effects, Atmos. Chem. Phys., 15, 6023–6034, https://doi.org/10.5194/acp-15-6023-2015, 2015.

Yao, L., Wang, D., Fu, Q., Qiao, L., Wang, H., Li, L., Sun, W., Li, Q., Wang, L., Yang, X., Zhao, Z., Kan, H., Xian, A., Wang, G., Xiao, H., and Chen, J.: The effects of firework regulation on air quality and public health during the Chinese Spring Festival from 2013 to 2017 in a Chinese megacity, Environ. Int., 126, 96–106, https://doi.org/10.1016/j.envint.2019.01.037, 2019.

Retama, A., Neria-Hernández, A., Jaimes-Palomera, M., Rivera-Hernández, O., Sánchez-Rodríguez, M., López-Medina, A., and Velasco, E.: Fireworks: a major source of inorganic and organic aerosols during Christmas and New Year in Mexico city, Atmos. Environ., 2, 100013, https://doi.org/10.1016/j.aeaoa.2019.100013, 2019.

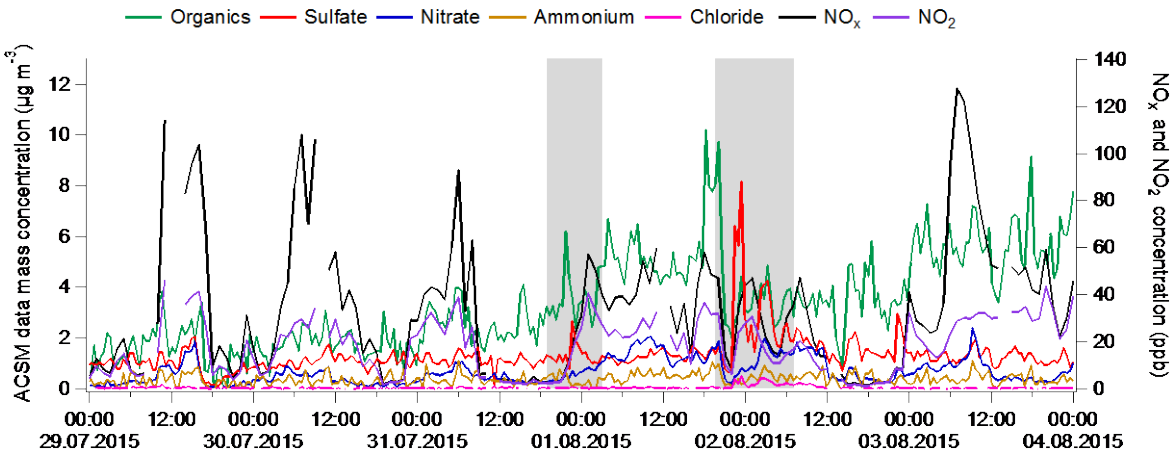

Figure S7: Time series of the non-refractory aerosol components (measured with the ACSM), NO_2 and NO_x concentration. The fireworks episodes are underlain in grey color.

Line 29 and later – The use of SoFi to separate highly correlated sources such as the two firework sources is the reason for this paper. The consideration of Cl displacement is interesting and has evidence to support it, why does it therefore come after 2 purely speculative thoughts about possible alternative sources. Promote this point and consider the speculations as alternatives. One of these - the separation of bonfires from fireworks may have been helped by considering the ACSM data.

We have rearranged the text from line 26 onwards as follows:

Chemical reactions of KCl with H_2SO_4 will result in a release of gaseous HCl and may explain the absence of particulate Cl in the fireworks-II factor profile. The time series variations in both fireworks suggest that fireworks-I might be related to the main fireworks celebration while fireworks-II might result from burning of leftover crackers after the main fireworks day, as well as the influence of other sources such as bonfires, which are a common activity during Swiss National Day celebrations. Another possibility could be the advection of fireworks clouds from nearby cities where grand firework displays and bonfires are carried out at large scale to celebrate the Swiss National Day.

General Comment-

The authors use the term 'trace' elements. I would not consider S or Fe trace elements in ambient PM. I suggest the authors just refer to them as elements.

We removed "trace" from the manuscript.

Pg 1 Line 13 - Source Finder software, please quote version number, supplier and country
Done.

Line 19 - The abstract is partly written in the present tense – 'experiences' should read 'experienced', 'concentrations are similar' should read 'concentrations were similar'

We corrected the grammatical error in abstract.
Further, there were minor contributions (on the order of a few percent) of sea salt and industrial sources. The regionally influenced secondary sulfate factor showed negligible resuspension, and concentrations were similar throughout the day. The significant loads of the traffic-related and road dust factors with strong diurnal variations highlight the continuing importance of vehicle-related air pollutants at this site.

Pg 2 Line 29 – clarify that you are talking about off line sampling systems

We added the word "offline" in the text.

Line 33 – the sampler don't specifically need those analysis techniques, they require techniques with high precision and low detection limits – such as these methods

We modified this line as follows:
These offline analyses require high precision and low detection limit techniques such as synchrotron radiation induced X-ray fluorescence spectrometry (SR-XRF) of aerosol samples collected with a RDI, particle induced X-ray emission (PIXE) with the streaker sampler and graphite furnace atomic absorption spectrometry (GFAAS) with the SEAS.

Pg 3 Line 28 – delete XACT manufacturer already provided line 4
Done.

Line 30 – with should read at Line 31 onwards – be consistent with how you name equipment – model, make, supplier, country
Done.

Line 31 – quote filter manufacturer
Done.

Pg 4 Line 2 – TEOM and FDMS in full then in brackets or just the abbreviation, not a mixture
Done.

Line 20 – can values be applied to individual data points; this implies that individual points can be used for a-value constraining. Is this true? Certain sections in a time series can but individual points cannot be separated out in this way.

Yes, it is possible to apply an *a*-value on individual data points because PMF renormalizes the factors at the end.

Line 28 – this is not the first use of sofi in the manuscript - the reference, version number and supplier should go there.

Done, except reference. The first use of SoFi is in the abstract section. One should not use references in the abstract.

Pg 5 Line 1 – 'PMF' rather than 'model'
Done.
Line 4 – 'identify' rather than 'find'
Done.
Line 4 – this only helps to identify the high concentration peaks and whether then influence the mean will depend on the distribution of data (see Cl results in fig 4)

We partially agree with the reviewer#2. CBPF gives directional information of sources contributing to pollutant concentrations at the sampling site.

Line 22 – Bi a major component of fireworks –a reference, some evidence would be good here and even justify the exclusion of other elements.

We deleted Bi a major tracer of fireworks from line 22 and added the reference for Bi on Pg8 line 12. Concerning exclusion of elements, please see the response in the major comments section.
We added a sentence on Pg 8 line 12 as follows:
Bi is used in crackling stars (Dragon's eggs) in the form of bismuth trioxide or subcarbonate as a non-toxic substitute for toxic lead compounds (Perrino et al., 2011).
Perrino, C., Tiwari, S., Catrambone, M., Torre, S. D., Rantica, E., and Canepari, S.: Chemical characterization of atmospheric PM in Delhi, India, during different periods of the year including Diwali festival, Atmos. Pollut. Res., 2, 418–427, https://doi.org/10.5094/apr.2011.048, 2011.

Pg 6 Line 1 - need a description on xij
Done.

Line 16 – listed s1-s4 but only s2 and s3 relate to this point

We removed S1, S2 and S4 according to text change in the revised manuscript.

Pg 7 Line 18 – how do you know it is coarse Cl, you have two measures of Cl one is non-refractory Cl- in PM1 and one is Cl in PM10?

We replaced "coarse" with PM_{10} in line 18.

Pg 8 Line 6 –are these elements really the main components of fireworks by mass, surely you need a reference here to justify this.

The fireworks factors are mostly dominated by K, S, and Cl, among the elements analysed here. Moreover, Ti, Cu, Ba and Bi are key tracers of these factors.

We have added references in line 6:

(Moreno et al., 2007; Wang et al., 2007; Vecchi et al., 2008; Perrino et al., 2011; Tian et al., 2014; Kong et al., 2015; Lin, 2016; Pongpiachan et al., 2018).

Moreno, T., Querol, X., Alastuey, A., Minguillón, M. C., Pey, J., Rodriguez, S., Miró, J. V., Felis, C., and Gibbons, W.: Recreational atmospheric pollution episodes: Inhalable metalliferous particles from firework displays, Atmos. Environ., 41, 913–922, https://doi.org/10.1016/j.atmosenv.2006.09.019, 2007.

Perrino, C., Tiwari, S., Catrambone, M., Torre, S. D., Rantica, E., and Canepari, S.: Chemical characterization of atmospheric PM in Delhi, India, during different periods of the year including Diwali festival, Atmos. Pollut. Res., 2, 418–427, https://doi.org/10.5094/apr.2011.048, 2011.

Wang, Y., Zhuang, G., Xu, C., and An, Z.: The air pollution caused by the burning of fireworks during the lantern festival in Beijing, Atmos. Environ., 41, 417–431, https://doi.org/10.1016/j.atmosenv.2006.07.043, 2007.

Vecchi, R., Bernardoni, V., Cricchio, D., D'Alessandro, A., Fermo, P., Lucarelli, F., Nava, S., Piazzalunga, A., and Valli, G.: The impact of fireworks on airborne particles, Atmos. Environ., 42, 1121–1132, https://doi.org/10.1016/j.atmosenv.2007.10.047, 2008.

Kong, S. F., Li, L., Li, X. X., Yin, Y., Chen, K., Liu, D. T., Yuan, L., Zhang, Y. J., Shan, Y. P., and Ji, Y. Q.: The impacts of firework burning at the Chinese Spring Festival on air quality: insights of tracers, source evolution and aging processes, Atmos. Chem. Phys., 15, 2167–2184, https://doi.org/10.5194/acp-15-2167-2015, 2015.

Lin, C.-C.: A review of the impact of fireworks on particulate matter in ambient air, J. Air Waste Manage. Assoc., 66, 12, 1171–1182, https://doi.org/10.1080/10962247.2016.1219280, 2016.

Pongpiachan, S., Iijima, A., and Cao, J.: Hazard quotients, hazard indexes, and cancer risks of toxic metals in PM_{10} during firework displays, Atmosphere, 9, 144, https://doi.org/10.3390/atmos9040144, 2018.

Tian, Y. Z., Wang, J., Peng, X., Shi, G. L., and Feng, Y. C.: Estimation of the direct and indirect impacts of fireworks on the physicochemical characteristics of atmospheric PM_{10} and $PM_{2.5}$, Atmos. Chem. Phys., 14, 9469–9479, https://doi.org/10.5194/acp-14-9469-2014, 2014.

Line 7 – chlorate and perchlorate (line 11) will also be detected as Cl in XRF

Indeed, the Xact measures total chlorine including all particulate Cl compounds such that we cannot distinguish them with the Xact measurements.

Line 16 – the sentence starting 'A pronounced: : :) should really come at te start of the para
Done.

Line 29 – this consideration of Cl displacement is interesting and at has evidence to support it, why does it therefore come after 2 purely speculative thoughts. Promote this point and consider the speculations as alternatives.

Please see the response above in the major comment.

Pg 11 – line 6 – there is no fig S12

We corrected it as Fig. S9.

Response to Reviewer #3

We kindly thank the reviewer#3 for taking our manuscript into consideration and we value the comments raised to improve the manuscript. A point-by-point answer (in regular typeset) to the reviewers' remarks (in italic typeset) follows. Changes to the manuscript are indicated in blue font.
In the following page and lines references refer to the manuscript version reviewed by anonymous Reviewer#3.

The paper "Source apportionment of highly time resolved trace elements during a firework episode from a rural freeway site in Switzerland" by Rai et al. deals with Positive Matrix Factorization analysis of a dataset of 1-h resolved trace elements. Despite the authors declare the existence of much more information on high time resolved scale (mass concentration by TEOM, equivalent black carbon by MAAP, ACSM data), they carried out the analysis on elements only. This limits strongly the information provided by the study (e.g. they can apportion only the mass related to elements, that they estimated to be about 20% of PM10 mass). Thus, the results cannot be representative of the total contribution of the sources to the measured PM. Furthermore, lots of constraints were implemented to reach the final solution. In some cases, both source profiles and temporal trends were constrained. So many constraints to the model make questionable the validity of the results, also considering that these constraints are not adequately supported by a methodological description of the way they were obtained, as explained in more detail

below. Whether the paper is well structured and well written in most parts (even if some obscure descriptions remain), the scientific aspect is not fully convincing.

Major concerns:

Page 5, line 15: excluding mass data (mentioned at p.4 l.2) should be carefully discussed as it strongly reduces the interest of the results, preventing an absolute quantification of the factor contributions to the measured PM. Furthermore, maybe the authors decided to analyse separately ACSM data, but at least equivalent BC information could be of help in source resolution.

This issue was also raised by Reviewer #2 (major comments section) and our response is presented in both places for clarity. The exclusion of elements was done based on online (Xact 625) and offline (ICP analysis) elemental quality comparison as discussed in Furger et al. (2017). We modified the text on Pg 5 line 20:

Elements (% of data points below MDL, r^2 value) which had more than 50 % of data points below MDL and low r^2 (0.5) between Xact and offline data were not included in the PMF input, such as: V (98 %, 0.57), Co (100 %, 0.05), Ni (32 %, 0.22), As (96 %, 0.5), Se (62 %, 0.3), Cd (87 %, 0.18), Sn (15 %, 0.27), Sb (6%, 0.42), Hg (13 %, 0.12) and Pt (98 %, not measured on the filters). The element Bi (93% data points below MDL) was an exception to include in the PMF input due to an excellent correlation between Xact and offline data (r^2 = 0.98) during fireworks peaks. The detailed description of the Xact data quality is given in the previous study (Furger et al., 2017).

Concerning ACSM and BC data, the same issue was also raised by Reviewer#1 and Reviewer#2. We repeat here the same. In our opinion, the combination of PM_1 data for Q-ACSM, $PM_{2.5}$ for MAAP and PM_{10} data for Xact may introduce artefacts in the ME-2 analysis. We have used NO_x, MAAP and Q-ACSM data sets in the manuscript to compare some of the ME-2 factor time series and diurnal patterns. We are not planning to publish a separate paper on the other data. A major focus was the exploration of the use of the Xact for source apportionment of inorganic elements / metals in Europe where the concentrations are considerably lower than in polluted areas in Asia.

Furger, M., Minguillón, M. C., Yadav, V., Slowik, J. G., Hüglin, C., Fröhlich, R., Petterson, K., Baltensperger, U., and Prévôt, A. S. H.: Elemental composition of ambient aerosols measured with high temporal resolution using an online XRF spectrometer, Atmos. Meas.Tech., 10, 2061–2076, https://doi.org/10.5194/amt-10-2061-2017, 2017.

Page 6, lines 11-12. "The unconstrained PMF solutions yielded mixed factor solutions. Therefore, it was essential to constrain specific factor profiles and the time series in the PMF analysis to avoid mixing (see details in the Supplement, section S1, Fig. S1)". This is the weakest aspect of all. The way in which the factor profiles/time series are constrained is the key point for all the rest of the analysis. Constraints determination strongly affects the final results (see described differences between the preliminary analysis and the constrained one) and merits detailed description and attention. Opposite, its description was moved to the Supplemental Material, and what is reported there is a not sufficient to determine the robustness of the approach. The following information should have been provided: 1) How many factors were present in the final analyses of the fireworks and non-fireworks periods? 2) Were the sources other than fireworks and sea-salt comparable between the datasets? (In terms of profile and tracer

species?) 3) Were 2 firework-related factors identified in the analysis of the firework-days subset? 4) What about the residual of S in the unconstrained 9 factor solution? 5) The need to constrain both profile and temporal trend of the sulphate source is very suspicious (the whole "secondary sulfate" factor was constrained in the final solution).

We agree with the reviewer#3. We have rewritten the section S1 below and we moved this section into the main text. However, we would like to respond point by point to the reviewer's five questions.

The input data set was divided into two parts: fireworks days (FD; 31 July–4 August) and non-fireworks days (NFD; all days except 31 July–4 August). To obtain a specific fireworks profile, we further selected only fireworks hours (FH; 31 July 21:00–1 August 07:00 LT) as PMF input data. The PMF analysis was performed on the NFD, FD, FH and the complete datasets separately for three to ten factors, with each of these solutions investigated with ten seeds (each seed represents a different pseudorandom initialization).

1) Seven factors were resolved in the NFD PMF analysis while a five-factor solution was identified in the FH PMF analysis.
2) The unconstrained NFD PMF analysis resolved factors such as sea salt, secondary sulfate, traffic-related, road dust, background dust, industrial and a K-rich factor. The FD and FH constrained PMF analyses resolved a five-factor solution with secondary sulfate, sea salt, fireworks, background dust and a K-rich factor with fireworks related elements. The traffic-related and road dust factors were resolved in FD and FH PMF analyses in seven and eight-factor solution, which were comparable to NFD PMF analysis. The fireworks factor contribution was going down in seven and eight-factor solution than the five-factor solution. The industrial factor in the FD and FH PMF analysis was resolved in eight-factor solution where it was mainly characterised by high contribution to Pb (67 %) and Zn (30 %) whereas in NFD PMF analysis the relative contribution to Pb and Zn were 90 % and 87 %, respectively.
3) The FD and FH constrained PMF analyses identified two fireworks-related factors, which were comparable to the final two fireworks-related factors profiles.
4) The scaled residual of S in the unconstrained nine-factor solution was between -0.46 and 0.85.
5) We tested several approaches for the secondary sulfate constraint: a) constraining only the profile; b) constraining only the time series to preserve secondary sulfate temporal trend during fireworks; c) constraining the entire time series along with factor profile; d) constraining the factor profile together with a segment of the time series (i.e., only during fireworks days). From all the above four tests, unmixed secondary sulfate was possible only in case of c and d, and we prefer the approach in d as it provides maximum freedom to the algorithm. We suggest that the need to constrain both the profile and part of the time series is driven by the very high concentration and variation in composition during the fireworks period. Because the signal-to-noise is very high, imperfections in the model description exert a strong influence on Q, and the model therefore tries to compensate by assigning fireworks mass to other factors. The double constraint tactic in d avoids this problem, while minimizing overall constraints on the solution.

These points, as well as the requested general information regarding the PMF analysis, are added to the manuscript beginning at Page 6 line 9:

In a first step, we examined a range of solutions with three to ten factors at ten seeds (number of PMF repeats) from unconstrained runs. The unconstrained PMF solution resulted in mixed factors, such as sea salt mixed with fireworks, even for higher numbers of factors (Fig. S1). This is likely because of the very high concentration and variation in composition of fireworks emissions during the fireworks period. Because the signal-to-noise is very high, imperfections in the model description exert a strong influence on *Q*, and the model therefore tries to compensate by assigning fireworks mass to other factors. This was particularly evident for the sea salt and secondary sulfate factors, where constraints on factor profiles and/or time series were necessary to obtain clean separation. Here we discuss the method for achieving this separation.

The input data set was divided into two parts: fireworks days (FD; 31 July–4 August) and non-fireworks days (NFD; all days except 31 July–4 August). To obtain a specific fireworks profile, we further selected only fireworks hours (FH; 31 July 21:00–1 August 07:00 LT) as input data. The PMF analysis was performed on the NFD, FD, FH and the complete datasets separately for three to ten factors, with each of these solutions investigated with ten seeds (each seed represents a different pseudorandom initialization).

The unconstrained NFD PMF analysis resolved seven factors at all ten seeds such as sea salt, secondary sulfate, traffic-related, road dust, background dust, industrial and a K-rich factor. The sea salt factor profile shows excellent correlation (r^2= 0.99) between the Cl and the identified sea salt factor time series. Solutions with less than seven factors showed significant scaled residuals for elements and time series, while solutions with more than seven factors revealed a split of the traffic-related, industrial and background dust factors. The NFD analysis therefore provides a sea salt profile that can be used as a constraint in the complete dataset.

The unconstrained PMF analysis of the complete dataset identified a secondary sulfate factor (most of the S is apportioned in this factor, with 91 % of the factor mass) in the nine-factor solution (Fig. S1). The identified secondary sulfate factor time series correlated very well with ACSM sulfate (r^2 = 0.91) (Fig. S1) at one seed out of ten seeds while r^2 was $\leq$ 0.88 for the remaining nine seeds. The scaled residual (over time series) of S in this solution was within the range of -0.46 to 0.85. Although these r^2 are quite similar, the solution characteristics are notably different. For the r^2 = 0.91 solution the secondary sulfate factor did not respond significantly to the fireworks event, while the other factors time series, such as the sea salt and a mixed traffic plus K-rich factors, were enhanced during the fireworks peaks. For the other nine seeds, visible contamination (i.e. concentration spikes) during the fireworks plumes were observed, suggesting mathematical mixing. S is one of the major components of fireworks emissions, the composition of which is highly variable. Because of their high sensitivity (and thus high signal-to-uncertainty ratio), imperfections in the model description of the fireworks composition yields high-signal residuals which strongly influence *Q*. The model responds by apportioning fireworks residuals to the other factors during the fireworks days. A similar issue also occurred for the sea salt factor due to the significant amount of Cl in the fireworks factor profile. Therefore, such events are often excluded from traditional PMF analyses (i.e., time periods removed from the input matrix), to avoid modelling errors due to the pulling of a solution by outliers. Here we take a different approach, exploiting the rotational control available in ME-2 to isolate environmentally reasonable, unmixed solutions.

We then performed the constrained PMF analysis on the FD and FH datasets. Here we constrained the secondary sulfate factor profile (*a*-value 0.1) and the time series (*a*-value 0.01) using the results of the 9-factor unconstrained PMF analysis of the NFD dataset. We tested several approaches for the secondary sulfate constraint: a) constraining factor profile only; b) constraining the factor time series during fireworks days only; c) constraining both the factor profile and the entire factor time series; d) constraining the factor profile and the factor time series during fireworks days only. Of the above methods, only c and d yielded secondary sulfate factors without visible mixing from the fireworks period. The approach d was used for PMF analysis as it provides maximum freedom to the algorithm.

In the FD and FH PMF analyses, the sea salt factor profile (*a*-value 0.1) was also constrained from the NFD unconstrained seven-factor PMF analysis. To resolve the unmixed sea salt factor time series from the fireworks, the background Cl concentration was calculated for the fireworks data points (K > 220 ng m^{-3}) only. A Cl concentration < 30 ng m^{-3} was considered as a background Cl concentration, and the fireworks data points were replaced with the linear interpolation between the background Cl concentrations adjacent to the fireworks peaks. In this way 42 % of the data points were interpolated during the fireworks days. The calculated background Cl during the FD was constrained (with *a* -value 0.01) in the sea salt factor time series. After applying all the above four constraints, the FH PMF analysis identified the fireworks factor profile on the basis of the K / S elemental concentration ratio (~2.76) in black powder (Dutcher et al., 1999), and on the concentration peak of 42 µg m^{-3}, which is close to the total elemental concentration peak of 48.4 µg m^{-3} on 1 August 23:00 LT in the factor time series. The FD PMF analysis also identified fireworks factor but the highest peak was 30 µg m^{-3} on 1 August 23:00 LT in the factor time series and the K / S elemental concentration ratio was 2.55 in the factor profile. Therefore, the fireworks factor profile from FH PMF analysis was considered for the final complete dataset PMF analysis. The FD and FH PMF analyses resolved a five-factor solution with secondary sulfate, sea salt, fireworks, background dust and a K-rich factor with fireworks related elements. In the K-rich factor, the K / S ratio was slightly higher (3.56) than the black powder ratio. The common factors resolved by FD, FH and NFD PMF were comparable in terms of factor time series and factor profile.

In the final complete dataset PMF analysis, the factor profiles of fireworks, secondary sulfate and sea salt were constrained (*a*-value 0.1) while the time series of secondary sulfate and the calculated background Cl concentration interpolation were constrained during the fireworks period only (*a*-value 0.01). The solution that best represented the input data was an eight-factor solution, consisting of factors interpreted as sea salt, secondary sulfate, traffic-related, industrial, two dust-related and fireworks-related (two factors).

Residual analysis (Q-contribution over time series) of the PMF runs showed significant structure in the residuals (Q maximum value was 15 during fireworks period as shown in Fig. S3) for solutions having up to seven factors. Increasing the number of factors to eight gave evidence of structure removal, with mostly random errors remaining, by another fireworks-II factor which was explained by K, S, Ba, Ti, Cu, Bi, while a further increase led to a new mixed factor of traffic-related and background dust which however had a noisy diurnal pattern (Fig. S3). All the variables were approximately unimodal scaled residuals between ±3 (Paatero and Hopke, 2003) (Fig. S5).

Pag 6, line 13: "obvious structure": completely obscure what the authors mean.

We meant significant structure in residuals. We modified the text on Page 6 line 13 as follows:

Residual analysis (Q-contribution over the time series) of the PMF runs showed significant structure in the residuals ((Q maximum value was 15 during fireworks period as shown in Fig. S3) for solutions having up to seven factors.

Pag 6, line 28: "both the sea salt and secondary sulfate factor time series were also constrained with a-value 0.01". Further constraint implemented. Please note that a small a-value was used. Is it consistent with uncertainty estimates for the non-firework sub-set and for the sulfate factor identified in the preliminary 9-factor solution? Please also note that the constraints come from two different analyses.

We understand the concern of the reviewer#3. The selected *a*-values are not intended to reflect the uncertainties y in the factor time series of secondary sulfate and sea salt during the fireworks period; we now assess these using a different method, as discussed below. Rather, the selected values are empirically chosen to provide a clean separation of these factors from the fireworks emissions. We performed a sensitivity analysis on the small *a*-value from 0 to 0.1 over partial (fireworks period only) time series of secondary sulfate and sea salt. The structure during the fireworks period in the sea salt and the secondary sulfate factor time series was mixing with the fireworks factor time series for *a*-values > 0.01.

We have now added the following text on page 6 line 28:

The small *a*-value (0.01) for the sea salt and the secondary sulfate factor time series (for the fireworks period only) were estimated based on sensitivity analyses on the *a*-value from 0 to 0.1 with an increment of 0.01. The time series of both factors were showing fireworks peaks during the fireworks period for *a*-values greater than 0.01.

In the original manuscript, section 3.3 presented an analysis of the uncertainty of the time series across the entire campaign. However, this analysis did not account for the tight constraints applied to the sea salt and secondary sulfate factors during the fireworks period, and as a result these uncertainties were underestimated. We have now added the following text (page 7 line 12), which describes the uncertainty estimates of these factors during the fireworks period, and updated Fig. 3a accordingly.

During the non-fireworks period, uncertainties in the source apportionment results are assessed by a bootstrap analysis as described above. However, this approach cannot be used to assess uncertainties in the sea salt and secondary sulfate factors during the fireworks period, as during this period these factor time series are constrained with an artificially low *a*-value selected to optimize deconvolution. For these two factors, uncertainties during the fireworks period are determined by our ability to accurately predict the factor time series. The secondary sulfate and sea salt factors cases are discussed separately below.

Secondary sulfate concentrations during the fireworks period were estimated from the linear fit of the secondary sulfate factor to ACSM sulfate during the entire non-fireworks period. Uncertainties of ±5 % were calculated as the standard deviation of the actual secondary sulfate concentrations to the predicted values and included for the fireworks period only in Fig. 3a.

As described above, the sea salt factor time series during the four-day fireworks period was investigated to determine measurements that were affected or not affected by fireworks, where the measurements determined to be affected were replaced with a linear interpolation between the nearest good points. To determine the uncertainties of

this approach, we applied this calculation to random segments of the non-fireworks data. Specifically, the four day-long sequence of affected/non-affected time points determined during the fireworks period was applied to a randomly chosen segment of data, and the standard deviation of measurement data to the estimated values calculated by interpolation was determined. This analysis was repeated for 38 randomly selected locations through the non-fireworks data, and a mean standard deviation of ±42 % was determined. This value is used as the uncertainty of the sea salt factor time series (during the fireworks period only) in Fig. 3a.

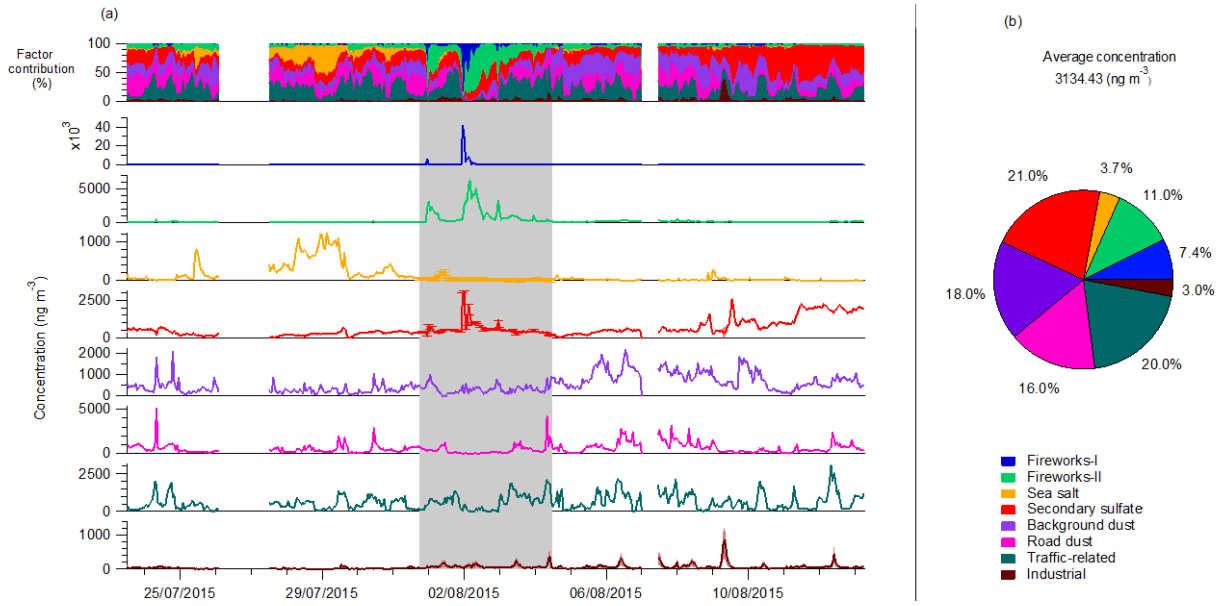

Figure 3: (a) Time series of the PM_{10} elemental sources and relative contributions of the different sources over time; shaded areas indicate the uncertainties (interquartile) of selected bootstrap runs; grey background color represent the fireworks period; estimated uncertainty of the secondary sulfate (± 5%) and the sea salt factors (± 42%) during fireworks period are added as error bars; (b) Mean relative contributions of PM_{10} elemental sources.

Page 7, line 19: obvious. It was checked in the preliminary analysis at 9-factors and then constrained both as far profile and temporal patterns are concerned in the final solution.

This factor (secondary sulfate) was identified in the unconstrained PMF solution at a specific seed where it was mostly dominated by S and had a high correlation with ACSM sulfate. However, the high and variable S concentrations during the fireworks period led to mixing between the fireworks and the secondary sulfate factors during this period. Therefore we constrained part of the secondary sulfate time series (only during fireworks days) to avoid mixing along with factor profile.

Page 8, "Fireworks" paragraph. Considering that the fireworks profile was constrained, it sounds very strange that two fireworks sources were identified in the final analysis. As previously required, the existence of two fireworks sources should be supported by their identification at least in the unconstrained analysis of the fireworks period. If

not, the strength of the imposed constrain should be verified to get if it artificially generates the presence of two factors.

Based on the suggested changes due to the previous comments, we believe that we have responded to this concern as well. We have already discussed the residuals structure in Fig. S3 from 4 to 10 factors solution. In the final solution, the secondary sulfate, sea salt and fireworks-I factor profiles were constrained along with the factor time series (for the fireworks period only) of sea salt and secondary sulfate. Because of significant scaled residuals in the 7-factor solution, we found that fireworks related elements such as K, Ba, Ti, Cu, Bi had significant residuals during fireworks days (scaled residual over time: ±8) which is consistent with Fig. S8. Both analyses (residual and Fig. S8) indicate that the fireworks composition was highly variable and not well explained by a single factor. We identified a K-rich factor in both the fireworks PMF and in the non-fireworks PMF analyses which were dominated by these elements along with other elements (Si, S, Fe, Mn, Zn, Pb). Although the second fireworks factor profile yielded a slightly higher K / S ratio (3.56) than the black powder ratio (2.76), we decided to keep it based on the improved residual structure and the factor time series which captured the fireworks variability.

Page 9, lines 1-4 and Figure 4. Completely obscure. I interpret "normalized" as "divided by", but in this case how can the negative values be justifiable? Furthermore, what is "composition"? Average contribution of the factor to each element?

The similar issue was also raised by Reviewer #1, and our response is presented in both places for clarity. The PMF results (Fig. 2) describe potentially complex and time-dependent sources as a single factor (or linear combination of factors). This is a fundamental limitation of the model, and may not accurately describe the behaviour or a complex source (e.g., residuals may be significant). In contrast, Fig. 4 provides an estimate of overall fireworks composition and temporal variability, complementing the PMF results (which are shown for reference). One can then see both the explanatory power and limitations of the SA model for this source.

We moved Fig. 4 to the supplement as Fig. S8 and removed ± SD from the figure as suggested by reviewer#1.

We added in the supplement on page 8 line 4:

Fig. S8 provides an estimate of the overall fireworks composition and temporal variability, complementing the PMF results (which are shown for reference). The figure is constructed in two stages. First, the time series of fireworks contributions to each element is estimated by subtracting the non-fireworks factors (NFF) from the original measurements. Then, the estimated fireworks contribution for each element is normalized by the total fireworks element contribution, and the displayed statistics are calculated. This is represented mathematically below, and the expression has been added to the main text. Note that the variation in fireworks profiles implied by this figure supports the representation of fireworks by 2 fireworks factors.

$$normalized\ concentration_{ij} = \frac{x_{ij} - \left(g_{ik} f_{kj}\right)_{k=NFF}}{\sum_j \left(x_{ij} - \left(g_{ik} f_{kj}\right)_{k=NFF}\right)} \quad \text{(S1)}$$

where X represents the input data matrix for PMF, while G and F represent the factor time series and factor profiles driven by six non-fireworks factors (NFF). Here *i* and *j* denote time series and variables, respectively.

NFF and fireworks measurements have some uncertainties, and therefore for elements and/or time periods in which the concentration of fireworks is low, positive and negative values fluctuating around zero are expected. Here the negative values occur mostly for Si (for which fireworks are a minor fraction of the total signal), while the other elements were mostly captured very well. We used the factor composition for the factor profiles (fingerprints). We have already added the mathematical expressions for the factor composition as well as for the factor relative contribution on Page 7, lines 26-27.

Page 11, lines 22-23: "We established that data sets including extreme events such as fireworks can be apportioned by ME-2 without disturbing the model solutions". Untrue. The imposed constraints completely modified the output of the unconstrained analysis.

We have discussed the unconstrained nine-factor solution which was basically mixed with the fireworks in the factor time series during fireworks period. To avoid mixing, we used the ME-2 method by restricting the fireworks structure in the S and Cl driven factors time series.

We have modified the text as follows:

We show that the rotational control available in ME-2 provides a means for treating extreme events such as fireworks within a PMF analysis.

Minor comments

Page 2, Line 12: A reference to: "Fe in brake lining can reach up to 60 % by weight" is needed.

Done. (Chan and Stachowiak, 2004; Schauer et al., 2006)

Chan, D. and Stachowiak, G. W.: Review of automotive brake friction materials, Proc Inst. Mech. Eng. Part D: J Automob. Eng., 218, 953–966, https://doi.org/10.1243/0954407041856773, 2004.

Schauer, J. J., Lough, G. C., Shafer, M. M, Christensen, W. C., Arndt, M. F., DeMinter, J. T., and Park, J. S.: Characterization of emissions of metals emitted from motor vehicles, Research report (Health Effects Institute), 133, 1–76; discussion 77, 2006.

Page 2, line 27: add "among others" after "Wang et al., 2018". Indeed, the list is far from being complete (see e.g.: Li et al. 2017 http://dx.doi.org/10.1016/j.jenvman.2017.02.059; Zhou et al., 2018 https://doi.org/10.5194/acp-18-2049-2018 among the most recent). If the authors intend providing a full list, a much more detailed research has to be done.

Done.

Page 3, lines 10-12. "The later, being essential in particular when separating extreme events such as fireworks which are most often excluded from the PMF input matrix (Ducret-Stich et al., 2013; Norris et al., 2014) to avoid distortion in the PMF solution due to unusually high emissions". This sentence is questionable. As reported by Paatero et al., (doi:10.5194/amt-7-781-2014) wrong decision on the outlier status of data can introduce serious modelling errors. Please also note that opposite to what stated by the authors, examples in the literature tried to

exploit fireworks tracers to quantify the source contribution, with different approaches (e.g. Scerri et al., 2018 https://doi.org/10.1016/j.chemosphere.2018.07.104, Ji et al., 2018 https://doi.org/10.1016/j.scitotenv.2018.01.304, Vecchi et al., 2008 http://dx.doi.org/10.1016/j.atmosenv.2007.10.047)

We modified the text in the manuscript as follows:

The rotational control available in ME-2 provides a means for treating extreme events such as fireworks within a PMF analysis. Such events are often excluded from the PMF input matrix to avoid modelling errors due to the pulling of a solution by outliers (Ducret-Stich et al., 2013; Norris et al., 2014; Paatero et al., 2014).

Regarding the papers mentioned by the reviewer, it was shown that fireworks are not necessarily outliers as considered in the PMF analysis. However, these articles have discussed different methods to apportion fireworks contribution in the PMF analysis e.g. Scerri et al. (2018) has down weighted some of the elements (not specific to fireworks-related elements) as "weak" variables without discussing the influence of fireworks on the other non-fireworks factors. The down weighting approach is not clear in this paper due to lack of criteria defining down weighting random elements. In contrast Vecchi et al. (2018) reported the up weighting of fireworks tracer by a factor of 2 to highlight its role during fireworks. At the same time, they down weighted some of the variables by the factor of 2 to 4 with trial and error method until the model resolved fireworks sources. This approach may have worked to resolve fireworks contribution but no discussion has been provided for other non-fireworks sources. They discussed the other sources in a separate paper (Bernardoni et al., 2011) with a slightly different PMF input set on the same data by excluding fireworks-related tracers. Ji et al. (2018) quantified fireworks factor on the basis of signal to noise ratio instead of up/down weighing elements specific to fireworks which yielded the mixed factors with fireworks (in terms of factor profile and time series) in their PMF analysis. This mixing issue can be resolved by using ME-2 approach as adopted in our study.

Bernardoni, V., Vecchi, R., Valli, G., Piazzalunga, A., and Fermo, P.: PM_{10} source apportionment in Milan (Italy) using time-resolved data, Sci. Total Environ., 409, 4788–4795, https://doi.org/10.1016/j.scitotenv.2011.07.048, 2011.

Ji, D., Cui, Y., Li, L., He, J., Wang, L., Zhang, H., Wang, W., Zhou, L., Maenhaut, W., Wen, T., and Wang, Y.: Characterization and source identification of fine particulate matter in urban Beijing during the 2015 Spring Festival, Sci. Total Environ., 430–440, 628–629, https://doi.org/10.1016/j.scitotenv.2018.01.304, 2018.

Scerri, M. M., Kandler, k., Weinbruch, S., Yubero, E., Galindo, N., Prati, P., Caponi, L., and Massabò, D.: Estimation of the contributions of the sources driving $PM_{2.5}$ levels in a Central Mediterranean coastal town, Chemosphere, 211 465–481, https://doi.org/10.1016/j.chemosphere.2018.07.104, 2018.

Vecchi, R., Bernardoni, V., Cricchio, D., D'Alessandro, A., Fermo, P., Lucarelli, F., Nava, S., Piazzalunga, A., and Valli, G.: The impact of fireworks on airborne particles, Atmos. Environ., 42, 1121–1132, https://doi.org/10.1016/j.atmosenv.2007.10.047, 2008.

Page 7, line 28: "absolute mass". It should be recalled that it refers only to the mass related to elements, as no PM mass was inserted in the analysis.

We have rewritten it as follows:

Fig. 3a shows the time series of the factors contributions in ng m^{-3} (bottom panels) and relative contributions (top panel) of the retrieved PM_{10} factors.

Page 9, line 25-26: "The two dust factors together explain 95 % of Ca, with no other factor explaining more than 93 %". Obscure. If already explained at 95%, how can other factors explain Ca for more than 93%?

We apologize for the misunderstanding. For clarity, we have rewritten it as:

The two dust factors together explain 95 % of Ca, while the remaining factors explain only 5% of Ca.

Page 9, lines 29-30: "In general, Ca is commonly associated with mineral dust, construction activities, vehicular emissions and iron/steel plants". References are needed.

Done.

(Lee and Pacyna, 1999; Vega et al., 2001; Bukowiecki et al., 2010; Crilley et al., 2016; Maenhaut, 2017)

Lee, D. S. and Pacyna, J. M.: An industrial emissions inventory of calcium for Europe, Atmos. Environ. 33, 1687–1697, https://doi.org/10.1016/S1352-2310(98)00286-6, 1999.

Crilley, L. R., Lucarelli, F., Bloss, W. J., Harrison, R. M., Beddows, D. C., Calzolai, G., Nava, S., Valli, G., Bernardoni, V., and Vecchi, R.: Source apportionment of fine and coarse particles at a roadside and urban background site in London during the 2012 summer ClearfLo campaign, Environ. Pollut., 220, 766–778, https://doi.org/10.1016/j.envpol.2016.06.002, 2016.

Vega, E., Mugica, V., Reyes, E., Sanchez, G., Chow, J. C., and Watson, J. G.: Chemical composition of fugitive dust emitters in Mexico City, Atmos. Environ., 35, 4033–4039, https://doi.org/10.1016/S1352-2310(01)00164-9, 2001.

Bukowiecki, N., Lienemann, P., Hill, M., Furger, M., Richard, A., Amato, F., Prévôt, A. S. H., Baltensperger, U., Buchmann, B., and Gehrig, R.: PM_{10} emission factors for non-exhaust particles generated by road traffic in an urban street canyon and along a freeway in Switzerland, Atmos. Environ., 44, 2330–2340, https://doi.org/10.1016/j.atmosenv.2010.03.039, 2010.

Maenhaut, W.: Source apportionment revisited for long-term measurements of fine aerosol trace elements at two locations in southern Norway, Nucl. Instrum. Methods Phys. Res. Sect. B, 417, 133–138 https://doi.org/10.1016/j.nimb.2017.07.006, 2017.

Source apportionment of highly time resolved trace elements during a firework episode from a rural freeway site in Switzerland

Pragati Rai[1], Markus Furger[1], Jay Slowik[1], Francesco Canonaco[1], Roman Fröhlich[1], Christoph Hüglin[2], María Cruz Minguillón[3], Krag Petterson[4], Urs Baltensperger[1] and André S.H. Prévôt[1]

[1]Laboratory of Atmospheric Chemistry, Paul Scherrer Institute, Villigen PSI, 5232, Switzerland
[2]Laboratory for Air Pollution / Environmental Technology, Empa, 8600 Dübendorf, Switzerland
[3]Institute of Environmental Assessment and Water Research (IDAEA), CSIC, 08034 Barcelona, Spain
[4]Cooper Environmental Services (CES), 9403 SW Nimbus Avenue, Beaverton, OR 97008, USA

Correspondence to: André S. H. Prévôt (andre.prevot@psi.ch) and Markus Furger (markus.furger@psi.ch)

Abstract. Trace element measurements in PM_{10} were performed with 1 h time resolution at a rural freeway site during summer 2015 in Switzerland using the Xact 625 multi-metals monitor. On average the Xact elements (without accounting for oxygen and other associated elements) make up about 20 % of the total PM_{10} mass (14.6 µg m^{-3}). Subsequently, a source apportionment by positive matrix factorization (PMF) implemented via the Source Finder software (SoFi Pro version 6.2, PSI, Switzerland) was applied. Eight different sources were identified for elemental PM_{10} (notable elements in brackets): fireworks-I (K, S, Ba, Cl), fireworks-II (K), sea salt (Cl), secondary sulfate (S), background dust (Si, Ti), road dust (Ca), traffic-related (Fe) and industrial (Zn, Pb). The major components were secondary sulfate and traffic-related followed by background dust and road dust factors, explaining 21 %, 20 %, 18 % and 16 % of the analysed PM_{10} elemental mass, respectively, with the factor mass not corrected for oxygen content. Further, there ~~are~~ were minor contributions (on the order of a few percent) of sea salt and industrial sources. The regionally influenced secondary sulfate factor ~~experiences~~ showed negligible resuspension, and concentrations ~~are~~ were similar throughout the day. The significant loads of the traffic-related and road dust factors with strong diurnal variations highlight the continuing importance of vehicle-related air pollutants at this site. Enhanced control of PMF using SoFi Pro allowed for a successful apportionment of transient sources such as the two firework factors and sea salt, which remained mixed when analysed by unconstrained PMF.

1 Introduction

Ambient particulate matter (PM) plays a major role in affecting human health and air quality. Trace elements represent a minor fraction of the atmospheric aerosol on a mass basis, but they can act as specific markers for several emission sources. The short- or long-term exposure of ambient particulate matter (PM) has significant negative effects on human health (Dao et al., 2012; Ancelet et al., 2012; Zhao and Hopke, 2004; Pope and Dockery, 2006; Dockery et al., 1993; Zhou et al., 2018). Cakmak et al. (2014) found significant association of acute changes in cardiovascular and respiratory physiology with $PM_{2.5}$ metals in Ontario, Canada. In Stockholm, Meister et al. (2012) estimated a 1.7 % increase in daily mortality per 10 µg m^{-3}

increase in the coarse fraction of PM. Metallic components of PM, especially the fine fraction of ~~trace~~ elements such as Fe, Ni, Cu, V, Pb and Zn, appear to be a significant cause of both pulmonary and cardiovascular diseases (Kelly and Fussell, 2012). Airborne particles and associated (trace) elements originate from various emission sources, such as motor vehicles, power plants, construction activities, in a broad size range. Among them, traffic-related emissions are of particular interest (Brauer et al., 2002). Traffic-derived PM has a high risk of respiratory illness, asthma and cardiovascular diseases, resulting in an increased rate in mortality (Kelly and Fussell, 2011). Traffic-related PM is emitted mainly as exhaust emissions (tailpipe exhaust from gasoline and diesel engines) and non-exhaust emissions (resuspension of road dust and brake and tire wear emissions) (Lawrence et al., 2013; Lin et al., 2015; Thorpe and Harrison, 2008; Zhou et al., 2018; Grigoratos and Martini, 2015; Amato et al., 2014b; Bukowiecki et al., 2010). Exhaust emissions are predominantly in the fine fraction of PM, whereas non-exhaust emissions contribute mostly to the coarse fraction (Amato et al., 2011; Thorpe and Harrison, 2008). Exhaust emission-related elements are comprised of Pb, Zn, Ni and V (Lin et al., 2015; Minguillon et al., 2012), while the non-exhaust emissions are dominated by Fe, Cu, Ba, Ca, Sb, Sn, Cr and Zn from brake lining and tire wear. The presence of Fe in brake lining can reach up to 60 % by weight (Chan and Stachowiak, 2004; Schauer et al., 2006). Brake pads are usually filled with $BaSO_4$, while Sb, Sn and Mo sulfides are often added as lubricants, and Cu, Cr and Zn are major additives to lubricating oils and normally used to improve friction (Thorpe and Harrison, 2008; Amato et al., 2014a). Sb has been identified as a major tracer of brake wear, due to significant (1–5 %) percentage of Sb in brake linings in the form of stibnite (Sb_2S_3) (Grigoratos and Martini, 2015; Bukowiecki et al., 2009). It has been reported that asphalt pavement-induced particles were characterized mainly by high concentrations of Cu, Cr, Ni, As and Pb (Yu, 2013) as well as Ca, Si, Mg, Al, Fe, P, S, Cl, K, V, Mn, Na (Fullova et al., 2017). Therefore, it is important to monitor traffic emissions for health risk assessment, the study of which relies heavily on the source apportionment (SA) of PM using chemically speciated data (Zhou et al., 2018).

Source quantification and characterization is an important step in understanding the relationship between source emissions, ambient concentrations, and health and environmental effects. SA by receptor models has been widely used in recent years to identify and apportion the contributions of various sources to the airborne PM concentrations. Positive Matrix Factorization (PMF) is one of the most widely used receptor models for SA of trace elements (Rahman et al., 2011; Ancelet et al., 2012; Cesari et al., 2014; Ducret-Stich et al., 2013; Kim et al., 2003; Rai et al., 2016; Zhang et al., 2013; Harrison et al., 2011; Hedberg et al., 2005). However, a very limited number of studies are available for trace elements emission sources with high time resolution (hourly or sub-hourly) (Visser et al., 2015; Crilley et al., 2016; Bukowiecki et al., 2010; Richard et al., 2011; Dall'Osto et al., 2013; Manousakas et al., 2015; Jeong et al., 2019; Wang et al., 2018, among others). Hourly ~~trace~~ elements data can be used to explore the diurnal patterns of emissions from traffic, biomass burning and industrial sources, thereby yielding more accurate and exposure-relevant SA results. Currently, there are very few offline instruments available for field sampling of elements with high time resolution, such as the rotating drum impactor (RDI) (Bukowiecki et al., 2008), the streaker sampler (PIXE International Corporation) (Lucarelli et al., 2011) and the semi-continuous elements in aerosol sampler (SEAS) (Kidwell and Ondov, 2001). The large quantity of samples generated by these samplers requires a labour

intensive and time consuming offline analysis. These offline ~~analysis~~ analyses require high precision and low detection limit techniques such as~~needs~~ synchrotron radiation induced X-ray fluorescence spectrometry (SR-XRF) of aerosol samples collected with a RDI, ~~Particle~~ particle induced X-ray emission (PIXE) with the streaker sampler, and graphite furnace atomic absorption spectrometry (GFAAS) with the SEAS. In practice, the offline samplers lead to undesirable trade-offs between time resolution and data coverage even for short duration field campaigns, whereas highly time-resolved long-term measurements are impractical. A recently introduced online high time resolution instrument can collect samples and perform analysis for elements simultaneously in a near real time scenario for long-term measurements without waiting for laboratory analysis. ~~A recently introduced online high time resolution instrument can collect samples and perform analysis for metals simultaneously in a near real time scenario without waiting for laboratory analysis.~~ The XRF-based Xact 620, 625 and the newer 625i ambient metals monitors (Cooper Environmental Services, Beaverton, Oregon, USA) have been developed in recent years and have been used in several field studies (Fang et al., 2015; Cooper et al., 2010; Furger et al., 2017; Park et al., 2014; Phillips-Smith et al., 2017; Tremper et al., 2018; Chang et al., 2018; Liu et al., 2019). However, only ~~two~~ six studies included SA on Xact data (Park et al., 2014; Fang et al., 2015; Phillips-Smith et al., 2017;Chang et al., 2018; Liu et al., 2019; Ji et al., 2018).

The main focus of this work is the exploration of the use of the Xact for source apportionment in Europe where the concentrations are considerably lower than in polluted areas in Asia. In the present study, we conducted SA using PMF to characterize the source ~~emissions~~ contributions of highly time-resolved metals during a three-week campaign at a traffic-influenced site in Härkingen, Switzerland. PMF was implemented through the multilinear engine-2 (ME-2) solver and controlled via SoFi, which allows for a comprehensive and systematic exploration of the solution space (Bozzetti et al., 2016; Canonaco et al., 2013). The rotational control available in ME-2 provides a means for treating extreme events such as fireworks within a PMF analysis. Such events are often excluded from the PMF input matrix to avoid modelling errors due to the pulling of a solution by outliers ~~The later, being essential in particular when separating extreme events such as fireworks which are most often excluded from the PMF input matrix~~ (Ducret-Stich et al., 2013; Norris et al., 2014) ~~to avoid distortion in the PMF solution due to unusually high emissions~~. Although a few studies have already been carried out in the past at this location (Lanz et al., 2010; Hueglin et al., 2006; Furger et al., 2017), none of them have reported SA on ~~trace~~ elements.

2 Experimental setup and data analysis

2.1 Sampling location

PM_{10} sampling was performed from 23 July until 13 August 2015 in Härkingen, Switzerland, a permanent station of the Swiss Air Pollution Monitoring Network (NABEL) (Fig. 1). Extreme firework episodes were captured during the Swiss National Day Celebration (1 August). The site is situated next to the A1 freeway, which is the main traffic route between eastern (Zurich) and western (Bern) Switzerland. The measurement site is bordered by agricultural areas to the west and

north while there are villages in the south and east direction. There is a metal processing company to the south-east across the freeway which manufactures wheels for passenger cars and commercial vehicles, and some small scale industrial buildings to the north-west. The emissions reaching the measurement site depend on wind direction. The site is strongly influenced by local road traffic emissions when winds come from the southern sector, while the northern wind sector represents the air constituents from a rural area. A detailed description of the sampling site can be found in previous studies (Furger et al., 2017; Hueglin et al., 2006)

2.2 Sampling and analysis

Sampling and analysis was conducted with an Xact 625 ambient metals monitor ~~(Cooper Environmental Services, Beaverton, Oregon, USA)~~ equipped with a PM_{10} inlet. The instrument was set up to quantify 24 elements (Si, S, Cl, K, Ca, Ti, V, Cr, Mn, Fe, Co, Ni, Cu, Zn, As, Se, Cd, Sn, Sb, Ba, Pt, Hg, Pb and Bi) with 1 h time resolution. In addition, 24-h PM_{10} samples were collected by a ~~Digital DA-80H~~ HiVol sampler (Digitel DA-80H, DIGITEL Hegnau, Switzerland) with quartz fiber filters (Pallflex XP56 Tissuquartz 2500QAT-UP, Pall, AG, Switzerland). Ten of these 24-h PM_{10} samples were analysed by inductively coupled plasma optical emission spectrometry (ICP-OES) for the concentrations of Na, Mg, Al, P, S, K, Ca, Ti and Fe. Moreover, the station was equipped with other instruments such as a tapered element oscillating microbalance filter dynamics measurement system (TEOM FDMS 8500, Thermo Fischer Scientific, MA, USA) ~~(tapered element oscillating microbalance)~~ for 10 min PM_{10} mass concentration measurements, a multi angle absorption photometer (MAAP, Thermo 5012, Thermo Fischer Scientific, MA, USA) for balck carbon (BC) measurements in $PM_{2.5}$ and standard meteorological sensors (temperature, wind speed and direction, precipitation). The trace gases were measured with conventional instruments by the Swiss National Air Pollution Monitoring Network, NABEL (Empa, 2011). The time resolution of all these instruments was 1 h. The station also provided hourly traffic counts for the freeway in the form of total number of vehicles, number of heavy-duty vehicles (HDV), and the number of light-duty vehicles (LDV). NO_x was measured by chemiluminescence spectroscopy (Horiba APNA 370). Specifically for the campaign, a quadrupole aerosol chemical speciation monitor ~~Q-ACSM~~ (~~quadrupole aerosol chemical speciation monitor~~ Q–ACSM 140-145, Aerodyne Inc~~.~~, Billerica, MA, USA) with vacuum aerodynamic diameters smaller than 1µm (non-refractory-PM_1) was deployed (Ng et al., 2011; Crenn et al., 2015) and the data were used for comparison of the factors during the SA analysis.

2.3 PMF using ME-2

Positive matrix factorization is one of the most common receptor models based on a weighted least squares fit (Paatero and Tapper, 1994). It is used to describe the variability of a multivariate dataset as the linear combination of a set of constant factor profiles and their corresponding time series as shown in Eq. (1) in cell notation:

$$x_{ij} = \sum_{k=1}^{p} g_{ik} f_{kj} + e_{ij} , \quad (1)$$

where **X**, **G**, **F** and **E** represent the data matrix, factor time series, factor profiles and residual matrices, respectively, while *i*, *j* and *k* indices denote time, element, and factor number. The index *p* represents the total number of factors in the PMF solution. The PMF model iteratively solves Eq. (1) by minimizing the object function (Q), defined as:

$$Q = \sum_i \sum_j \left(\frac{e_{ij}}{s_{ij}}\right)^2, \quad (2)$$

Here, s_{ij} corresponds to the measurement uncertainty (error matrix) for the input point *ij*.

The PMF algorithm was solved using ME-2 (Paatero, 1999), which enables an efficient exploration of the solution space by introducing *a priori* information to **G** and / or **F** into the PMF model. Using the constraining technique of the *a*-value, one or more factor profile/factor time series can be confined by the scalar *a* ($0 \leq a \leq 1$), which can be applied to the entire profile/time series or to individual variables/data points of the profile/time series. The scalar *a* defines how much the resolved factors are allowed to deviate from the input profile/time series, according to:

$$f'_{kj} = f_{kj} \pm a \times f_{kj}\,, \quad (3)$$

$$g'_{ik} = g_{ik} \pm a \times g_{ik}\,, \quad (4)$$

where the subscript *j* varies between 0 and the number of variables and *i* varies between 0 and the number of measured data points in time. f_{kj} and g_{ik} are the starting value used as a *priori* knowledge from the base case solution in this SA study, and f'_{kj} and g'_{ik} are the resulting values in the solution. Normalization in Eq. (3) and (4) can lead to the resulting values slightly outside the specified *a*-value boundaries. This method reduces the available solution space and directs the solution towards an optimized and environmentally meaningful solution. The Source Finder software SoFi Pro (Canonaco et al., 2013) which is coded in the Igor Pro software environment (Wavemetrics, Inc., Portland, OR, USA) was used for the ~~model~~ PMF configuration and analysis.

2.4 Conditional bivariate polar function (CBPF) plots

CBPF is a data analysis tool to ~~find~~ identify the direction of source contributions and was applied to the PMF source factors. Polar plots are used to present the CBPF analyses, where the number of events with a concentration greater than the ~~90~~th ith percentile (0 to 100) is plotted as a function of both wind speed and direction, as shown in Eq. (5):

$$CBPF = \frac{m_{\theta,r}}{n_{\theta,r}}, \quad (5)$$

where $m_{\theta,r}$ is the number of samples in wind sector θ and wind speed sector *r* with a concentration greater than the ~~90~~th ith percentile and $n_{\theta,r}$ is the total number of samples with the same wind direction and speed (Carslaw and Beevers, 2013). The resultant CBPF polar plots present the probability that high concentrations of a pollutant correspond to a particular wind direction and speed and can give insight into the contributions from local and regional sources.

3 SA method and solutions selection

3.1 PMF input preparation

In our study, the PMF input consists of a data matrix and an error matrix of hourly ~~trace~~ element measurements, where the rows represent the time series (456 points with 1 h steps) and the columns contain the ~~trace~~ elements (14 variables). The input preparation of PMF was done by excluding some specific ~~trace~~ elements for better source apportionment results. A common approach for the choice of species to include in the PMF input depends on: 1) the percentage of data below detection limit (Polissar et al., 1998), and 2) Xact data comparison with offline 24-h PM_{10} filters (Pearson coefficient of determination r^2). The minimum detection limits (MDL), r^2 and data points below MDL ~~for 1 h sampling~~ of Xact ~~trace~~ elements are listed in Furger et al. (2017). The MDLs were given by the manufacturer and were calculated by using the sensitivity of the element and counts in the region of interest of a blank section of the tape from where 1σ interference-free detection limits are reported. Elements (% of data points below MDL, r^2 value) which had more than 50 % of data points below MDL and low r^2 (< 0.5) between Xact and offline data were not included in the PMF input, such as:~~(e.g.~~ V (98 %, 0.57), Co (100 %, 0.05), Ni (32 %, 0.22), As (96 %, 0.5), Se (62 %, 0.3), Cd (87 %, 0.18), Sn (15 %, 0.27), Sb (6%, 0.42), Hg (13 %, 0.12) and Pt (98 %, not measured on the filters)~~, except Bi (93 %), which is a major tracer of fireworks and contains spikes during the fireworks episode~~. ~~Some of the trace elements such as Ni, Hg, Sn and Sb were also excluded due to poor data quality.~~ The element Bi (93% data points below MDL) was an exception to include in the PMF input due to an excellent correlation between Xact and offline data (r^2 = 0.98) during fireworks peaks. The detailed description of the Xact data quality is given in the previous study (Furger et al., 2017). Missing data points in time (e.g. a power failure during sampling or a filter tape change) were removed from the data and error matrices. In the present work, if the ~~trace~~ element concentration was less than or equal to the MDL provided, the error matrix element s_{ij} was calculated using the Eq. (6), and if the concentration was greater than the MDL provided, the error matrix element s_{ij} was calculated using Eq. (7) (Reff et al., 2007; Tian et al., 2016; Polissar et al., 1998):

$$s_{ij} = \frac{5}{6} \times MDL_j \,, \tag{6}$$

$$s_{ij} = \sqrt{(p_j \times x_{ij})^2 + (MDL_j)^2} \,, \tag{7}$$

where **X** indicates the data matrix, while subscripts i and j are indices for time and elements. In this study, an estimated analytical uncertainty (p_j) of 10 % was used to derive the error matrix data set (Kim et al., 2005; Kim and Hopke, 2007; Tian et al., 2016; Ji et al., 2018), which did not change the PMF solution. The metal-specific analytical uncertainty was also considered from the previous studies (Jeong et al., 2016; Phillips-Smith et al., 2017), where it was calculated on the basis of high/medium-concentration metal standards laboratory experiments and the additional 5-10% flow rate accuracy, which yielded similar PMF solutions compared to an overall 10 % analytical uncertainty.

~~In this study, the p_J is the analytical uncertainty taken as 10 % for all of the chemical species.~~

3.2 PMF setup

An important step in the PMF analysis is the selection of the number of factors by the user, as mathematical diagnostics alone are insufficient for choosing the correct number of factors (Ulbrich et al., 2009; Canonaco et al., 2013). The selection of factors is often based on an analysis of total Q or Q/Q_{exp}, scaled residuals (e_{ij}/s_{ij}), comparison of time series of the factor with external tracers, as well as diurnal patterns, and the evaluation of the residual time series as a function of the number of resolved factors.

In a first step, we examined a range of solutions with three to ten factors at ten seeds (number of PMF repeats) from unconstrained runs. The unconstrained PMF solution resulted in mixed factors, such as sea salt mixed with fireworks, even for higher numbers of factors (Fig. S1). This is likely because of the very high concentration and variation in composition of fireworks emissions during the fireworks period. Because the signal-to-noise is very high, imperfections in the model description exert a strong influence on *Q*, and the model therefore tries to compensate by assigning fireworks mass to other factors. This was particularly evident for the sea salt and secondary sulfate factors, where constraints on factor profiles and/or time series were necessary to obtain clean separation. Here we discuss the method for achieving this separation.

The input data set was divided into two parts: fireworks days (FD; 31 July–4 August) and non-fireworks days (NFD; all days except 31 July–4 August). To obtain a specific fireworks profile, we further selected only fireworks hours (FH; 31 July 21:00–1 August 07:00 LT) as input data. The PMF analysis was performed on the NFD, FD, FH and the complete datasets separately for three to ten factors, with each of these solutions investigated with ten seeds (each seed represents a different pseudorandom initialization).

The unconstrained NFD PMF analysis resolved seven factors at all ten seeds such as sea salt, secondary sulfate, traffic-related, road dust, background dust, industrial and a K-rich factor. The sea salt factor profile shows excellent correlation (r^2= 0.99) between the Cl and the identified sea salt factor time series. Solutions with less than seven factors showed significant scaled residuals for elements and time series, while solutions with more than seven factors revealed a split of the traffic-related, industrial and background dust factors. The NFD analysis therefore provides a sea salt profile that can be used as a constraint in the complete dataset.

The unconstrained PMF analysis of the complete dataset identified a secondary sulfate factor (most of the S is apportioned in this factor, with 91 % of the factor mass) in the nine-factor solution (Fig. S1). The identified secondary sulfate factor time series correlated very well with ACSM sulfate (r^2 = 0.91) (Fig. S1) at one seed out of ten seeds while r^2 was ≤ 0.88 for the remaining nine seeds. The scaled residual (over time series) of S in this solution was within the range of -0.46 to 0.85. Although these r^2 are quite similar, the solution characteristics are notably different. For the r^2 = 0.91 solution the secondary sulfate factor did not respond significantly to the fireworks event, while the other factors time series, such as the sea salt and a mixed traffic plus K-rich factors, were enhanced during the fireworks peaks. For the other nine seeds, visible contamination (i.e. concentration spikes) during the fireworks plumes were observed, suggesting mathematical mixing. S is

one of the major components of fireworks emissions, the composition of which is highly variable. Because of their high sensitivity (and thus high signal-to-uncertainty ratio), imperfections in the model description of the fireworks composition yields high-signal residuals which strongly influence *Q*. The model responds by apportioning fireworks residuals to the other factors during the fireworks days. A similar issue also occurred for the sea salt factor due to the significant amount of Cl in the fireworks factor profile. Therefore, such events are often excluded from traditional PMF analyses (i.e., time periods removed from the input matrix), to avoid modelling errors due to the pulling of a solution by outliers. Here we take a different approach, exploiting the rotational control available in ME-2 to isolate environmentally reasonable, unmixed solutions.

We then performed the constrained PMF analysis on the FD and FH datasets. Here we constrained the secondary sulfate factor profile (*a*-value 0.1) and the time series (*a*-value 0.01) using the results of the 9-factor unconstrained PMF analysis of the NFD dataset. We tested several approaches for the secondary sulfate constraint: a) constraining factor profile only; b) constraining the factor time series during fireworks days only; c) constraining both the factor profile and the entire factor time series; d) constraining the factor profile and the factor time series during fireworks days only. Of the above methods, only c and d yielded secondary sulfate factors without visible mixing from the fireworks period. The approach d was used for PMF analysis as it provides maximum freedom to the algorithm.

In the FD and FH PMF analyses, the sea salt factor profile (*a*-value 0.1) was also constrained from the NFD unconstrained seven-factor PMF analysis. To resolve the unmixed sea salt factor time series from the fireworks, the background Cl concentration was calculated for the fireworks data points (K > 220 ng m^{-3}) only. A Cl concentration < 30 ng m^{-3} was considered as a background Cl concentration, and the fireworks data points were replaced with the linear interpolation between the background Cl concentrations adjacent to the fireworks peaks. In this way 42 % of the data points were interpolated during the fireworks days. The calculated background Cl during the FD was constrained (with *a* -value 0.01) in the sea salt factor time series. After applying all the above four constraints, the FH PMF analysis identified the fireworks factor profile on the basis of the K / S elemental concentration ratio (~2.76) in black powder (Dutcher et al., 1999), and on the concentration peak of 42 µg m^{-3}, which is close to the total elemental concentration peak of 48.4 µg m^{-3} on 1 August 23:00 LT in the factor time series. The FD PMF analysis also identified fireworks factor but the highest peak was 30 µg m^{-3} on 1 August 23:00 LT in the factor time series and the K / S elemental concentration ratio was 2.55 in the factor profile. Therefore, the fireworks factor profile from FH PMF analysis was considered for the final complete dataset PMF analysis. The FD and FH PMF analyses resolved a five-factor solution with secondary sulfate, sea salt, fireworks, background dust and a K-rich factor with fireworks related elements. In the K-rich factor, the K / S ratio was slightly higher (3.56) than the black powder ratio. The common factors resolved by FD, FH and NFD PMF were comparable in terms of factor time series and factor profile.

In the final complete dataset PMF analysis, the factor profiles of fireworks, secondary sulfate and sea salt were constrained (*a*-value 0.1) while the time series of secondary sulfate and the calculated background Cl concentration interpolation were constrained during the fireworks period only (*a*-value 0.01). The solution that best represented the input data was an eight-

factor solution, consisting of factors interpreted as sea salt, secondary sulfate, traffic-related, industrial, two dust-related and fireworks-related (two factors).

Residual analysis (Q-contribution over time series) of the PMF runs showed significant structure in the residuals (Q maximum value was 15 during fireworks period as shown in Fig. S3) for solutions having up to seven factors. Increasing the number of factors to eight gave evidence of structure removal, with mostly random errors remaining, by another fireworks-II factor which was explained by K, S, Ba, Ti, Cu, Bi, while a further increase led to a new mixed factor of traffic-related and background dust which however showed a noisy diurnal pattern (Figs. S1, S2, S3, S4). All the variables were approximately unimodal scaled residuals between ±3 (Paatero and Hopke, 2003) (Fig. S5).

3.3 Uncertainty estimate of PMF results

The statistical and rotational uncertainties were explored by the bootstrap (BS) resampling strategy (Efron, 1979) and the exploration of the *a*-value space of the constrained information as well as random initialization of the unconstrained information. Briefly, the bootstrap algorithm generates new input matrices by randomly resampling variables from the original input matrix. Each newly generated PMF input matrix had a total number of samples equal to the original matrix (456 samples); although some of the original 456 samples were represented several times, while others were not represented at all. A systematic investigation of the *a*-value space in combination with each individual BS run is computationally impractical and was therefore replaced by random initialization of the *a*-value of the secondary sulfate, sea salt and fireworks-I factor profiles between 0 and 0.5 with an increment of 0.1 for 1000 BS runs. Moreover, to avoid rejection of many solutions due to mixing of the sea salt factor time series and the secondary sulfate time series with the fireworks factor peaks, both the sea salt and secondary factor time series (for the fireworks period only) were also constrained with an *a*-value 0.01. The small *a*-value (0.01) for the sea salt and the secondary sulfate factor time series (for the fireworks period only) were estimated based on sensitivity analyses on the *a*-value from 0 to 0.1 with an increment of 0.01. The time series of both factors were showing fireworks peaks during the fireworks period for *a*-values greater than 0.01. Solutions were selected and retained based on the correlation (correlation of coefficient Pearson *r*) of the time series between the factors of the base case and the factors of the BS runs. Solutions with low correlation and some solutions with high correlation have a factor of completely different type, i.e. mixed or split or otherwise altered factor profile/time series based on visual inspection. These kinds of solutions were rejected. This approach was used only for uncertainty assessment rather than uncertainty exploration to find the environmentally reasonable solution.

We also performed separate random bootstrap analyses for 1000 times on the correlation (*r*) between the time series of a base case factor and the respective external marker, e.g. the secondary sulfate factor vs ACSM sulfate, and the traffic-related factor vs NO_x to assess the acceptable uncertainty of the r value. The resulting correlation coefficients were represented in probability density functions (PDF) over 1000 bootstrap runs for both bootstrap analysis methods. In total 86 % of the bootstrap runs were classified as environmentally good solutions. The average *a*-value retained by the selected bootstrap runs was 0.233, 0.255 and 0.241 for the fireworks-I, sea salt and secondary sulfate factor profiles, respectively. The spread of

the *a*-value for these three factors is presented as mean, median and interquartile in the supplement (Fig. S6). The selected solutions factor profiles are represented as box whisker plot in the sequence of p10 (10^{th} percentile), p25 (25^{th} percentile), p50 or median (50^{th} percentile), p75 (75^{th} percentile) and p90 (90^{th} percentile) in Fig. ~~1~~2.

During the non-fireworks period, uncertainties in the source apportionment results are assessed by a bootstrap analysis as described above. However, this approach cannot be used to assess uncertainties in the sea salt and secondary sulfate factors during the fireworks period, as during this period these factor time series are constrained with an artificially low *a*-value selected to optimize deconvolution. For these two factors, uncertainties during the fireworks period are determined by our ability to accurately predict the factor time series. The secondary sulfate and sea salt factors cases are discussed separately below.

Secondary sulfate concentrations during the fireworks period were estimated from the linear fit of the secondary sulfate factor to ACSM sulfate during the entire non-fireworks period. Uncertainties of ±5 % were calculated as the standard deviation of the actual secondary sulfate concentrations to the predicted values and included for the fireworks period only in Fig. 3a.

As described above, the sea salt factor time series during the four-day fireworks period was investigated to determine measurements that were affected or not affected by fireworks, where the measurements determined to be affected were replaced with a linear interpolation between the nearest good points. To determine the uncertainties of this approach, we applied this calculation to random segments of the non-fireworks data. Specifically, the four day-long sequence of affected/non-affected time points determined during the fireworks period was applied to a randomly chosen segment of data, and the standard deviation of measurement data to the estimated values calculated by interpolation was determined. This analysis was repeated for 38 randomly selected locations through the non-fireworks data, and a mean standard deviation of ±42 % was determined. This value is used as the uncertainty of the sea salt factor time series (during the fireworks period only) in Fig. 3a

4 Results and discussion

4.1 Overview of retrieved factors

The solution that best represented the input data was the eight-factor solution. The eight factors from the PMF results are as follows:

1. Two fireworks factors with prominent relative contributions of Bi, Ba, K, S, Ti, Cu and Cl, which are important components of fireworks (Kong et al., 2015; Vecchi et al., 2008);
2. A sea salt factor explaining a large fraction of Cl in the ~~coarse~~ PM_{10} fraction;
3. A secondary sulfate factor mostly dominated by S and highly correlated with ACSM sulfate; (Fig. S1~~7~~);
4. Two dust factors, one dominated by Ca and showing traffic rush hours peaks, and the other dominated by Si without a clear diurnal pattern;

5. A traffic-related factor characterized by Fe, Cr, Cu, Mn, Zn and Ba;
6. An industrial factor showing relatively high contributions of Pb and Zn.

4.2 Detailed factor description

In this section the final results of the elemental PM_{10} source apportionment are presented and validated. Fig. ~~1~~ 2 represents the fractional composition of the factor ~~composition~~ profile ($f_{kj}/\sum_j f_{kj}$) (left y-axis; colored box whisker plots for each factor) and relative contribution ($\sum_i g_{ik}f_{kj}/\sum_k\sum_i g_{ik}f_{kj}$) of each factor to each variable (right y-axis; black box whisker plots). Fig. 3a shows the time series of the ~~absolute~~ factors contributions in ng m^{-3} (bottom panels) and of the relative contributions (top panel) of the retrieved elemental PM_{10} factors. ~~Fig. 2a shows the time series of the absolute mass (bottom panels) and relative contributions (top panel) of the retrieved PM_{10} factors.~~ The variability of these time series across all good solutions was relatively low. Fig. ~~2b~~ 3b reports the averaged total PM_{10} elemental mass (excluding the fireworks factors) and relative contributions of the PM_{10} elemental sources. The reported variabilities/uncertainties (which correspond to the interquartile range among selected bootstrap runs) are an indication of the high stability of the solution. The diurnal variations of the absolute concentrations of the identified factors and some of their corresponding external tracers are presented in Fig. ~~3~~4. CBPF analysis was performed at 90th percentile (Fig. 5) as well as ~~(Fig. S8)~~at different percentile ranges (Fig. S16) to validate some of the identified sources and their characterization.

Fireworks: The fireworks factor profiles and time series are shown in Fig. ~~1~~ 2 and Fig. ~~2a~~ 3a respectively. The fireworks factors are mostly dominated by K, S, Cl, Ti, Cu, Ba and Bi, which are the ~~main~~ chemical elemental species of fireworks (Moreno et al., 2007; Wang et al., 2007; Vecchi et al., 2008; Perrino et al., 2011; Tian et al., 2014; Kong et al., 2015; Lin, 2016; Pongpiachan et al., 2018).~~.~~ Ba and Cu compounds are used to produce green and blue fireworks. The presence of Cl in fireworks-I suggests that the chloride salt might be the main chemical form in the fireworks, such as barium chloride. K is one of the major components of fireworks, which contain 74 % of KNO_3 in black powder as the oxidizing agent for the burning process (Drewnick et al., 2006). The ACSM inorganics concentrations during the fireworks episodes indicate that neither particulate nitrate nor ammonium is generated in the fireworks in significant amounts (Fig. S7). Consistent with previous measurements of submicron fireworks aerosol (Drewnick et al., 2006; Vecchi et al., 2008; Jiang et al., 2015), nitrate was not enhanced during the fireworks period, suggesting conversion of KNO_3 to other forms of nitrogen. The NO_2 / K mass ratio (1.66) on the main fireworks hour (1 August 23:00 LT) (see Fig. S7) is close to the atomic ratio of NO_2 / K (1.17). This measured ratio is also in agreement with the NO_2 / K^+ (2.03) ratio observed during Chinese Spring Festival in Shanghai (Yao et al., 2019). However, the NO_2 and/or NO_x variation was not significant during the fireworks peaks in the present study (Fig. S7), which is in agreement with the former studies (Vecchi et al., 2008; Retama et al., 2019; Yao et al., 2019). The K / S ratio of 2.72 in the fireworks-I factor profile is in good agreement with the K / S elemental concentration ratio (~2.76) in black powder (Dutcher et al., 1999). Other K compounds in black powder can be in the form of perchlorate or chlorate (Wang et al., 2007). Bi is used in crackling stars (Dragon's eggs) in the form of bismuth trioxide or subcarbonate as a non-toxic substitute for toxic lead compounds (Perrino et al., 2011). ~~Bi is used to produce crackling sounds in fireworks~~.

The Ba / K ratio of 0.031-0.054 for fireworks-I and fireworks-II is close to the value 0.057 reported in (Pongpiachan et al., 2018). Fireworks particles are usually present in large amounts in the fine fraction, staying longer in the atmosphere (Richard et al., 2011; Moreno et al., 2007).

~~A pronounced increase in both fireworks factor time series is observed when the fireworks traditionally begin.~~The diurnal patterns of ~~these~~ the fireworks-related elements exhibit a peak at 23:00 LT (or CEST) during the fireworks period (Furger et al., 2017) in accordance with the fireworks-I diurnal variation (Fig. ~~3c~~4c). ~~A pronounced increase in both fireworks factor time series is observed when the fireworks traditionally begin.~~ Both fireworks factors contain two sharp peaks. The fireworks-I factor concentration started to increase on 31 July 2015 22:00 LT and formed the extreme peak within 1 h at 23:00 LT (~5 µg m^{-3}). After that it decayed quickly (10 times lower concentration than maximum fireworks concentration) within 1 h and remained more or less constant until 1 August 2015 21:00 LT. It again started to increase from 22:00 LT and formed a second sharp peak on 1 August 2015 23:00 LT, followed by a gradual decay over the next 6 to 10 h. Fireworks-II presents a slightly different pattern in its time series. It started to increase from 31 July 2015 22:00 LT and depicted its highest peak at 00:00 LT (~3.6 µg m^{-3}) with a quite slow decay until 1 August 2015 06:00 LT. The concentration remained slightly higher than fireworks-I over daytime. It then started to increase again from 1 August 2015 17:00 LT and yielded the highest peak on 2 August 04:00 LT with 6.7 µg m^{-3}. It remained higher until 2 August 2015 08:00 LT and slowly decayed until the afternoon, followed by further prominent peaks at 23:00 LT on 2 August and 3 August. Chemical reactions of KCl with H_2SO_4 will result in a release of gaseous HCl and may explain the absence of particulate Cl in the fireworks-II factor profile. The time series variations in both fireworks suggest that fireworks-I might be related to the main fireworks celebration while fireworks-II might result from burning of leftover crackers after the main fireworks day, as well as the influence of other sources such as bonfires, which are a common activity during Swiss National Day celebrations. Another possibility could be the advection of fireworks clouds from nearby cities where grand firework displays and bonfires are carried out at large scale to celebrate the Swiss National Day. ~~The aging induced by reactions of KCl with acids like HNO_3 may cause the absence of particulate Cl by release of HCl. This could explain the absence of Cl in the fireworks II factor profile.~~ The average relative contributions of fireworks-I and fireworks-II to the analysed mass were 7.4 % and 11 % respectively (Fig. 3b).

Fig. S8~~4~~ represents an estimate of overall fireworks composition and temporal variability, complementing the PMF results~~the fireworks data points for each element~~. A K concentration > 220 ng m^{-3} was used as the criterion to separate fireworks data points (65 data points) from the whole data set. The detailed description is mentioned in the supplement. ~~The mean values (with one standard deviation) of the elements normalized by the averaged values of the total fireworks concentration are presented as box whisker plots (fireworks I factor composition as red dots and fireworks II factor composition as green dots). This figure highlights the fact that m~~Most of the elements are well captured by two fireworks factors, such as S, K, Fe, Cu, Ba etc., since they lie within the fireworks data distribution. In contrast, there are some elements that are not contributing to fireworks, e.g. Ca and Cr, while some elements are explained by only one firework, e.g., Si, Cl and Pb. This indicates that a single fireworks factor is not enough to represent the fireworks data variability.

Sea salt: The sea salt factor was mainly composed of Cl (81 % of the factor ~~composition~~mass) as shown in the factor profile (Fig. ~~1~~2), with no diurnal pattern (Fig. ~~3e~~4e). The average relative contribution of the sea salt factor to the analysed mass was 3.7 % (Fig. ~~2b~~3b). Sea salt also includes Na and Mg, which were not measured by the Xact but analysed by ICP-OES for 24-h offline filters. Based on the high correlation of Na and Cl in a previous study, Cl alone can be used as a marker for sea salt particles (Vallius, 2005). The existence of sea salt particles was confirmed by a low Mg / Na ratio in the ~~24 h~~ filter data, ~~for days with Cl concentration, with Mg / Na~~ equalling 0.13 and 0.16 for 28 July and 30 July, respectively, in line with a ratio of 0.132 to 0.185 for marine aerosol (Chesselet et al., 1972). For the remaining 8 filter samples Mg / Na was higher than 0.18, probably due to absence of sea salt (Fig. ~~S9~~S10). A comparison with ACSM data revealed that Cl was mainly present in the fine fraction (PM_1) during firework days, ~~and mainly in the coarse mode~~ while during the rest of the campaign it was in PM_{10} (Fig. S1~~0~~). The measured Cl / K and Cl / Ca ratios (0.27 and 0.33 respectively) from Xact do not lie in the range of road salt snow samples (150±39 and 103±22, respectively) collected near the roadside (≤50 m) in USA (Williams et al., 2000), which validates our interpretation as a sea salt factor. In addition, the highest Cl concentrations were observed only in the last week of July, with westerly winds at higher wind speed (5–8 m s^{-1}) (Fig. ~~S10~~S11, ~~S11~~S12). This result is in agreement with the CBPF plot where the high concentration of the sea salt factor dominates for westerly winds with high wind speed (Figs. ~~S8~~4, S16), and confirms previous studies (Visser et al., 2015; Twigg et al., 2015).

Dust: The PMF analysis resolved two dust-related factors, i.e., a road dust (Ca-rich) and a background dust (Si-rich) factor, with average relative contributions to the analysed mass of 18 % and 16 %, respectively (Fig. ~~2b~~3b). The road dust factor was mainly composed of Ca (68 % of ~~total~~ the factor ~~composition~~mass) followed by Si (26 %), with relative contributions of 89 % to Ca, 19 % to Si and 12 % to Mn, while the background dust factor highly contributed to Ti, Si, Mn, Fe and Ca, with 65 %, 58 %, 22 %, 16 % and 6 %, respectively. The two dust factors together explain 95 % of Ca, while the remaining factors explain only 5% of Ca. ~~The two dust factors together explain 95 % of Ca, with no other factor explaining more than 93 %.~~ The solution with two dust factors resulted in reduced scaled residuals for Si and Ca compared to a solution with one dust factor (Fig. ~~S12~~S13). The scatter plot of the absolute concentrations of Si and Ca also indicates the presence of two different sources (Fig. ~~S13~~S14). The high relative contribution of Ca in road dust has also been found in other source apportionment studies (Ducret-Stich et al., 2013; Bukowiecki et al., 2010). In general, Ca and Si ~~is~~ are commonly associated with mineral dust, construction activities, vehicular emissions and iron/steel plants (Lee and Pacyna, 1999; Vega et al., 2001; Bukowiecki et al., 2010; Crilley et al., 2016; Maenhaut, 2017). Iron/steel plants produce furnace slacks, a glass-like by-product which consists of Ca, Si, Mg and Al oxides. The higher fraction of crustal elements such as Ca and Si in road dust might be a consequence of the widespread use of asphalt/concrete to make roads (Fullova et al., 2017; Li et al., 2004). The sampling site is located close to the freeway and must be influenced by wear and tear of the asphalt/concrete roads because of heavy traffic. Ca has been associated with construction activities in previous studies (Bernardoni et al., 2011; Crilley et al, 2016), which have been found to peak during the day and decreased to almost zero outside of normal working times (08:00 until 17:00 LT). This evidence is not supported by the road/background dust factor diurnal pattern in this study. Further evidence of non-construction activity is found in the Xact elemental ratio of Ca / S (0.62) which is not in the agreement with

the pure gypsum Ca / S ratio (1.25) used for construction work (Hassan et al., 2014), where they are the main constituents. The background dust factor profile exhibits elements associated with mineral dust, such as Ti, Si and Fe. These and other terrestrial elements are commonly present in soil as oxides (Rudnick and Gao, 2003). The background dust factor also contains a significant fraction of the measured Mn, which is one of the most abundant compounds in the earth's crust, where it occurs in the form of MnO_2 (Taylor and McLennan, 1995). Since the sampling site is adjacent to agricultural fields in the north and west directions, the contribution of these elements to this factor can be expected. A similar background factor with high contributions of Si, Ti and Ca was found by Richard et al. (2011) at an urban site in Switzerland.

The separation of two dust factors is in line with Amato et al. (2009), where ME-2 yielded a road dust factor distinct from a mineral dust factor. The CBPF plot shows that higher concentrations of the road dust factor are associated with the southern wind sector, while the background dust factor is influenced by the southwest and northeast wind sectors (Figs. 5, ~~S8~~S16). The diurnal pattern of the road dust factor shows morning rush hour traffic peaks similar to NO_x, ~~black carbon (~~BC~~)~~, ~~heavy duty vehicle (~~HDV~~)~~ count and traffic-related factor (Fig. ~~3a~~4a, ~~3b~~4b) indicating resuspension of road dust is due to the vehicle fleet. A similar relationship between road dust and the traffic-related source was observed in a previous study (Amato et al., 2009). Resuspension of road dust in the early morning traffic is not triggered by wind speed (Fig. ~~S14~~S15), but by the traffic fleet, whereas in the afternoon, an increase in wind speed leads to resuspension of dust deposited on the road as well as resuspension of agricultural soil dust near the sampling site. Therefore, meteorology plays a vital role for the contribution of the background dust factor.

Traffic-related: The traffic-related factor ~~composition~~ profile was mostly dominated by Fe (73 % of ~~total~~ the factor ~~composition~~mass) and contributed strongly to Cr (96 %), Fe (76 %), Cu (71 %), Mn (50 %), Zn (31 %), Ba (26 %) and Si (12 %). Its average relative contribution to the analysed mass was 20 % (Fig. ~~2b~~3b). Coarse particles from brake/disc wear could appear as flakes and mainly consist of iron oxides (Wahlström et al., 2010). The higher fraction of Fe in the traffic-related source has been found in several previous studies (Visser et al., 2015; Amato et al., 2014a; Bukowiecki et al., 2010; Dall'Osto et al., 2013; Crilley et al., 2016). However, the ratio of Fe to other elements is variable between studies. Fe, Cr, Cu, Zn, Mn and Ba are the most abundant trace elements in brake pads, brake lining and thus attributed to tire/brake wear (Thorpe and Harrison, 2008; Grigoratos and Martini, 2015; Gianini et al., 2012) and engine wear. Si is one of the brake lining components used as abrasive to increase friction, and as fillers to reduce manufacturing costs, respectively (Thorpe and Harrison, 2008; Grigoratos and Martini, 2015). This factor is characterized by a strong diurnal peak coinciding with the morning rush hour at 08:00 LT, similar to NO_x and BC (Fig. ~~3b~~4b). The ~~light duty vehicle (~~LDV~~)~~ and HDV counts start to increase from 05:00 LT (Fig. ~~3a~~4a), ~~-~~unlike the primary traffic emission NO_x and BC. The similar diurnal pattern of this factor might be due to the high braking load for vehicles during peak traffic hours, resulting in increased emissions of vehicle wear particles.

Secondary sulfate: This source is characterized by sulfur (S) and is most likely due to the regional background contribution of secondary sulfate due to conversion of SO_2 to SO_4^{2-}, consistent with the results of many previous source apportionment studies (Dall'Osto et al., 2013; Richard et al., 2011). It explains the highest fraction of S (91 % of ~~total~~ the factor

~~composition~~mass) with relative contributions to S (73%) and Pb (30%) (Fig. ~~1~~2). The average relative contribution of this factor to the analysed mass is 21 % (Fig. ~~2b~~3b). Similar factor profiles were found in previous studies (Visser et al., 2015; Dall'Osto et al., 2013). This factor correlates well with ACSM SO_4^{2-} measurements (r^2 = 0.91), suggesting a dominant contribution from the submicron fraction and thus a slow rate of dry deposition. Combined with SO_2 oxidation processes occurring on timescales of hours to days, it is thus reasonable that the secondary sulfate factor does not exhibit a clear diurnal variation (Fig. ~~3f~~4f) and is consistent with regional rather than local sources. The time series of secondary sulfate exhibits peaks during the fireworks event (Fig. ~~2a~~3a), in agreement with the ACSM SO_4^{2-} time series (Fig. S9~~12~~). The secondary sulfate factor and the ACSM SO_4^{2-} capture the highest peak at midnight on 2 August 2015, while fireworks-I formed a peak at 23:00 LT on 1 August 2015. The time series of ACSM SO_4^{2-} and ACSM NH_4^+ show significant correlation (Fig. ~~S12~~S9), indicating the formation of ammonium sulfate particles except for the main fireworks peaks.

Industrial: This factor is characterised by high relative contributions to Zn (50 %) and Pb (63 %), with a low contribution to the analysed mass (in the order of 3 %, Fig. ~~2b~~3b). The profile is shown in Fig. 2 and the time series in Fig. 3a. The time series contains a few spikes after 4 August, when the wind was predominantly from the south and south-east sector, suggesting an industrial emission. A similar factor profile was observed in previous source apportionment studies (Crilley et al., 2016; Richard et al., 2011) from local point source emissions without any link to specific industrial activities. Amato et al. (2010) and Dall'Osto et al. (2013) also reported a PMF factor with high concentrations of Zn and Pb and attributed it to emissions from smelters in Barcelona, while Vossler et al. (2016) reported a similar factor profile from coal combustion processes in Ostrava. ~~A similar factor profile was observed in previous source apportionment studies (Crilley et al., 2016; Dall'Osto et al., 2013; Richard et al., 2011; Vossler et al., 2016; Amato et al., 2010). The profile is shown in Fig. 1 and time series in Fig. 2a. The time series contains a few spikes after 4 August when the wind was predominantly from the south and south east sector, suggesting industrial emissions.~~ Industrial emissions play a minor role in this study area, as it is surrounded by only a few small scale industrial buildings (logistics businesses approximately 500 m to the north-west, and a wheel manufacturing company to the south-east across the freeway). The CPBF plot confirms the dominance of high concentrations in the south-east direction (Fig. ~~S8~~5). The diurnal cycle shows a clear peak at 10:00 LT (Fig. ~~3g~~4g) which is related to a few peaks.

5 Conclusion

A source apportionment study of elements in PM_{10} measured at a traffic-influenced site in Härkingen, Switzerland; during the summer of 2015 was conducted using the ME-2 implementation of PMF. The PMF model was able to resolve and evaluate the contributions and compositions of eight sources: two fireworks factors, sea salt, secondary sulfate, background dust, road dust, traffic-related, and an industrial source. The use of ME-2 allowed the use of constraints via the *a*-value approach, which improved the factor resolution relative to conventional PMF. We show that the rotational control available in ME-2 provides a means for treating extreme events such as fireworks within a PMF analysis.~~We established that data sets~~

~~including extreme events such as fireworks can be apportioned by ME-2 without disturbing the model solutions~~. This was only achievable when controlling problematic factors, i.e., factors that tend to mix within the constraining technique. Two dust factors with different time profiles and two fireworks factors were identified by the PMF model resulting in better representation of data variability. An S-rich (secondary sulfate) factor, which can typically be attributed to regional background/transported secondary sulfate, was correlated with fine mode non-refractory sulfate measured by an ACSM. The traffic-related factor followed the diurnal pattern of traffic rush hours similar to NO_x and BC with concentrations up to 4 times higher during daytime relative to night-time. This result emphasizes the large influence of highway traffic on the composition of elemental PM_{10}. The small contribution of the industrial factor confirms the low influence of local daily activities from the surroundings.

It was shown that high time resolution elements data sets enable a fully resolved SA, with considerable improvements compared to 24-h filter analysis, where the attribution to specific sources is possible only on a larger time scale and is mostly based on seasonal variations.

Data availability

The datasets are available upon request to the corresponding author.

Author contribution

PR performed SA analysis and wrote the manuscript. MF, RF and CH performed measurement. MF and RF analysed data for Xact and ACSM, respectively. FC provided expertise on software for SA analysis. MCM provided ICP-MS and ICP-AES analysis data. KP lent Xact® 625 for measurement. UB, ASHP, MF, FC and JS were involved with the supervision and conceptualisation. All authors commented on the paper and assisted in the interpretation of the results.

Competing interests

Krag Petterson is employed by Cooper Environmental Services, the manufacturer of the Xact® 625.

Acknowledgements

This study has been funded by the Swiss National Science Foundation (SNSF grants 200021_162448/1 and BSSGI0_155846), and by the Swiss Federal Office for the Environment (FOEN). We thank René Richter and Roland Scheidegger of PSI for their technical support during the measurement campaign. We are grateful to Chris Koch and Varun Yadav of Cooper Environmental Services for instructions on the instrument and numerous technical discussions. We thank the operators of the NABEL station for providing all kinds of support during the measurements.

References

Amato, F., Pandolfi, M., Escrig, A., Querol, X., Alastuey, A., Pey, J., Perez, N., and Hopke, P. K.: Quantifying road dust resuspension in urban environment by Multilinear Engine: A comparison with PMF2, Atmos. Environ., 43, 2770–2780, https://doi.org/10.1016/j.atmosenv.2009.02.039, 2009.

Amato, F., Nava, S., Lucarelli, F., Querol, X., Alastuey, A., Baldasano, J. M., and Pandolfi, M.: A comprehensive assessment of PM emissions from paved roads: Real-world emission factors and intense street cleaning trials, Sci. Total Environ., 408, 4309–4318, https://doi.org/10.1016/j.scitotenv.2010.06.008, 2010.

Amato, F., Pandolfi, M., Moreno, T., Furger, M., Pey, J., Alastuey, A., Bukowiecki, N., Prevot, A. S. H., Baltensperger, U., and Querol, X.: Sources and variability of inhalable road dust particles in three European cities, Atmos. Environ., 45, 6777–6787, https://doi.org/10.1016/j.atmosenv.2011.06.003, 2011.

Amato, F., Alastuey, A., de la Rosa, J., Sánchez de la Campa, A. M., Pandolfi, M., Lozano, A., Contreras González, J., and Querol, X.: Trends of road dust emissions contributions on ambient air particulate levels at rural, urban and industrial sites in southern Spain, Atmos. Chem. Phys., 14, 3533–3544, https://doi.org/10.5194/acp-14-3533-2014, 2014a.

Amato, F., Cassee, F. R., Denier van der Gon, H. A. C., Gehrig, R., Gustafsson, M., Hafner, W., Harrison, R. M., Jozwicka, M., Kelly, F. J., Moreno, T., Prevot, A. S. H., Schaap, M., Sunyer, J., and Querol, X.: Urban air quality: The challenge of traffic non-exhaust emissions, J. Hazard. Mater., 275, 31–36, https://doi.org/10.1016/j.jhazmat.2014.04.053, 2014b.

Ancelet, T., Davy, P. K., Mitchell, T., Trompetter, W. J., Markwitz, A., and Weatherburn, D. C.: Identification of particulate matter sources on an hourly time-scale in a wood burning community, Environ. Sci. Technol., 46, 4767–4774, https://doi.org/10.1021/es203937y, 2012.

Bernardoni, V., Vecchi, R., Valli, G., Piazzalunga, A., and Fermo, P.: PM_{10} source apportionment in Milan (Italy) using time-resolved data, Sci. Total Environ., 409, 4788–4795, https://doi.org/10.1016/j.scitotenv.2011.07.048, 2011.

Bozzetti, C., Daellenbach, K. R., Hueglin, C., Fermo, P., Sciare, J., Kasper-Giebl, A., Mazar, Y., Abbaszade, G., El Kazzi, M., Gonzalez, R., Shuster-Meiseles, T., Flasch, M., Wolf, R., Křepelová, A., Canonaco, F., Schnelle-Kreis, J., Slowik, J. G., Zimmermann, R., Rudich, Y., Baltensperger, U., El Haddad, I., and Prévôt, A. S. H.: Size-resolved identification, characterization, and quantification of primary biological organic aerosol at a European rural site, Environ. Sci. Technol., 50, 3425–3434, https://doi.org/10.1021/acs.est.5b05960, 2016.

Brauer, M., Hoek, G., Vliet, P. V., Meliefste, K., Fischer, P. H., Wijga, A., Koopman, L. P., Neijens, H. J., Gerritsen, J., Kerkhof, M., Heinrich, J., Bellander, T., and Brunekreef, B.: Air pollution from traffic and the development of respiratory

infections and asthmatic and allergic symptoms in children, Am. J. Respir. Crit. Care Med., 166, 1092–1098, https://doi.org/10.1164/rccm.200108-007OC, 2002.

Bukowiecki, N., Lienemann, P., Zwicky, C. N., Furger, M., Richard, A., Falkenberg, G., Rickers, K., Grolimund, D., Borca, C., Hill, M., Gehrig, R., and Baltensperger, U.: X-ray fluorescence spectrometry for high throughput analysis of atmospheric aerosol samples: The benefits of synchrotron X-rays, Spectrochim. Acta B, 63, 929–938, https://doi.org/10.1016/j.sab.2008.05.006, 2008.

Bukowiecki, N., Lienemann, P., Hill, M., Figi, R., Richard, A., Furger, M., Rickers, K., Falkenberg, G., Zhao, Y., Cliff, S. S., Prévôt, A. S. H., Baltensperger, U., Buchmann, B., and Gehrig, R.: Real-world emission factors for antimony and other brake wear related trace elements: size-segregated values for light and heavy duty vehicles, Environ. Sci. Technol., 43, 8072–8078, https://doi.org/10.1021/es9006096, 2009.

Bukowiecki, N., Lienemann, P., Hill, M., Furger, M., Richard, A., Amato, F., Prévôt, A. S. H., Baltensperger, U., Buchmann, B., and Gehrig, R.: PM_{10} emission factors for non-exhaust particles generated by road traffic in an urban street canyon and along a freeway in Switzerland, Atmos. Environ., 44, 2330–2340, https://doi.org/10.1016/j.atmosenv.2010.03.039, 2010.

Cakmak, S., Dales, R., Kauri, L. M., Mahmud, M., Ryswyk, K. V., Vanos, J., Liu, L., Kumarathasan, P., Thomson, E., Vincent, R., and Weichenthal, S.: Metal composition of fine particulate air pollution and acute changes in cardiorespiratory physiology, Environ. Pollut., 189, 208–214, https://doi.org/10.1016/j.envpol.2014.03.004, 2014.

Canonaco, F., Crippa, M., Slowik, J. G., Baltensperger, U., and Prévôt, A. S. H.: SoFi, an IGOR-based interface for the efficient use of the generalized multilinear engine (ME-2) for the source apportionment: ME-2 application to aerosol mass spectrometer data, Atmos. Meas. Tech., 6, 3649–3661, https://doi.org/10.5194/amt-6-3649-2013, 2013.

Carslaw, D. C. and Beevers, S. D.: Characterising and understanding emission sources using bivariate polar plots and k-means clustering, Environ. Modell. Softw., 40, 325–329, https://doi.org/10.1016/j.envsoft.2012.09.005, 2013.

Cesari, D., Genga, A., Ielpo, P., Siciliano, M., Mascolo, G., Grasso, F. M., and Contini, D.: Source apportionment of $PM_{2.5}$ in the harbour-industrial area of Brindisi (Italy): Identification and estimation of the contribution of in-port ship emissions, Sci. Total Environ., 497–498, 392–400, https://doi.org/10.1016/j.scitotenv.2014.08.007, 2014.

Chan, D. and Stachowiak, G. W.: Review of automotive brake friction materials, Proc Inst. Mech. Eng. Part D: J Automob. Eng., 218, 953–966, https://doi.org/10.1243/0954407041856773, 2004.

Chang, Y., Huang, K., Xie, M., Deng, C., Zou, Z., Liu, S., and Zhang, Y.: First long-term and near real-time measurement of trace elements in China's urban atmosphere: temporal variability, source apportionment and precipitation effect, Atmos. Chem. Phys., 18, 11793–11812, https://doi.org/10.5194/acp-18-11793-2018, 2018.

Chesselet, R., Morelli, J., and Buat-Menard, P.: Variations in ionic ratios between reference sea water and marine aerosols, J. Geophys. Res., 77, 5116–5131, https://doi.org/10.1029/JC077i027p05116, 1972.

Crenn, V., Sciare, J., Croteau, P. L., Verlhac, S., Fröhlich, R., Belis, C. A., Aas, W., Äijälä, M., Alastuey, A., Artiñano, B., Baisnée, D., Bonnaire, N., Bressi, M., Canagaratna, M., Canonaco, F., Carbone, C., Cavalli, F., Coz, E., Cubison, M. J., Esser-Gietl, J. K., Green, D. C., Gros, V., Heikkinen, L., Herrmann, H., Lunder, C., Minguillón, M. C., Močnik, G., O'Dowd, C. D., Ovadnevaite, J., Petit, J.-E., Petralia, E., Poulain, L., Priestman, M., Riffault, V., Ripoll, A., Sarda-Estève, R., Slowik, J. G., Setyan, A., Wiedensohler, A., Baltensperger, U., Prévôt, A. S. H., Jayne, J. T., and Favez, O.: ACTRIS ACSM intercomparison – Part 1: Reproducibility of concentration and fragment results from 13 individual Quadrupole Aerosol Chemical Speciation Monitors (Q-ACSM) and consistency with co-located instruments, Atmos. Meas. Tech., 8, 5063–5087, https://doi.org/10.5194/amt-8-5063-2015, 2015.

Crilley, L. R., Lucarelli, F., Bloss, W. J., Harrison, R. M., Beddows, D. C., Calzolai, G., Nava, S., Valli, G., Bernardoni, V., and Vecchi, R.: Source apportionment of fine and coarse particles at a roadside and urban background site in London during the 2012 summer ClearfLo campaign, Environ. Pollut., 220, 766–778, https://doi.org/10.1016/j.envpol.2016.06.002, 2016.

Cooper, J. A., Petterson, K., Geiger, A., Siemers, A., and Rupprecht, B.: Guide for developing a multi-metals, fenceline monitoring plan for fugitive emissions using X-ray based monitors, Cooper Environmental Services, Portland, Oregon, 1–42, 2010.

Dall'Osto, M., Querol, X., Amato, F., Karanasiou, A., Lucarelli, F., Nava, S., Calzolai, G., and Chiari, M.: Hourly elemental concentrations in $PM_{2.5}$ aerosols sampled simultaneously at urban background and road site during SAPUSS – diurnal variations and PMF receptor modelling, Atmos. Chem. Phys., 13, 4375–4392, https://doi.org/10.5194/acp-13-4375-2013, 2013.

Dao, L., Morrison, L., and Zhang, C.: Bonfires as a potential source of metal pollutants in urban soils, Galway, Ireland, Appl. Geochem., 27, 930–935, https://doi.org/10.1016/j.apgeochem.2012.01.010, 2012.

Dockery, D. W., Pope III, C. A., Xu, X., Spengler, J. D., Ware, J. H., Fay, M. E., Ferris, B. G., and Speizer, F. E.: An association between air pollution and mortality in six U.S. cities, The New England J. Med., 329, 1753–1759, https://doi.org/10.1056/NEJM199312093292401, 1993.

Drewnick, F., Hings, S. S., Curtius, J., Eerdekens, G., and Williams, J.: Measurement of fine particulate and gas-phase species during the New Year's fireworks 2005 in Mainz, Germany, Atmos. Environ., 40, 4316–4327, https://doi.org/10.1016/j.atmosenv.2006.03.040, 2006.

Ducret-Stich, R. E., Tsai, M.-Y., Thimmaiah, D., Kunzli, N., Hopke, P. K., and Phuleria, H. C.: PM_{10} source apportionment in a Swiss Alpine valley impacted by highway traffic, Environ. Sci. Pollut. Res., 20, 6496–6508, https://doi.org/10.1007/s11356-013-1682-1, 2013.

Dutcher, D. D., Perry, K. D., Cahill, T. A., and Copeland, S. A.: Effects of indoor pyrotechnic displays on the air quality in the Houston Astrodome, J. Air Waste Manage. Assoc., 49, 156–160, https://doi.org/10.1080/10473289.1999.10463790, 1999.

Efron, B.: Bootstrap methods: Another look at the Jacknife, The Ann. Stat., 7, 1–26, 1979.

Empa: Technischer Bericht zum Nationalen Beobachtungsnetz für Luftfremdstoffe (NABEL), available at: http//www.empa.ch, 2011.

Fang, T., Guo, H., Verma, V., Peltier, R. E., and Weber, R. J.: $PM_{2.5}$ water-soluble elements in the southeastern United States: automated analytical method development, spatiotemporal distributions, source apportionment, and implications for health studies, Atmos. Chem. Phys., 15, 11667–11682, https://doi.org/10.5194/acp-15-11667-2015, 2015.

Fullova, D., Durcanska, D., and Hegrova, J.: Particulate matter mass concentrations produced from pavement surface abrasion, MATEC Web of Conferences, 117, 00048, https://doi.org/10.1051/matecconf/201711700048, 2017.

Furger, M., Minguillón, M. C., Yadav, V., Slowik, J. G., Hüglin, C., Fröhlich, R., Petterson, K., Baltensperger, U., and Prévôt, A. S. H.: Elemental composition of ambient aerosols measured with high temporal resolution using an online XRF spectrometer, Atmos. Meas.Tech., 10, 2061–2076, https://doi.org/10.5194/amt-10-2061-2017, 2017.

Gianini, M. F. D., Fischer, A., Gehrig, R., Ulrich, A., Wichser, A., Piot, C., Besombes, J.-L., and Hueglin, C.: Comparative source apportionment of PM_{10} in Switzerland for 2008/2009 and 1998/1999 by positive matrix factorisation, Atmos. Environ., 54, 149–158, https://doi.org/10.1016/j.atmosenv.2012.02.036, 2012.

Grigoratos, T. and Martini, G.: Brake wear particle emissions: a review, Environ. Sci. Pollut. Res., 22, 2491–2504, https://doi.org/10.1007/s11356-014-3696-8, 2015.

Harrison, R. M., Beddows, D. C. S., and Dall'Osto, M.: PMF analysis of wide-range particle size spectra collected on a major highway, Environ. Sci. Technol., 45, 5522–5528, https://doi.org/10.1021/es2006622, 2011.

Hassan, A. K., Fares, S., and Abd El-Rahma, M.: Natural radioactivity levels and radiation hazards for gypsum materials used in Egypt. J. Environ. Sci. Technol., 7, 56–66, https://doi.org/10.3923/jest.2014.56.66, 2014.

Hedberg, E., Gidhagen, L., and Johansson, C.: Source contributions to PM_{10} and arsenic concentrations in Central Chile using positive matrix factorization, Atmos. Environ., 39, 549–561, https://doi.org/10.1016/j.atmosenv.2004.11.001, 2005.

Hueglin, C., Buchmann, B., and Weber, R. O.: Long-term observation of real-world road traffic emission factors on a motorway in Switzerland, Atmos. Environ., 40, 3696–3709, https://doi.org/10.1016/j.atmosenv.2006.03.020, 2006.

Jeong, C.-H., Wang, J. M., and Evans, G. J.: Source Apportionment of Urban Particulate Matter using Hourly Resolved Trace Metals, Organics, and Inorganic Aerosol Components, Atmos. Chem. Phys. Discuss., https://doi.org/10.5194/acp-2016-189, 2016.

Jeong, C.-H., Wang, J. M., Hilker, N., Debosz, J., Sofowote, U., Su, Y., Noble, M., Healy, R. M., Munoz, T., Dabek-Zlotorzynska, E., Celo, V., White, L., Audette, C., Herod, D., and Evans, G. J.: Temporal and spatial variability of traffic-related $PM_{2.5}$ sources: Comparison of exhaust and non-exhaust emissions, Atmos. Environ., 198, 55–69, https://doi.org/10.1016/j.atmosenv.2018.10.038, 2019.

Ji, D., Cui, Y., Li, L., He, J., Wang, L., Zhang, H., Wang, W., Zhou, L., Maenhaut, W., Wen, T., and Wang, Y.: Characterization and source identification of fine particulate matter in urban Beijing during the 2015 Spring Festival, Sci. Total Environ., 430–440, 628–629, https://doi.org/10.1016/j.scitotenv.2018.01.304, 2018.

Jiang, Q., Sun, Y. L., Wang, Z., and Yin, Y.: Aerosol composition and sources during the Chinese Spring Festival: fireworks, secondary aerosol, and holiday effects, Atmos. Chem. Phys., 15, 6023–6034, https://doi.org/10.5194/acp-15-6023-2015, 2015.

Kelly, F. J. and Fussell, J. C.: Air pollution and airway disease, Clin. Exp. Allergy, 41, 1059–1071, https://doi.org/10.1111/j.1365-2222.2011.03776.x, 2011.

Kelly, F. J. and Fussell, J. C.: Size, source and chemical composition as determinants of toxicity attributable to ambient particulate matter, Atmos. Environ., 60, 504–526, https://doi.org/10.1016/j.atmosenv.2012.06.039, 2012.

Kidwell, C. B. and Ondov, J. M.: Development and evaluation of a prototype system for collecting sub-hourly ambient aerosol for chemical analysis, Aerosol Sci. Technol., 35, 596–601, https://doi.org/10.1080/02786820118049, 2001.

Kim, E. and Hopke, P. K.: Source identifications of airborne fine particles using positive matrix factorization and U.S. Environmental Protection Agency positive matrix factorization, J. Air Waste Manage. Assoc., 57, 7, 811–819, https://doi.org/10.3155/1047-3289.57.7.811, 2007.

Kim, E., Hopke, P. K., and Edgerton, E. S.: Source identification of Atlanta aerosol by positive matrix factorization, J. Air Waste Manage. Assoc., 53, 731–739, https://doi.org/10.1080/10473289.2003.10466209, 2003.

Kim, E., Hopke, P. K., and Qin, Y.: Estimation of organic carbon blank values and error structures of the speciation trends network data for source apportionment, J. Air Waste Manage. Assoc., 55, 8, 1190–1199, https://doi.org/10.1080/10473289.2005.10464705, 2005.

Kong, S. F., Li, L., Li, X. X., Yin, Y., Chen, K., Liu, D. T., Yuan, L., Zhang, Y. J., Shan, Y. P., and Ji, Y. Q.: The impacts of firework burning at the Chinese Spring Festival on air quality: insights of tracers, source evolution and aging processes, Atmos. Chem. Phys., 15, 2167–2184, https://doi.org/10.5194/acp-15-2167-2015, 2015.

Lanz, V. A., Prévôt, A. S. H., Alfarra, M. R., Weimer, S., Mohr, C., DeCarlo, P. F., Gianini, M. F. D., Hueglin, C., Schneider, J., Favez, O., D'Anna, B., George, C., and Baltensperger, U.: Characterization of aerosol chemical composition with aerosol mass spectrometry in Central Europe: an overview, Atmos. Chem. Phys., 10, 10453–10471, https://doi.org/10.5194/acp-10-10453-2010, 2010.

Lawrence, S., Sokhi, R., Ravindra, K., Mao, H., Prain, H. D., and Bull, I. D.: Source apportionment of traffic emissions of particulate matter using tunnel measurements, Atmos. Environ., 77, 548–557, https://doi.org/10.1016/j.atmosenv.2013.03.040, 2013.

Lee, D. S. and Pacyna, J. M.: An industrial emissions inventory of calcium for Europe, Atmos. Environ. 33, 1687–1697, https://doi.org/10.1016/S1352-2310(98)00286-6, 1999.

Li, Z., Hopke, P. K., Husain, L., Qureshi, S., Dutkiewicz, V. A., Schwab, J. J., Drewnick, F., and Demerjian, K. L.: Sources of fine particle composition in New York city, Atmos. Environ., 38, 6521–6529, https://doi.org/10.1016/j.atmosenv.2004.08.040, 2004.

Lin, C.-C.: A review of the impact of fireworks on particulate matter in ambient air, J. Air Waste Manage. Assoc., 66, 12, 1171–1182, https://doi.org/10.1080/10962247.2016.1219280, 2016.

Lin, Y.-C., Tsai, C.-J., Wu, Y.-C., Zhang, R., Chi, K.-H., Huang, Y.-T., Lin, S.-H., and Hsu, S.-C.: Characteristics of trace metals in traffic-derived particles in Hsuehshan Tunnel, Taiwan: size distribution, potential source, and fingerprinting metal ratio, Atmos. Chem. Phys., 15, 4117–4130, https://doi.org/10.5194/acp-15-4117-2015, 2015.

Liu, Y., Zheng, M., Yu, M., Cai, X., Du, H., Li, J., Zhou, T., Yan, C., Wang, X., Shi, Z., Harrison, R. M., Zhang, Q., and He, K.: High-time-resolution source apportionment of $PM_{2.5}$ in Beijing with multiple models, Atmos. Chem. Phys., 19, 6595–6609, https://doi.org/10.5194/acp-19-6595-2019, 2019.

Lucarelli, F., Nava, S., Calzolai, G., Chiari, M., Udisti, R., and Marino, F.: Is PIXE still a useful technique for the analysis of atmospheric aerosols? The LABEC experience, X-Ray Spectrom., 40, 162–167, https://doi.org/10.1002/xrs.1312, 2011.

Manousakas, M., Diapouli, E., Papaefthymiou, H., Migliori, A., Karydas, A. G., Padilla-Alvarez, R., Bogovac, M., Kaiser, R. B., Jaksic, M., Bogdanovic-Radovic, I., and Eleftheriadis, K.: Source apportionment by PMF on elemental concentrations obtained by PIXE analysis of PM_{10} samples collected at the vicinity of lignite power plants and mines in Megalopolis, Greece, Nucl. Instr. Meth. Phys. Res. Sec. B, 349, 114–124, https://doi.org/10.1016/j.nimb.2015.02.037, 2015.

Maenhaut, W.: Source apportionment revisited for long-term measurements of fine aerosol trace elements at two locations in southern Norway, Nucl. Instrum. Methods Phys. Res. Sect. B, 417, 133–138 https://doi.org/10.1016/j.nimb.2017.07.006, 2017.

Meister, K., Johansson, C., and Forsberg, B.: Estimated short-term effects of coarse particles on daily mortality in Stockholm, Sweden, Environ. Health Perspect., 120, 431–436, https://doi.org/10.1289/ehp.1103995, 2012.

Minguillon, M. C., Querol, X., Baltensperger, U., and Prévôt, A. S. H.: Fine and coarse PM composition and sources in rural and urban sites in Switzerland: local or regional pollution?, Sci. Total Environ., 427–428, 191–202, https://doi.org/10.1016/j.scitotenv.2012.04.030, 2012.

Moreno, T., Querol, X., Alastuey, A., Minguillón, M. C., Pey, J., Rodriguez, S., Miró, J. V., Felis, C., and Gibbons, W.: Recreational atmospheric pollution episodes: Inhalable metalliferous particles from firework displays, Atmos. Environ., 41, 913–922, https://doi.org/10.1016/j.atmosenv.2006.09.019, 2007.

Ng, N. L., Herndon, S. C., Trimborn, A., Canagaratna, M. R., Croteau, P. L., Onasch, T. B., Sueper, D., Worsnop, D. R., Zhang, Q., Sun, Y. L., and Jayne, J. T.: An aerosol chemical speciation monitor (ACSM) for routine monitoring of the composition and mass concentrations of ambient aerosol, Aerosol Sci. Technol., 45, 780–794, https://doi.org/10.1080/02786826.2011.560211, 2011.

Norris, G., Duvall, R., Brown, S., and Bai, S.: EPA Positive Matrix Factorization (PMF) 5.0 fundamentals and user guide prepared for the United States Environmental Protection Agency Office of Reseach and Development, Washington DC, 2014.

Paatero, P.: The Multilinear Engine – A table-driven, least squares program for solving multilinear problems, including the n-way parallel factor analysis model, J. Comput. Graph. Stat., 8, 854–888, https://doi.org/10.1080/10618600.1999.10474853-1999, 1999.

Paatero, P. and Hopke, P. K.: Discarding or downweighting high-noise variables in factor analytic models, Anal. Chim. Acta, 490, 277–289, https://doi.org/10.1016/s0003-2670(02)01643-4, 2003.

Paatero, P. and Tapper, U.: Positive matrix factorization: A non-negative factor model with optimal utilization of error-estimates of data values, Environmetrics, 5, 111–126, https://doi.org/10.1002/env.3170050203, 1994.

Park, S. S., Cho, S. Y., Jo, M. R., Gong, B. J., Park, J. S., and Lee, S. J.: Field evaluation of a near-real time elemental monitor and identification of element sources observed at an air monitoring supersite in Korea, Atmos. Poll. Res., 5, 119–128, https://doi.org/10.5094/apr.2014.015-2014, 2014.

Perrino, C., Tiwari, S., Catrambone, M., Torre, S. D., Rantica, E., and Canepari, S.: Chemical characterization of atmospheric PM in Delhi, India, during different periods of the year including Diwali festival, Atmos. Pollut. Res., 2, 418–427, https://doi.org/10.5094/apr.2011.048, 2011.

Phillips-Smith, C., Jeong, C.-H., Healy, R. M., Dabek-Zlotorzynska, E., Celo, V., Brook, J. R., and Evans, G.: Sources of particulate matter components in the Athabasca oil sands region: investigation through a comparison of trace element measurement methodologies, Atmos. Chem. Phys., 17, 9435–9449, https://doi.org/10.5194/acp-17-9435–2017, 2017.

Polissar, A. V., Hopke, P. K., Paatero, P., Malm, W. C., and Sisler, J. F.: Atmospheric aerosol over Alaska: 2. Elemental composition and sources, J. Geophys. Res., 103, 19045–19057, https://doi.org/10.1029/98JD01212, 1998.

Pongpiachan, S., Iijima, A., and Cao, J.: Hazard quotients, hazard indexes, and cancer risks of toxic metals in PM_{10} during firework displays, Atmosphere, 9, 144, https://doi.org/10.3390/atmos9040144, 2018.

Pope III, C. A. and Dockery, D. W.: Health effects of fine particulate air pollution: Lines that connect, J. Air Waste Manage. Assoc., 56, 709–742, https://doi.org/10.1080/10473289.2006.10464485, 2006.

Rahman, S. A., Hamzah, M. S., Wood, A. K., Elias, M. S., Salim, N. A. A., and Sanuri, E.: Sources apportionment of fine and coarse aerosol in Klang Valley, Kuala Lumpur using positive matrix factorization, Atmos. Poll. Res., 2, 197–206, https://doi.org/10.5094/apr.2011.025, 2011.

Rai, P., Chakraborty, A., Mandariya, A. K., and Gupta, T.: Composition and source apportionment of PM_1 at urban site Kanpur in India using PMF coupled with CBPF, Atmos. Res., 178–179, 506–520, https://doi.org/10.1016/j.atmosres.2016.04.015, 2016.

Reff, A., Eberly, S. I., and Bhave, P. V.: Receptor modeling of ambient particulate matter data using positive matrix factorization: Review of existing methods, J. Air Waste Manage. Assoc., 57, 146–154, https://doi.org/10.1080/10473289.2007.10465319, 2007.

Retama, A., Neria-Hernández, A., Jaimes-Palomera, M., Rivera-Hernández, O., Sánchez-Rodríguez, M., López-Medina, A., and Velasco, E.: Fireworks: a major source of inorganic and organic aerosols during Christmas and New Year in Mexico city, Atmos. Environ., 2, 100013, https://doi.org/10.1016/j.aeaoa.2019.100013, 2019.

Richard, A., Gianini, M. F. D., Mohr, C., Furger, M., Bukowiecki, N., Minguillón, M. C., Lienemann, P., Flechsig, U., Appel, K., DeCarlo, P. F., Heringa, M. F., Chirico, R., Baltensperger, U., and Prévôt, A. S. H.: Source apportionment of size and time resolved trace elements and organic aerosols from an urban courtyard site in Switzerland, Atmos. Chem. Phys., 11, 8945–8963, https://doi.org/10.5194/acp-11-8945-2011, 2011.

Rudnick, R. L. and Gao, S.: Composition of the continental crust, Vol. 3, edited by: Rudnick, E., Book Section 2, 1–56, Elsevier Science, Philadelphia, 2003.

Schauer, J. J., Lough, G. C., Shafer, M. M, Christensen, W. C., Arndt, M. F., DeMinter, J. T., and Park, J. S.: Characterization of emissions of metals emitted from motor vehicles, Research report (Health Effects Institute), 133, 1–76; discussion 77, 2006.

Taylor, S. R. and McLennan, S. M.: The geochemical evolution of the continental crust, Rev. Geophys., 33, 241–265, 1995.

Thorpe, A. and Harrison, R. M.: Sources and properties of non-exhaust particulate matter from road traffic: A review, Sci. Total Environ., 400, 270–282, https://doi.org/10.1016/j.scitotenv.2008.06.007, 2008.

Tian, S. L., Pan, Y. P., and Wang, Y. S.: Size-resolved source apportionment of particulate matter in urban Beijing during haze and non-haze episodes, Atmos. Chem. Phys., 16, 1–19, https://doi.org/10.5194/acp-16-1-2016, 2016.

Tian, Y. Z., Wang, J., Peng, X., Shi, G. L., and Feng, Y. C.: Estimation of the direct and indirect impacts of fireworks on the physicochemical characteristics of atmospheric PM_{10} and $PM_{2.5}$, Atmos. Chem. Phys., 14, 9469–9479, https://doi.org/10.5194/acp-14-9469-2014, 2014.

Tremper, A. H., Font, A., Priestman, M., Hamad, S. H., Chung, T.-C., Pribadi, A., Brown, R. J. C., Goddard, S. L., Grassineau, N., Petterson, K., Kelly, F. J., and Green, D. C.: Field and laboratory evaluation of a high time resolution X-ray fluorescence instrument for determining the elemental composition of ambient aerosols, Atmos. Meas. Tech., 11, 3541–3557, https://doi.org/10.5194/amt-11-3541-2018, 2018.

Twigg, M. M., Di Marco, C. F., Leeson, S., van Dijk, N., Jones, M. R., Leith, I. D., Morrison, E., Coyle, M., Proost, R., Peeters, A. N. M., Lemon, E., Frelink, T., Braban, C. F., Nemitz, E., and Cape, J. N.: Water soluble aerosols and gases at a UK background site – Part 1: Controls of $PM_{2.5}$ and PM_{10} aerosol composition, Atmos. Chem. Phys., 15, 8131–8145, https://doi.org/10.5194/acp-15-8131-2015, 2015.

Ulbrich, I. M., Canagaratna, M. R., Zhang, Q., Worsnop, D. R., and Jimenez, J. L.: Interpretation of organic components from positive matrix factorization of aerosol mass spectrometric data, Atmos. Chem. Phys., 9, 2891–2918, https://doi.org/10.5194/acp-9-2891-2009, 2009.

Vallius, M.: Characteristics and sources of fine particulate matter in urban air. Ph.D. dissertation. Publications of the National Public Health Institute, Department of Environmental Health Kuopio, Finland, 2005.

Vecchi, R., Bernardoni, V., Cricchio, D., D'Alessandro, A., Fermo, P., Lucarelli, F., Nava, S., Piazzalunga, A., and Valli, G.: The impact of fireworks on airborne particles, Atmos. Environ., 42, 1121–1132, https://doi.org/10.1016/j.atmosenv.2007.10.047, 2008.

Vega, E., Mugica, V., Reyes, E., Sanchez, G., Chow, J. C., and Watson, J. G.: Chemical composition of fugitive dust emitters in Mexico City, Atmos. Environ., 35, 4033–4039, https://doi.org/10.1016/S1352-2310(01)00164-9, 2001.

Visser, S., Slowik, J. G., Furger, M., Zotter, P., Bukowiecki, N., Canonaco, F., Flechsig, U., Appel, K., Green, D. C., Tremper, A. H., Young, D. E., Williams, P. I., Allan, J. D., Coe, H., Williams, L. R., Mohr, C., Xu, L., Ng, N. L., Nemitz, E., Barlow, J. F., Halios, C. H., Fleming, Z. L., Baltensperger, U., and Prévôt, A. S. H.: Advanced source apportionment of size-resolved trace elements at multiple sites in London during winter, Atmos. Chem. Phys., 15, 11291–11309, https://doi.org/10.5194/acp-15-11291-2015, 2015.

Vossler, T., Černikovský, L., Novák, J., and Williams, R.: Source apportionment with uncertainty estimates of fine particulate matter in Ostrava, Czech Republic using positive matrix factorization, Atmos. Pollut. Res., 7, 503–512, https://doi.org/10.1016/j.apr.2015.12.004, 2016.

Wahlström, J., Olander, L., and Olofsson, U.: Size, shape, and elemental composition of airborne wear particles from disc brake materials, Tribol. Lett., 38, 15–24, 2010.

Wang, Q., Qiao, L., Zhou, M., Zhu, S., Griffith, S., Li, L., and Yu, J. Z: Source apportionment of $PM_{2.5}$ using hourly measurements of elemental tracers and major constituents in an urban environment: investigation of time-resolution influence, J. Geophys. Res. : Atmos., 123, 5284–5300, https://doi.org/10.1029/2017JD027877, 2018.

Wang, Y., Zhuang, G., Xu, C., and An, Z.: The air pollution caused by the burning of fireworks during the lantern festival in Beijing, Atmos. Environ., 41, 417–431, https://doi.org/10.1016/j.atmosenv.2006.07.043, 2007.

Williams, A. L., Stensland, G. J., Peters, C. R., and Osborne, J.: Atmospheric dispersion study of deicing salt applied to roads: first progress report, Illinois State Water Surv. Contract Report, 2000-05, Champaign, IL, 2000.

Yao, L., Wang, D., Fu, Q., Qiao, L., Wang, H., Li, L., Sun, W., Li, Q., Wang, L., Yang, X., Zhao, Z., Kan, H., Xian, A., Wang, G., Xiao, H., and Chen, J.: The effects of firework regulation on air quality and public health during the Chinese Spring Festival from 2013 to 2017 in a Chinese megacity, Environ. Int., 126, 96–106, https://doi.org/10.1016/j.envint.2019.01.037, 2019.

Yu, L., Wang, G., Zhang, R., Zhang, L., Song, Y., Wu, B., Li, X., An, K., and Chu, J.: Characterization and source apportionment of $PM_{2.5}$ in an urban environment in Beijing, Aerosol Air Qual. Res., 13, 574–583, https://doi.org/10.4209/aaqr.2012.07.0192, 2013.

Zhang, R., Jing, J., Tao, J., Hsu, S.-C., Wang, G., Cao, J., Lee, C. S. L., Zhu, L., Chen, Z., Zhao, Y., and Shen, Z.: Chemical characterization and source apportionment of $PM_{2.5}$ in Beijing: seasonal perspective, Atmos. Chem. Phys., 13, 7053–7074, https://doi.org/10.5194/acp-13-7053-2013, 2013.

Zhao, W. and Hopke, P. K.: Source apportionment for ambient particles in the San Gorgonio wilderness, Atmos. Environ., 38, 5901–5910, https://doi.org/10.1016/j.atmosenv.2004.07.011, 2004.

Zhou, S., Davy, P. K., Huang, M., Duan, J., Wang, X., Fan, Q., Chang, M., Liu, Y., Chen, W., Xie, S., Ancelet, T., and Trompetter, W. J.: High-resolution sampling and analysis of ambient particulate matter in the Pearl River Delta region of

southern China: source apportionment and health risk implications, Atmos. Chem. Phys., 18, 2049–2064, https://doi.org/10.5194/acp-18-2049-2018, 2018.

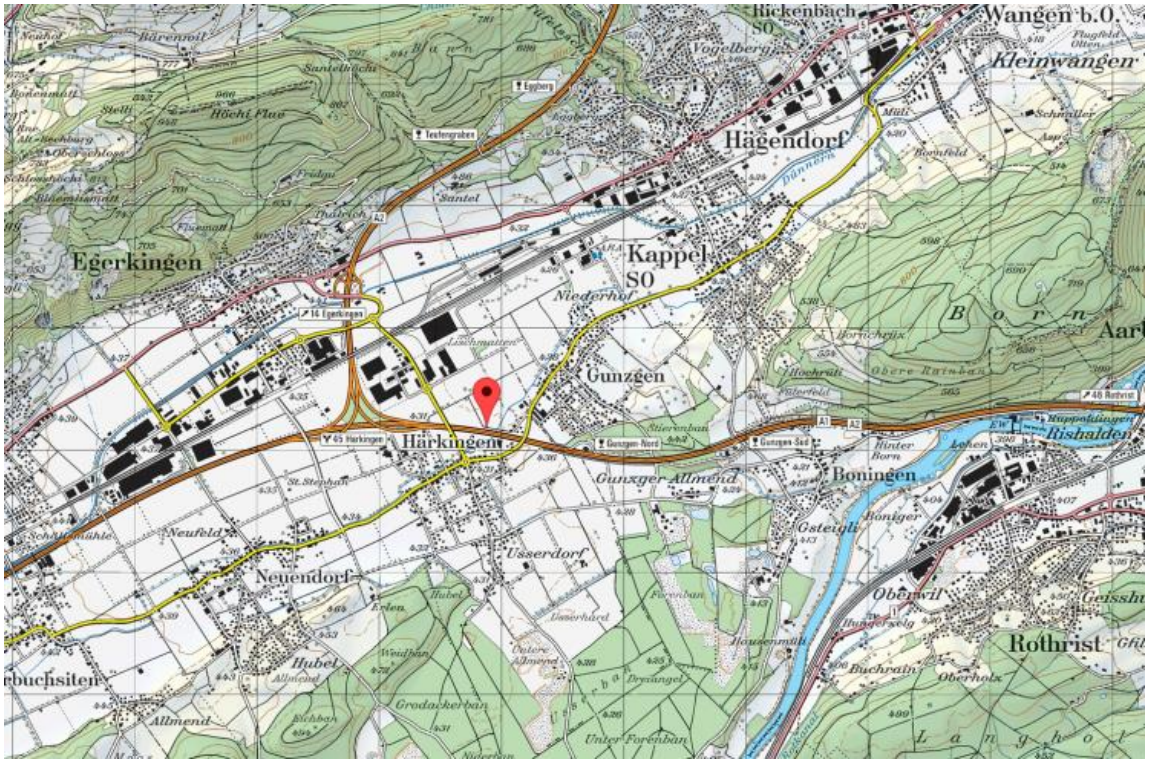

Figure 1: Map of the sampling location (NABEL site in Haerkingen), The site is marked with red google pin. Map reproduced by permission of swisstopo (JA100119).

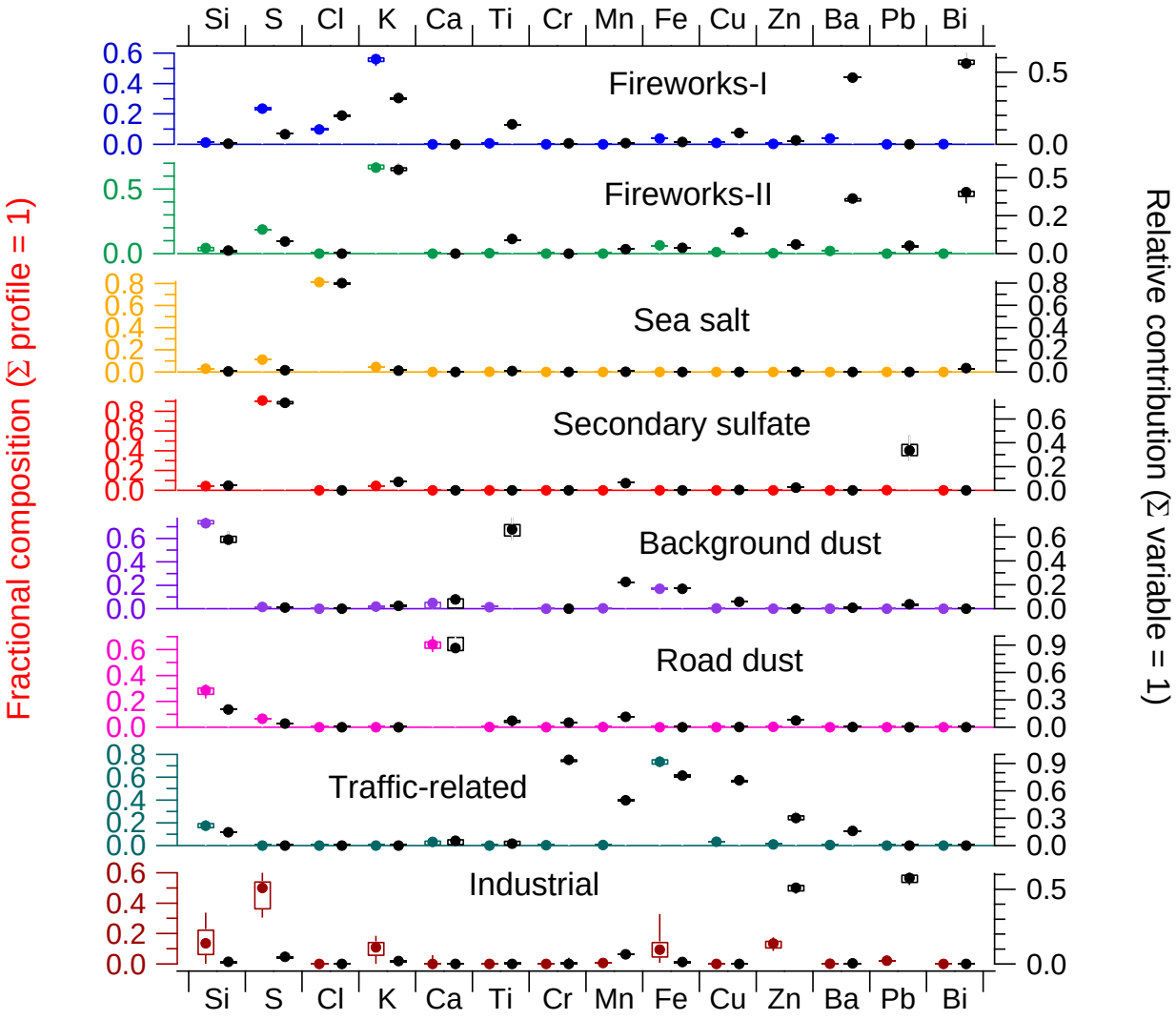

Figure 12: Source profiles of PMF results. The data and their corresponding uncertainty are given as box-whisker plot (bottom to top: p10-p25-p50-p75-p90) of good solutions from bootstrap runs. The left y-axis represents the fractional composition of the factor profile in row-wise (presented in coloured box whisker plot) for each factor in ng ng^{-1}, the right y-axis represents the relative contribution of each factor to each variable (indicated in black box-whisker plot).

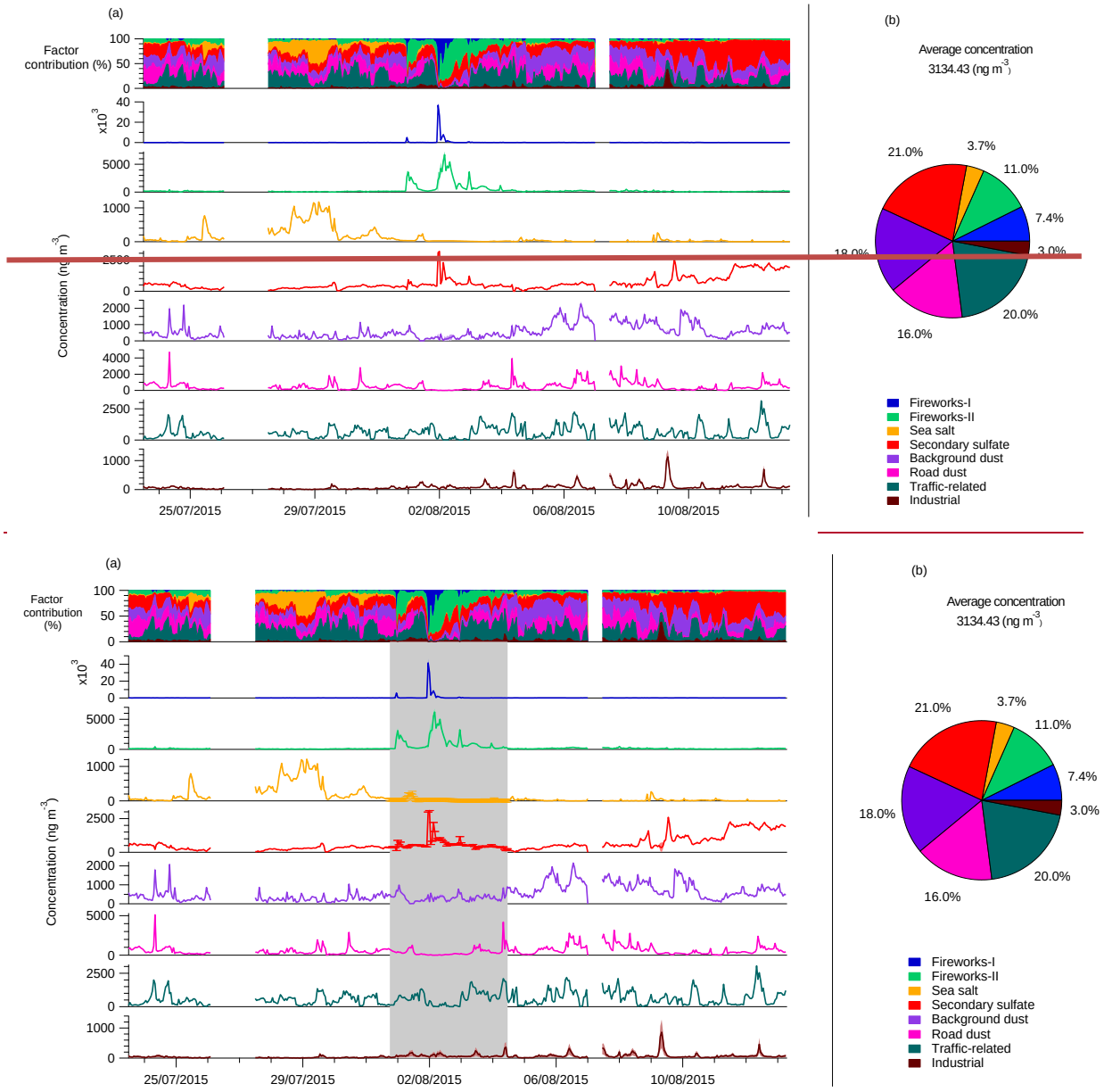

Figure ~~2~~3: (a) Time series of the PM_{10} elemental sources and relative contributions of the different sources over time; shaded areas indicate the uncertainties (interquartile) of selected bootstrap runs; grey background color represent the fireworks period; estimated uncertainty of the secondary sulfate (± 5%) and the sea salt factors (± 42%) during fireworks period are added as error bars; (b) Mean relative contributions of PM_{10} elemental sources.

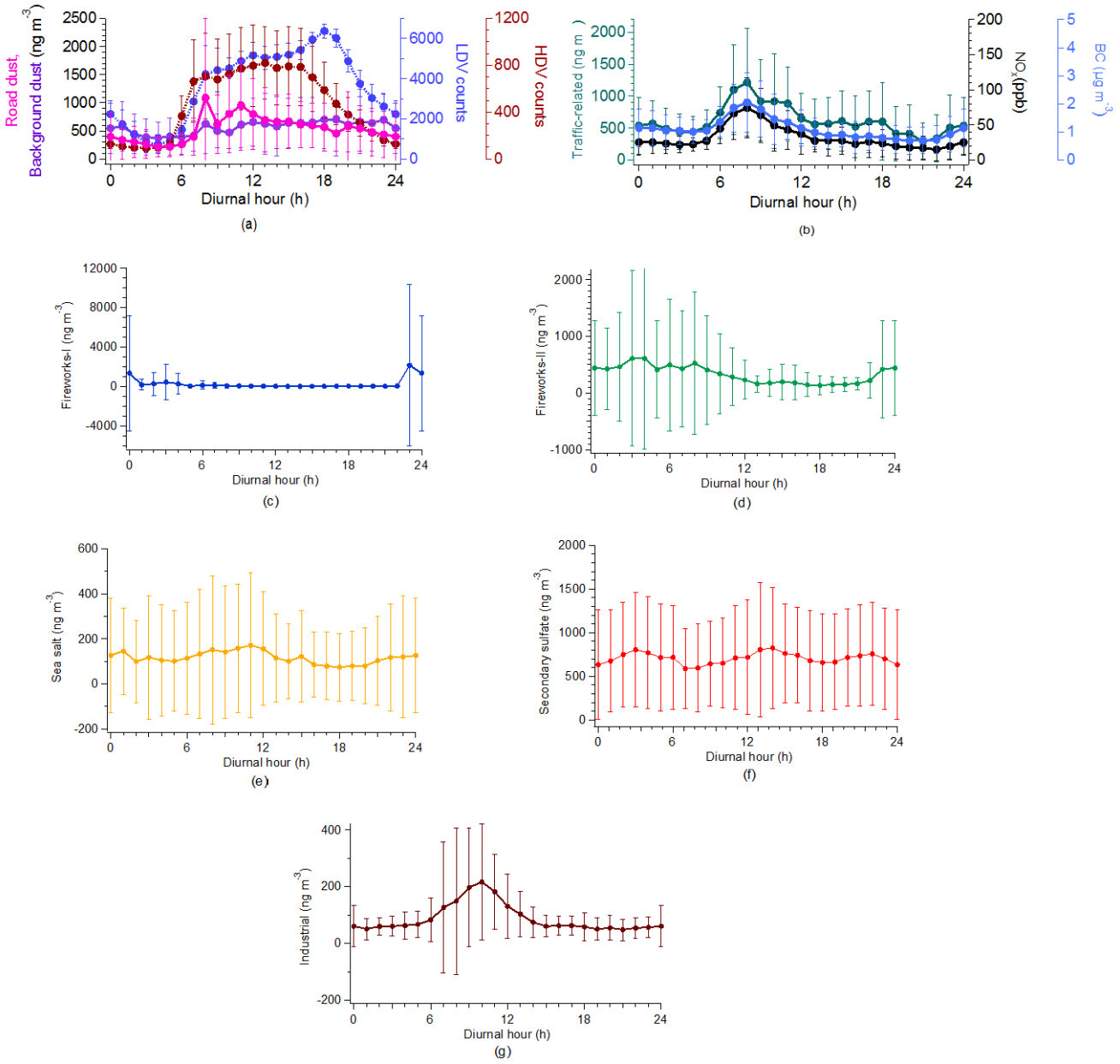

Figure ~~34~~: Mean diurnal patterns of the factors and of some corresponding external tracers with error bars (one standard deviation).

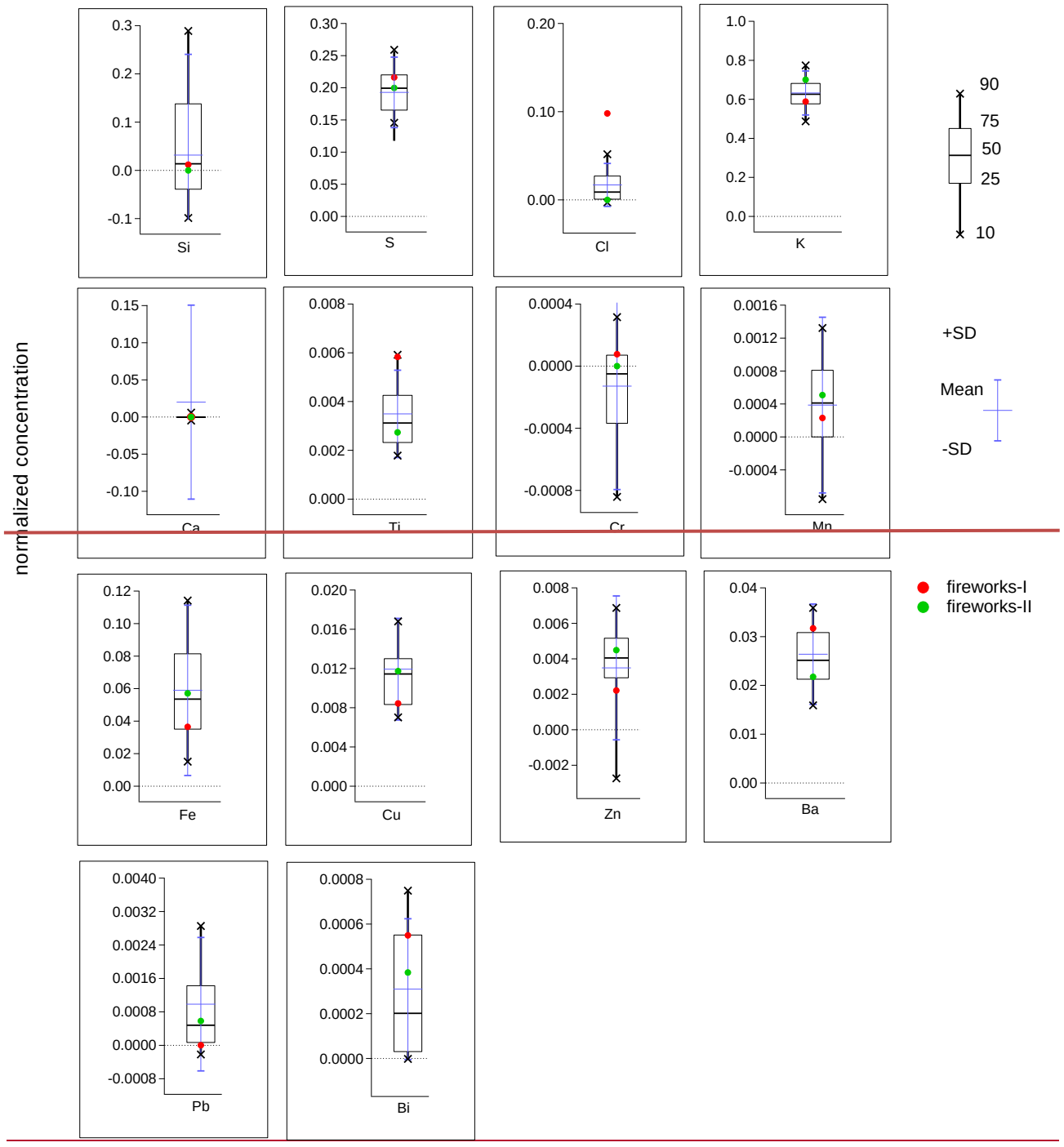

~~Figure 4: Representation of fireworks data points (normalized concentration) in terms of mean, median, 10-25-75-90th percentiles (bottom to top) and one standard deviation. Red and green dots denote the factor composition of fireworks-I and fireworks-II, respectively.~~

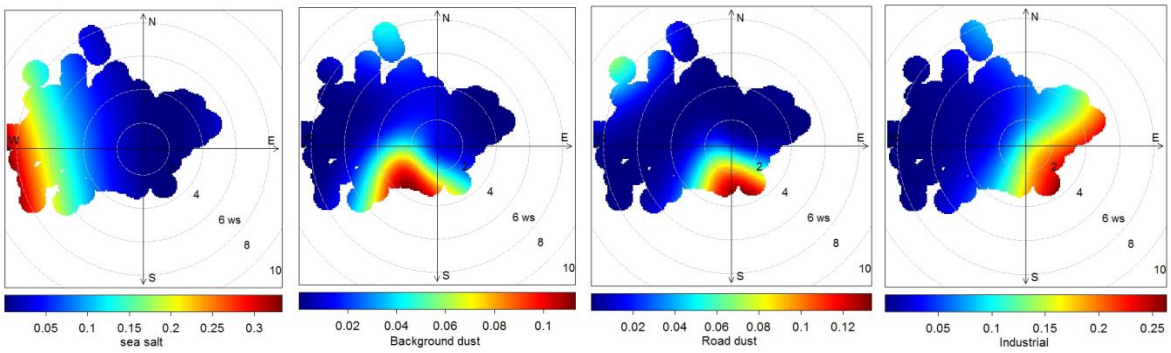

Figure 5: CBPF analysis (at 90th percentile) of factors in terms of wind speed (m s^{-1}) and wind direction. The color code represents the probability of the factor contribution.

Supplementary of

Source apportionment of highly time resolved trace elements during a firework episode from a rural freeway site in Switzerland

Pragati Rai et al.

Correspondence to: André S. H. Prévôt (andre.prevot@psi.ch) and Markus Furger (markus.furger@psi.ch)

S1. Preliminary source apportionment analysis and factor identification:

The first step in the source apportionment analysis is to perform a bilinear model without any *a* priori information in the modelled matrices (F and G) (unconstrained PMF) for different numbers of factors, e.g., three to ten factors (Crippa et al., 2014). The unconstrained PMF solution resulted in mixed factors, such as sea salt mixed with fireworks even for higher number of factors (Fig S1). The separation of the sea salt factor from fireworks was done as follows:

1. The input data set was divided into two parts: fireworks days (30 July–4 August) and Non-fireworks days (all days except 30 July–4 August).
2. Unconstrained PMF was performed at different number of factors on both data sets separately.
3. The fireworks profile and sea salt profile were selected from a PMF run conducted on fireworks data set and non-fireworks data set, respectively.
4. A secondary sulfate factor was observed (mostly characterized by elemental S with, 91% of total factor composition) at the 9 factor solution (Fig. S1), which correlates very well with ACSM sulfate (R^2 = 0.91).
5. The factor profiles of secondary sulfate, fireworks and sea salt were constrained in the PMF. In addition, the time series of the secondary sulfate factor was constrained too to avoid mixing between this time series and that of the firework factors.
6. Various sensitivity tests were performed by varying the *a* value of the constrained data.

Backward trajectory inspection revealed a predominance of continental air masses during the firework event, excluding the influence of sea salt. The absolute Cl concentration during fireworks period was used as background Cl concentration by replacing the fireworks data points with linear interpolation between two non-fireworks data points. This information was used to separate sea salt factor time series from fireworks time series. It was done by constraining the background Cl time series (only for fireworks data points) in the sea salt factor time series. ME-2 was performed from 4 to 10 factors on the whole data set with different seeds.

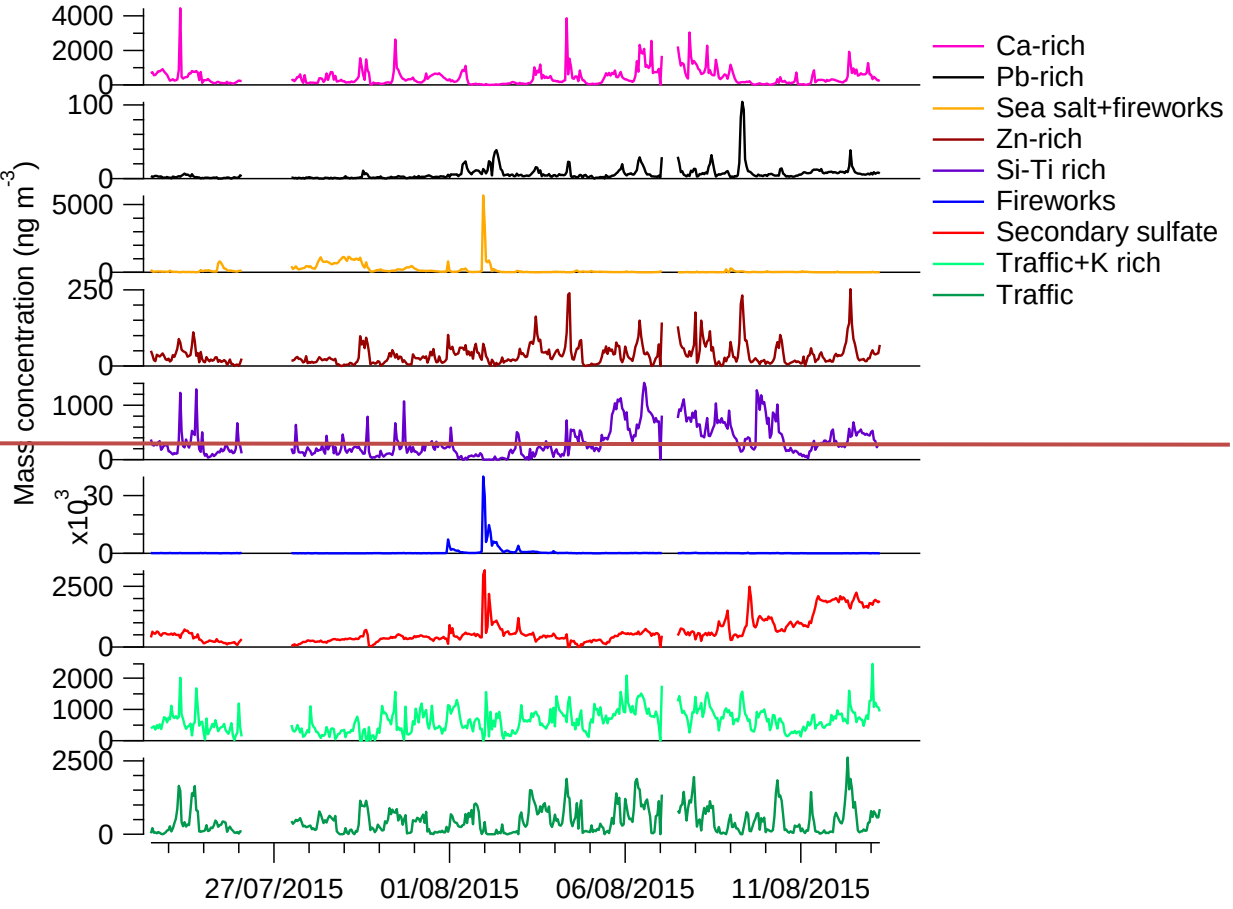
Mass concentration (ng m-3)
x10^3
4000
2000
0
100
0
5000
0
250
0
1000
0
30
0
2500
0
2000
1000
0
2500
0
27/07/2015
01/08/2015
06/08/2015
11/08/2015
Ca-rich
Pb-rich
Sea salt+fireworks
Zn-rich
Si-Ti rich
Fireworks
Secondary sulfate
Traffic+K rich
Traffic

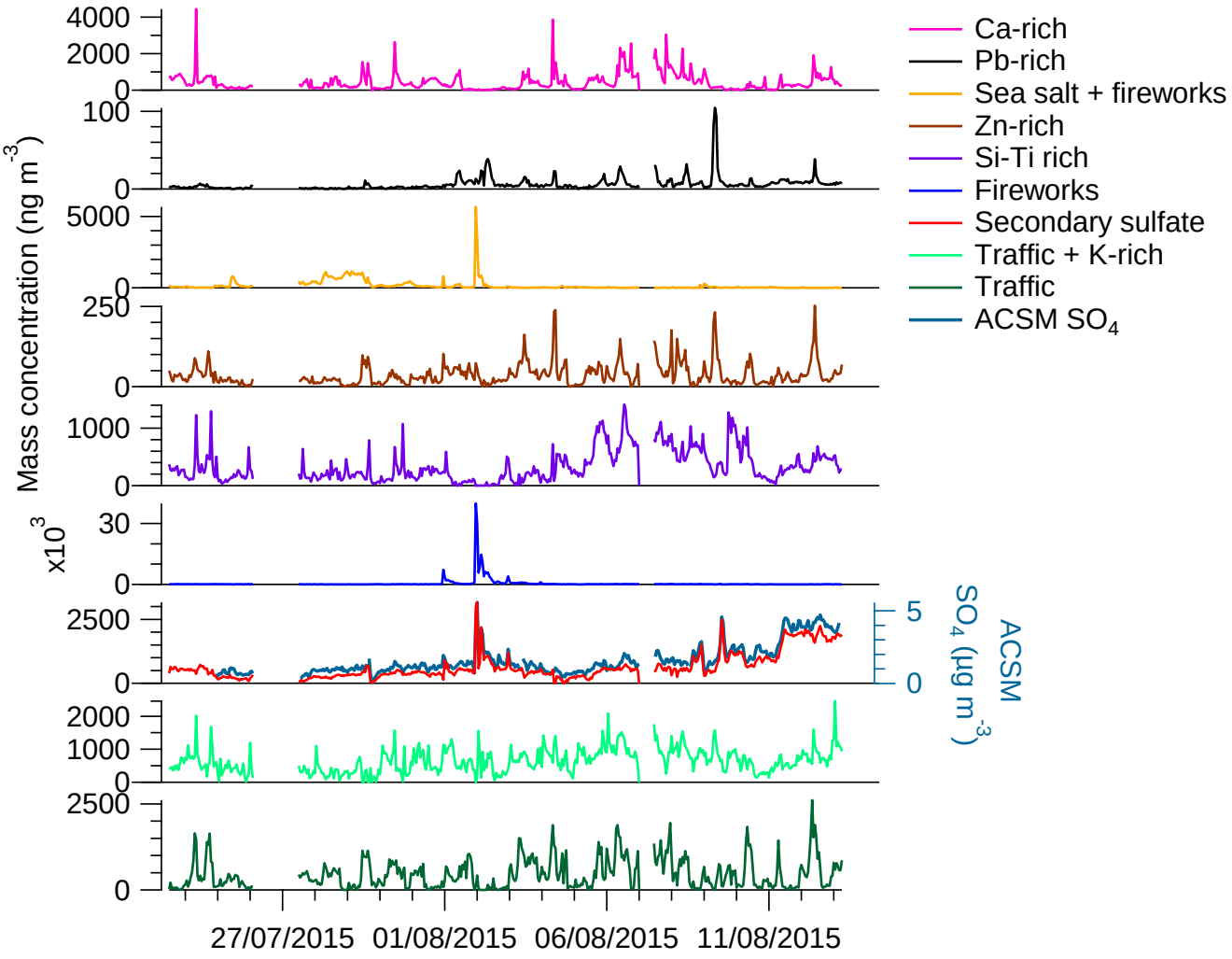

Figure S1: Unconstrained PMF with a nine-factor solution.

Based on $Q_{avg,}$ defined as $\frac{\Sigma_{i=1}^{m}\Sigma_{j=1}^{n}\left(\frac{e_{ij}}{s_{ij}}\right)^2}{n*m}$ (n: sample time series, m: number of variables), the model explains the data variability very well when allowing for eight factors (Fig S2). Furthermore, we access the change in time-dependent $Q_{avg,i}$, $\frac{\Sigma_{i=1}^{m}\Sigma_{j=1}^{n}\left(\frac{e_{ij}}{s_{ij}}\right)^2}{n}$, when increasing the number of factors i.e., $\Delta Q_{avg,i}$; contribution to Q for the (p)-factor solution minus that of the (p+1)-factor solution (Fig S3). A significant decrease in $\Delta Q_{avg,i}$ indicates that the structure in the residuals disappeared with the additional factor. The removed structure is evident up to eight factors. Increasing the number of factors to nine

yields a new mixed factor of the traffic-related and background dust factors (Fig. S1). Overall, a best ME-2 solution was observed up to a number of factors equal to eight.

For the 8-factor solution, we assess how well the different variables are explained by PMF using the quantity $\Delta Q_{avg,\ j}$ $\frac{\sum_{i=1}^{m}\sum_{j=1}^{n}\left(\frac{e_{ij}}{s_{ij}}\right)^2}{m}$ (Fig S4). $Q_{avg,j}$ shows that with 8 factors all variables are explained within their measurement uncertainty except Si and Pb. This might be linked to an underestimation of the measurement uncertainty itself.

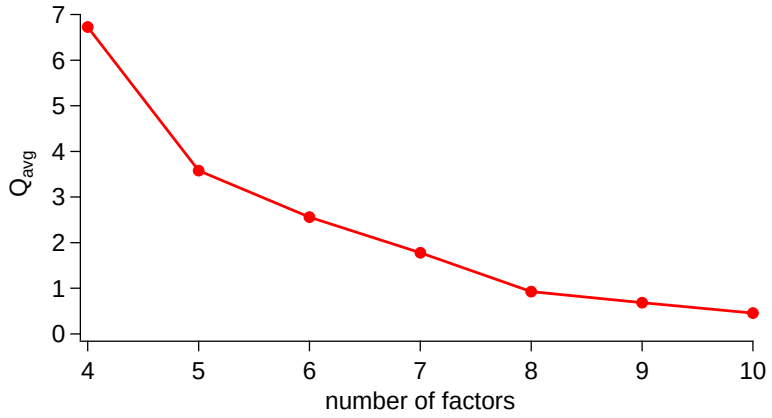

Figure S2: Q_{avg} as a function of the number of factors.

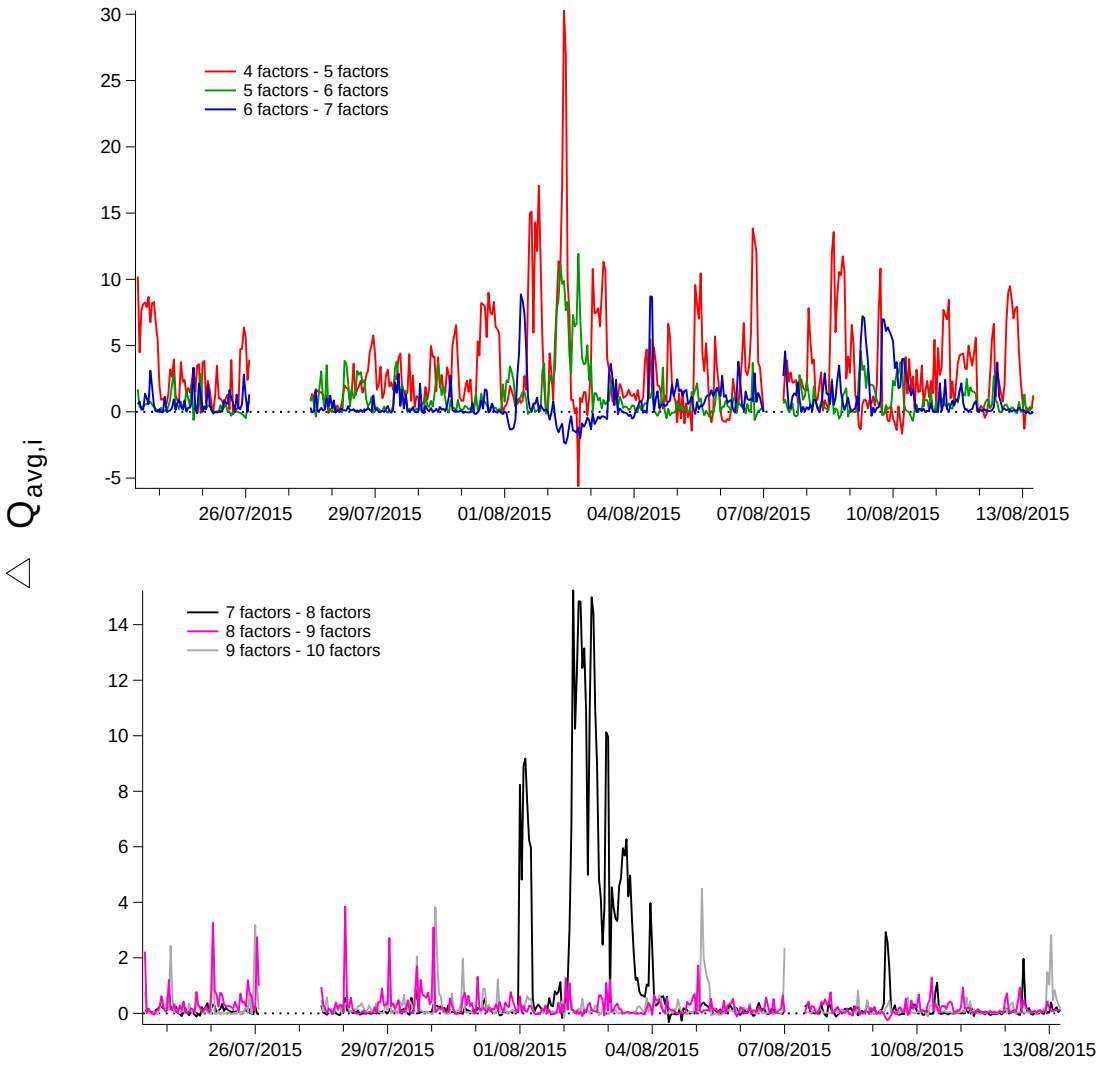

Figure S3: -Change in the time-dependent contribution of $Q_{avg,i}$ ($\Delta Q_{avg,i}$) as a function of the number of factors.

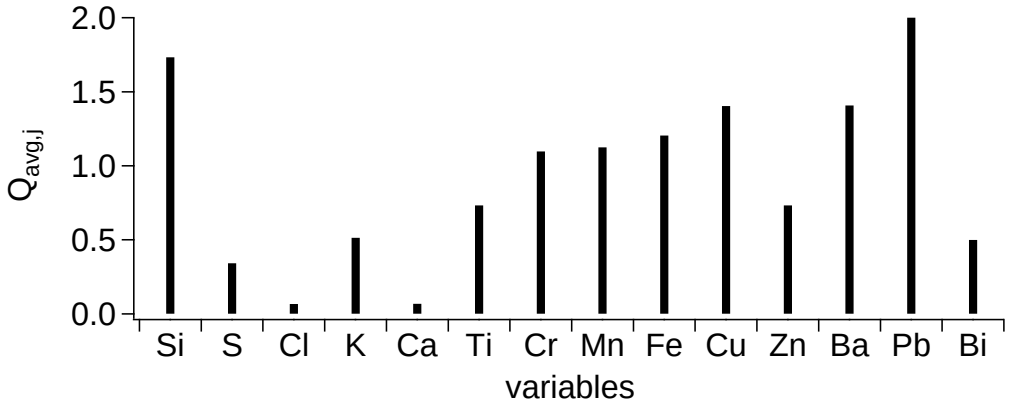

Figure S4: Q_{avg} as a function of variables for the eight-factor solution.

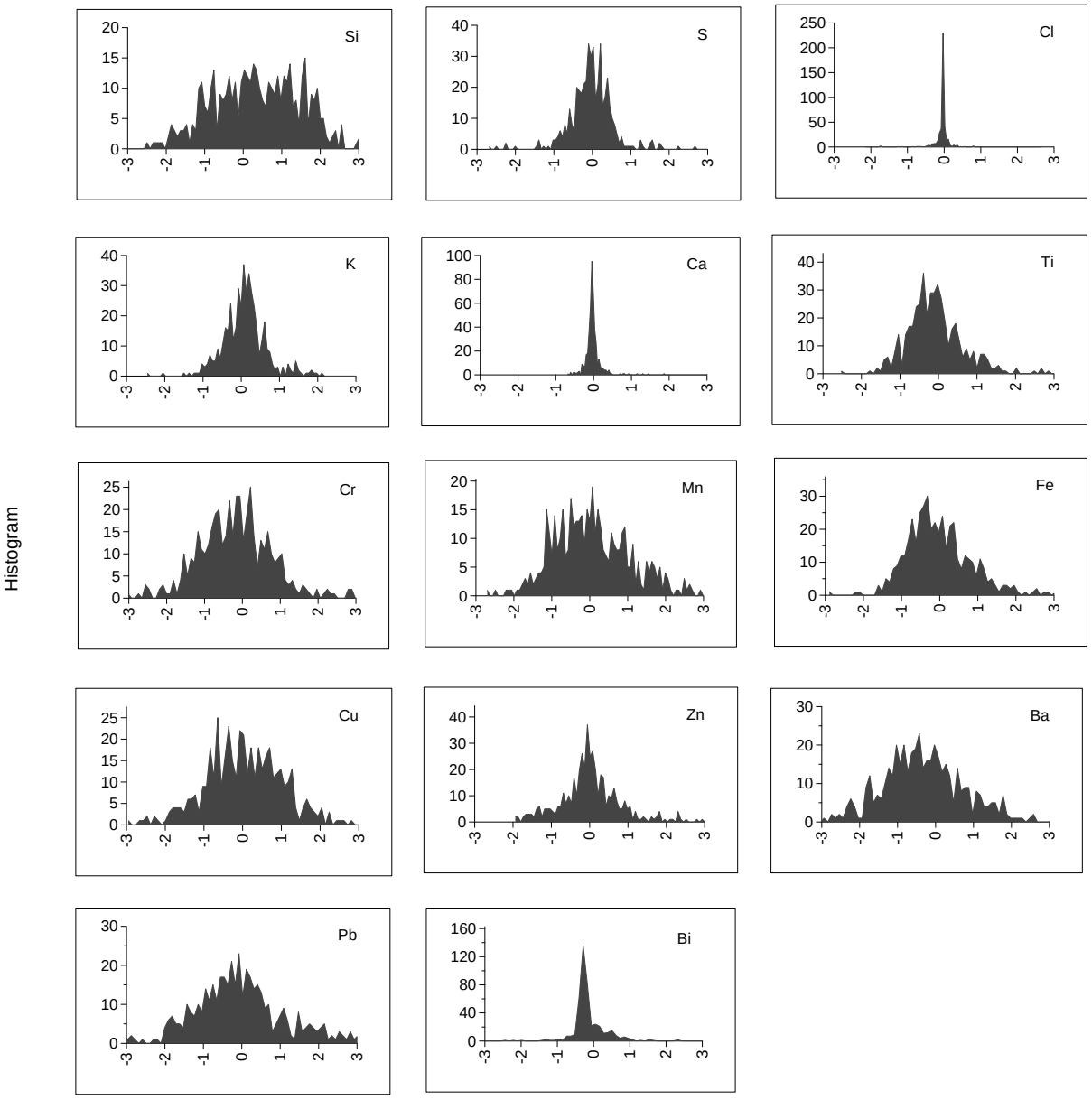

Figure S5: Histograms of variables as a function of residuals weighted by the uncertainty (residual/uncertainty) for the eight-factor solution.

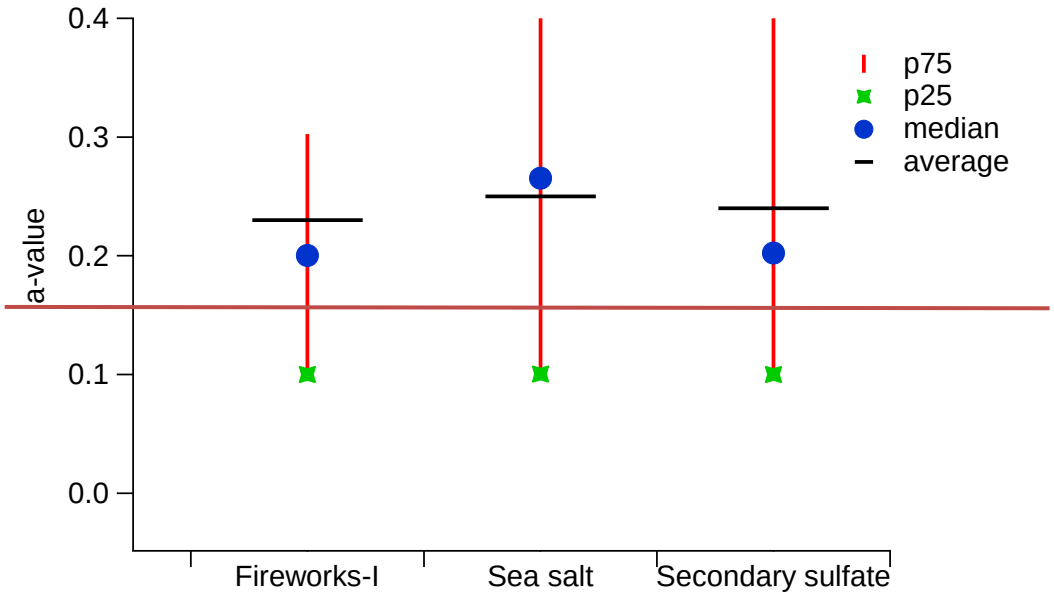

~~**Figure S6: *a*-value statistics of the accepted solutions. *a*-values between 0 to 0.5 were explored during BS analysis. The average *a*-value of the selected solutions was ranging from 0.2 to 0.3 for the constrained factors. The selected *a*-values were homogeneously distributed over that range.**~~

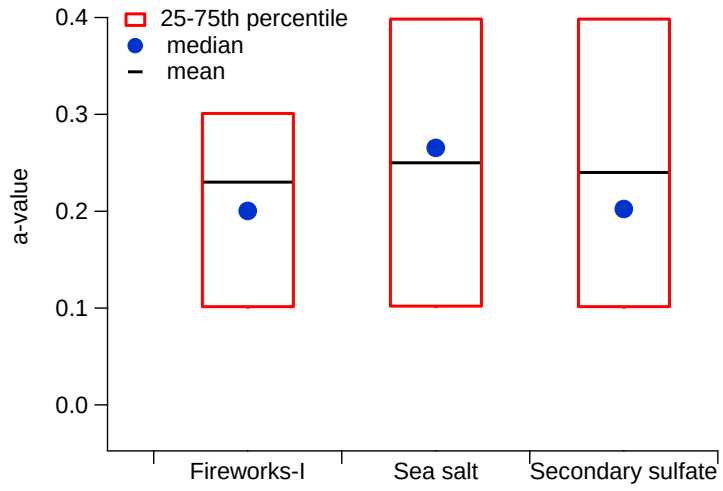

Figure S6: *a*-value statistics of the accepted solutions. *a*-values between 0 to 0.5 were explored during BS analysis. The average *a*-value of the selected solutions was ranging from 0.2 to 0.3 for the constrained factors. The selected *a*-values were homogeneously distributed over that range.

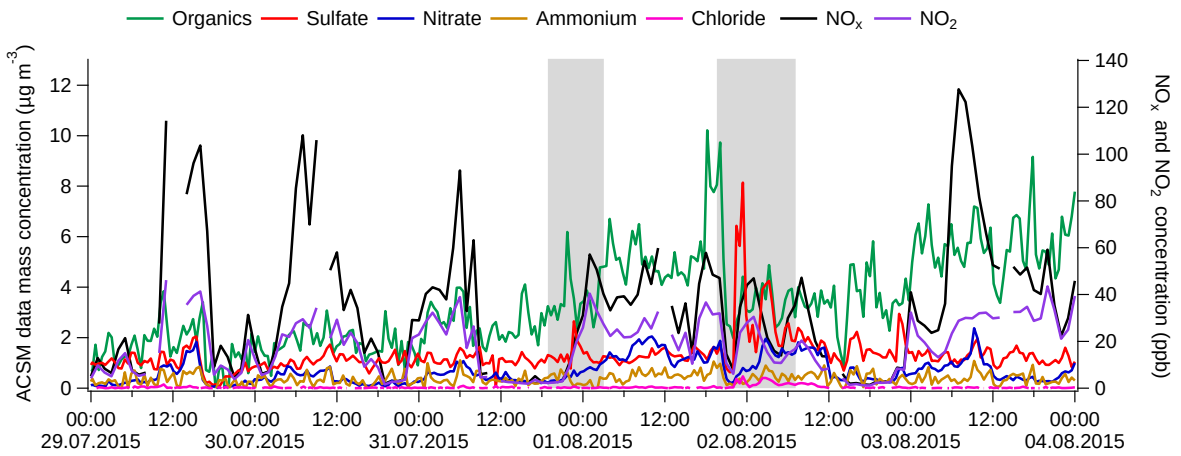

Figure S7: Time series of the non-refractory aerosol components (measured with the ACSM), NO_2 and NO_x concentration. The fireworks episodes are underlain in grey color.

Fig. S8 provides an estimate of the overall fireworks composition and temporal variability, complementing the PMF results (which are shown for reference). The figure is constructed in two stages. First, the time series of fireworks contributions to each element is estimated by subtracting the non-fireworks factors (NFF) from the original measurements. Then, the estimated fireworks contribution for each element is normalized by the total fireworks element contribution, and the displayed statistics are calculated. This is represented mathematically below, and the expression has been added to the main text. Note that the variation in fireworks profiles implied by this figure supports the representation of fireworks by 2 fireworks factors.

$$normalized\ concentration_{ij} = \frac{x_{ij} - \left(g_{ik} f_{kj}\right)_{k=NFF}}{\Sigma_j \left(x_{ij} - \left(g_{ik} f_{kj}\right)_{k=NFF}\right)} \quad \text{(S1)}$$

where X represents the input data matrix for PMF, while G and F represent the factor time series and factor profiles driven by six non-fireworks factors (NFF). Here *i* and *j* denote time series and variables, respectively.

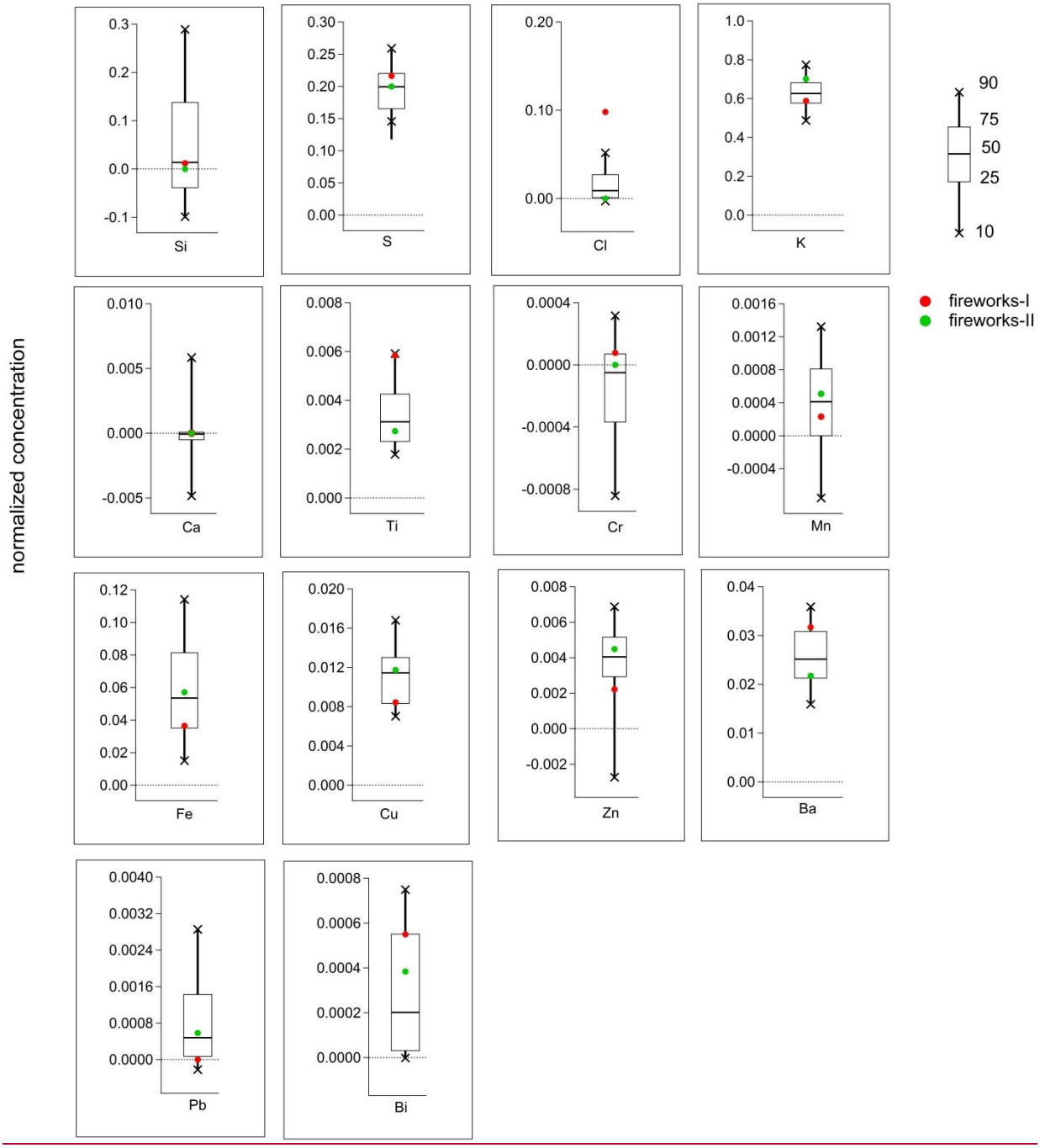

Figure S8: Representation of fireworks data points (normalized concentration) in terms of median and 10-25-75-90th percentiles (bottom to top). Red and green dots denote the factor profiles of fireworks-I and fireworks-II, respectively.

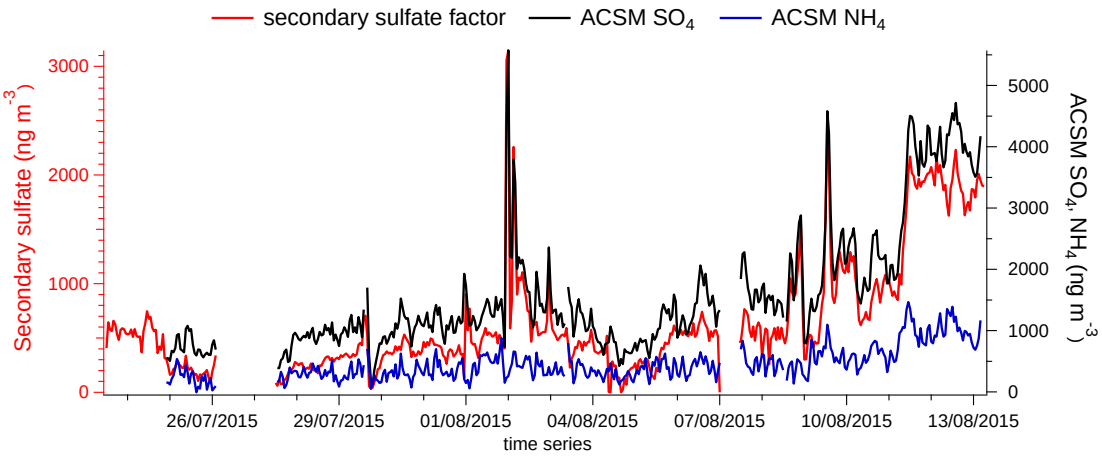

Figure S9~~7~~: Time series of the secondary sulfate factor (left y-axis) and mass concentration of SO_4, NH_4 from the ACSM (right y-axis).

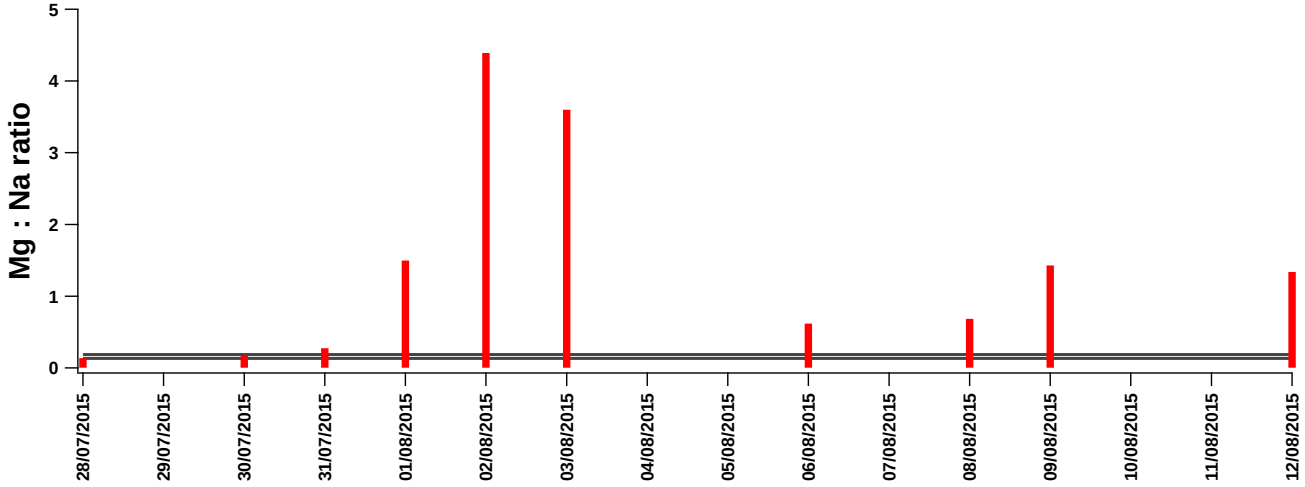

Figure S10~~9~~: Mg / ~~÷~~Na ratio (red bars) for 24-h filter data analysed by ICP-OES. The gray lines represent the Mg / ~~÷~~Na ratio range (0.132 -0.185) in marine aerosols. The Mg / Na ratio was 0.13 and 0.16 for 28 July and 30 July, respectively while for the rest of the days it was higher than 0.185.

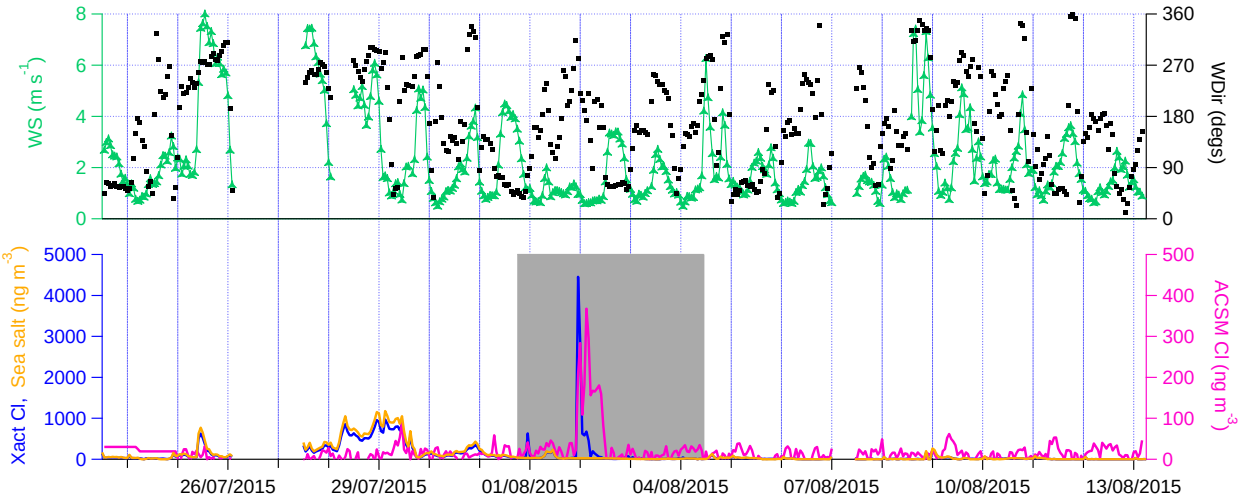

Figure S1~~0~~: Bottom panel: Time series of the Cl concentration from the Xact, sea salt factor (left y-axis) from the PMF solution, and ACSM chloride concentration (right y-axis). Top panel: Wind speed (WS in m s^{-1}) and wind direction (WDir in degree) during the measurement period. The grey area in the bottom panel represents fireworks days.

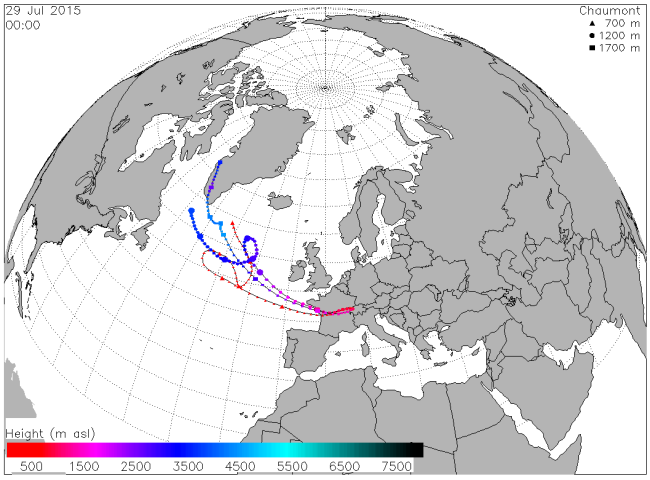

Figure S12~~1~~: Backward trajectory (produced from the FLEXTRA Trajectory Model; *https://folk.nilu.no/~andreas/flextra.html*) analysis at different heights during a sea salt event.

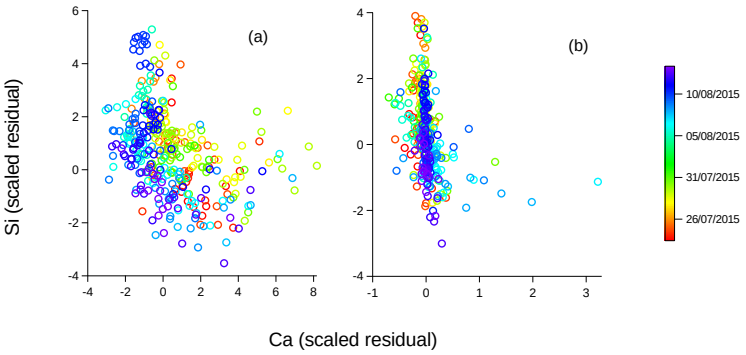

Figure S132: Scatter plot of Si vs. Ca scaled residuals: (a) PMF solution with one dust factor; (b) PMF solution with two dust factors.

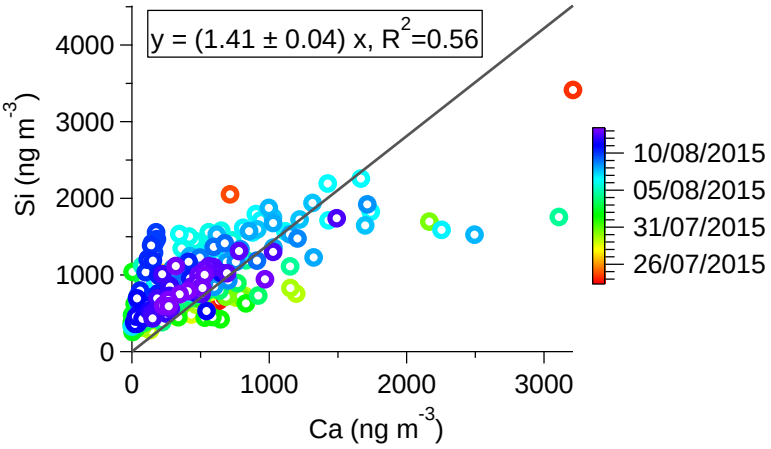

Figure S143: Scatter plot of Si vs. Ca.

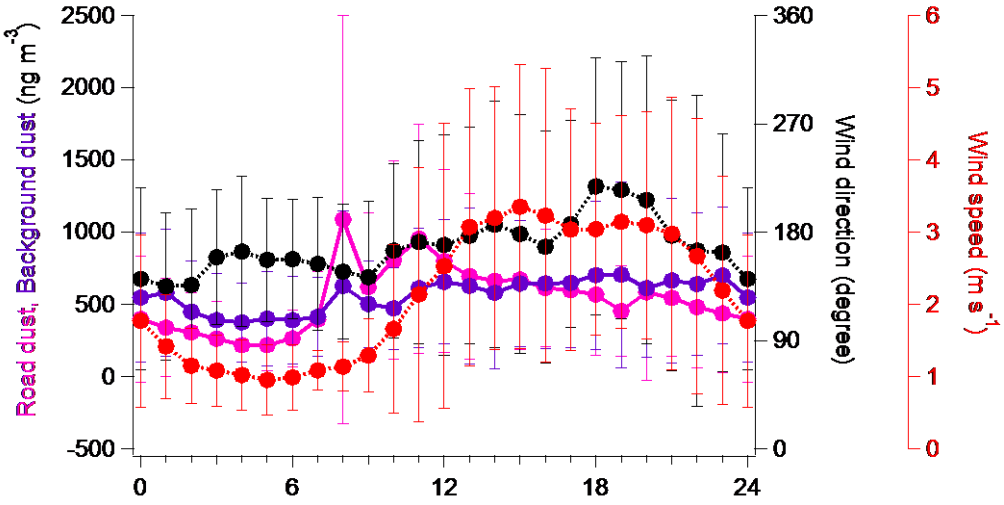

Figure S154: Mean diurnal variations of the two dust factors (left-y axis) along with wind speed and wind direction (right y-axes) with error bars (one standard deviation).

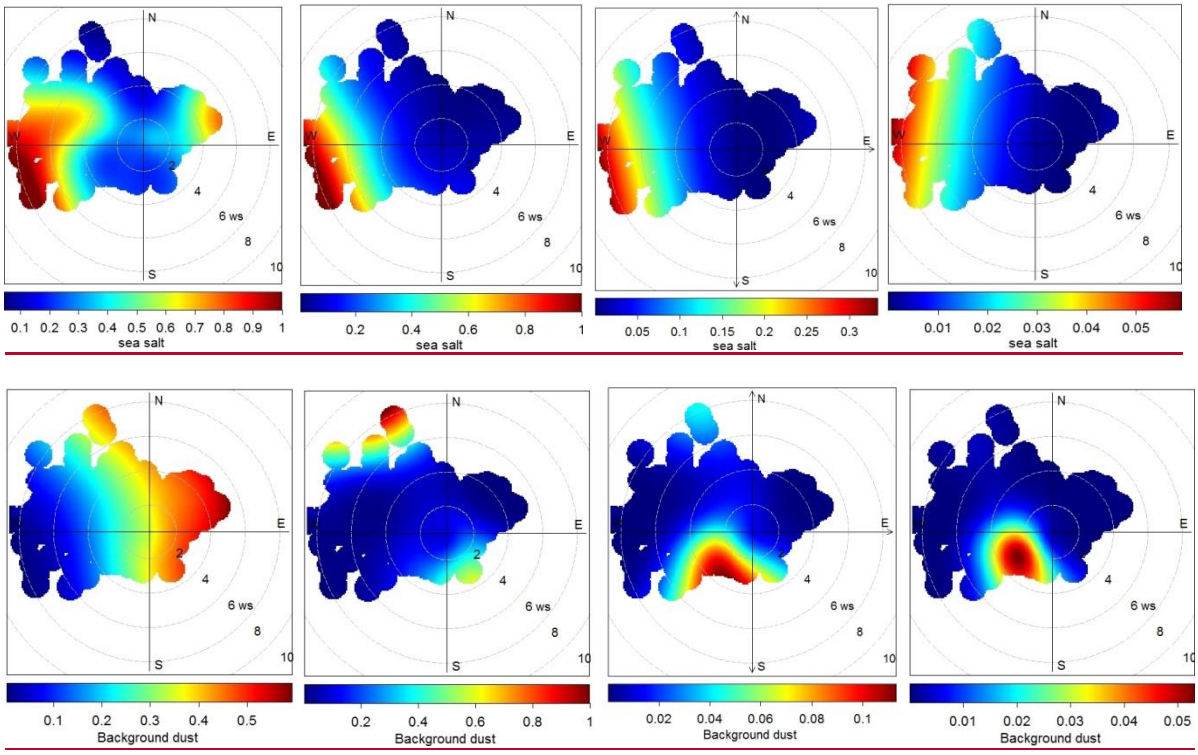

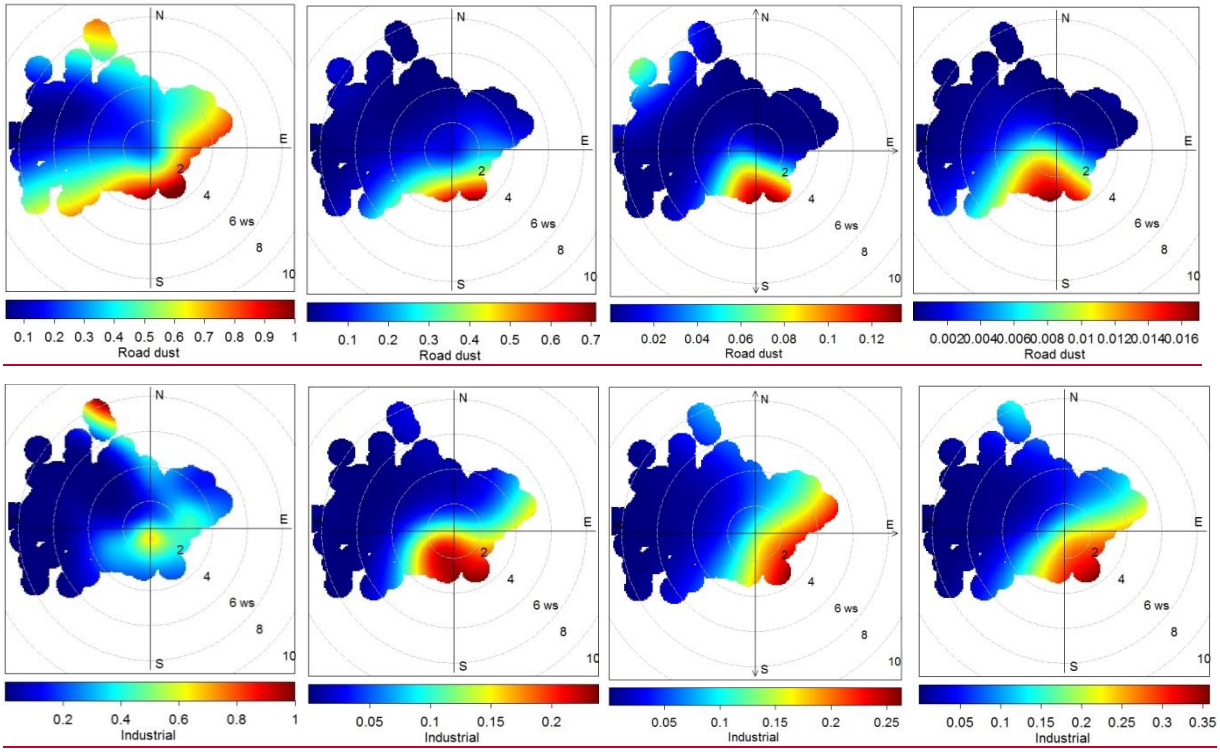

Figure S16: CBPF analysis (from left to right: 50th, 75th, 90th, 95th percentiles) of factors (sea salt, background dust, road dust, industrial) in terms of wind speed (m s^{-1}) and wind direction. The color code represents the probability of the factor contribution.

5

~~**References**~~

~~Crippa, M., Canonaco, F., Lanz, V. A., Äijälä, M., Allan, J. D., Carbone, S., Capes, G., Ceburnis, D., Dall'Osto, M., Day, D. A., DeCarlo, P. F., Ehn, M., Eriksson, A., Freney, E., Hildebrandt Ruiz, L., Hillamo, R., Jimenez, J. L., Junninen, H., Kiendler Scharr, A., Kortelainen, A. M., Kulmala, M., Laaksonen, A., Mensah, A. A., Mohr, C., Nemitz, E., O'Dowd, C.,~~

10 ~~Ovadnevaite, J., Pandis, S. N., Petäjä, T., Poulain, L., Saarikoski, S., Sellegri, K., Swietlicki, E., Tiitta, P., Worsnop, D. R., Baltensperger, U., and Prévôt, A. S. H.: Organic aerosol components derived from 25 AMS data sets across Europe using a consistent ME 2 based source apportionment approach, Atmos. Chem. Phys., 14, 6159 6176, https://doi.org/10.5194/acp 14 6159 2014, 2014.~~